AD-A151 226 RECEIVER OTTIMIZATION FOR DETECTION IN DOUBLY SPREAD COMMUNICATION CHANNE..(U) PENNSYLVANIA STATE UNIV UNIVERSITY PARK APPLIED RESEARCH LAB.. D M DRUMHELLER 1/2

UNCLASSIFIED 10 DEC 84 ARL/PSU/TM-84-185 F/G 17/2.1 NL

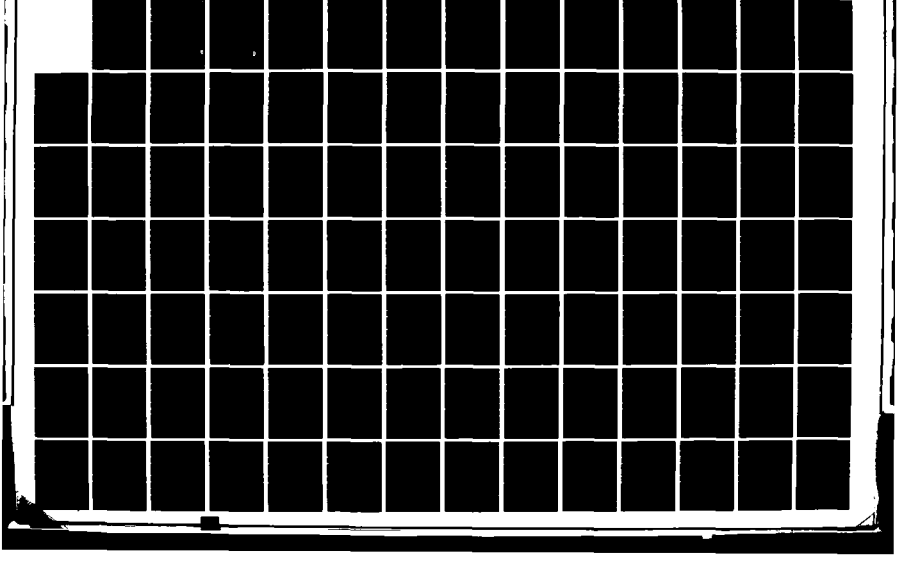

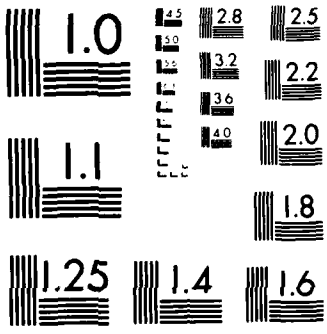

MICROCOPY RESOLUTION TEST CHART
NATIONAL BUREAU OF STANDARDS 1963 A

RECEIVER OPTIMIZATION FOR DETECTION IN DOUBLY SPREAD COMMUNICATION CHANNELS

David Mark Drumheller

Technical Memorandum
File No. TM 84-185
10 December 1984
Contract N00024-79-C-6043

Copy No. 12

The Pennsylvania State University
Intercollege Research Programs and Facilities
APPLIED RESEARCH LABORATORY
Post Office Box 30
State College, Pa. 16804

NAVY DEPARTMENT

NAVAL SEA SYSTEMS COMMAND

RECEIVER OPTIMIZATION FOR DETECTION IN DOUBLY SPREAD COMMUNICATION CHANNELS

David Mark Drumheller

Technical Memorandum
File No. TM 84-185
10 December 1984
Contract N00024-79-C-6043

Copy No. 12

The Pennsylvania State University
Intercollege Research Programs and Facilities
Applied Research Laboratory
Post Office Box 30
State College, PA 16804

NAVY DEPARTMENT

NAVAL SEA SYSTEMS COMMAND

Approved for Public Release

REPORT DOCUMENTATION PAGE		READ INSTRUCTIONS BEFORE COMPLETING FORM
1. REPORT NUMBER TM 84-185	2. GOVT ACCESSION NO. AD-A151 296	3. RECIPIENT'S CATALOG NUMBER
4. TITLE (and Subtitle) RECEIVER OPTIMIZATION FOR DETECTION IN DOUBLY SPREAD COMMUNICATION CHANNELS		5. TYPE OF REPORT & PERIOD COVERED Technical Memorandum 6. PERFORMING ORG. REPORT NUMBER
7. AUTHOR(s) David Mark Drumheller		8. CONTRACT OR GRANT NUMBER(s) N00024-79-C-6043
9. PERFORMING ORGANIZATION NAME AND ADDRESS Applied Research Laboratory Post Office Box 30 State College, PA 16804		10. PROGRAM ELEMENT, PROJECT, TASK AREA & WORK UNIT NUMBERS
11. CONTROLLING OFFICE NAME AND ADDRESS Naval Sea Systems Command Department of the Navy Washington, DC 20362		12. REPORT DATE 10 December 1984 13. NUMBER OF PAGES 116
14. MONITORING AGENCY NAME & ADDRESS(if different from Controlling Office)		15. SECURITY CLASS. (of this report) Unclassified 15a. DECLASSIFICATION/DOWNGRADING SCHEDULE
16. DISTRIBUTION STATEMENT (of this Report) Approved for public release. Distribution unlimited. Per NAVSEA - Case 84-1049.		
17. DISTRIBUTION STATEMENT (of the abstract entered in Block 20, if different from Report)		
18. SUPPLEMENTARY NOTES		
19. KEY WORDS (Continue on reverse side if necessary and identify by block number)		

20. ABSTRACT (Continue on reverse side if necessary and identify by block number)

The problem addressed in this thesis is the maximization of the expected matched filter receiver response to a signal that has been transmitted through a communication channel whose average scattering properties are known in terms of a scattering function. This is accomplished by altering the receiver processing signal given the channel scattering function and transmit signal. The channel is assumed to be doubly-spread, meaning that any signal propagated through it will exhibit both time and frequency spreading. The scattering

functions that describe these channels subtend a finite region in the delay-Doppler plane.

This thesis contains some of the background material necessary to understand the modeling of communication channels as random linear time-varying systems and the use of matched filter receivers for signal detection. This material includes a review of the properties of linear spaces, Fourier transforms, and the foundational material leading to the development of the scattering function.

ABSTRACT

The problem addressed in this thesis is the maximization of the expected matched filter receiver response to a signal that has been transmitted through a communication channel whose average scattering properties are known in terms of a scattering function. This is accomplished by altering the receiver processing signal given the channel scattering function and transmit signal. The channel is assumed to be doubly-spread, meaning that any signal propagated through it will exhibit both time and frequency spreading. The scattering functions that describe these channels subtend a finite region in the delay-dopper plane.

This thesis contains some of the background material necessary to understand the modeling of communication channels as random linear time-varying systems and the use of matched filter receivers for signal detection. This material includes a review of the properties of linear spaces, Fourier transforms, and the foundational material leading to the development of the scattering function.

TABLE OF CONTENTS

TABLE OF CONTENTS (continued)

LIST OF FIGURES

LIST OF FIGURES (continued)

LIST OF SYMBOLS

R^1	the field of real numbers
R^2	the set of real ordered pairs
C	the field of complex numbers
$L^1(R^1)$	the space of all Lebesque measurable functions mapping the field of real numbers to the field of complex numbers, and are magnitude integrable
$L^2(R^1)$	the space of all Lebesque measurable functions mapping the field of real numbers to the field of complex numbers, and are square integrable
$L^1(R^2)$	the space of all Lebesque measurable functions mapping the set of real ordered pairs to the field of complex numbers, and are magnitude integrable
$C^0(R^1)$	the space of all continuous bounded functions mapping the field of real numbers to the field of complex numbers
$\|\cdot\|_1$	the norm in the space $L^1(R^1)$
$\|\cdot\|_2$	the norm in the space $L^2(R^1)$
$\langle x,y \rangle$	the inner product of x(t) and y(t)
$x*y$	the convolution product of x(t) and y(t)
$\in$	denotes membership to a set
$\cap$	denotes the intersection of two sets
A/B	the set of all elements in set A but not in set B

ACKNOWLEDGEMENTS

I would like to thank all my committee members for their constructive criticism of the earlier drafts of my thesis. In particular, I would like to thank my thesis advisor, Dr. Dennis W. Ricker, for originally suggesting my thesis topic and providing me with the time and resources to pursue the research.

I would also like to thank my secretary, Janice Hall, who typed the first draft of my thesis and assisted in making revisions of later versions. The Applied Research Laboratory Editorial Department also deserves recognition for drawing some of the illustrations. Finally would like to thank Joseph A. Long for reviewing the final draft of this thesis.

This work was supported by the Applied Research Laboratory of The Pennsylvania State University under contract with Naval Sea Systems Command.

CHAPTER 1

GENERAL INTRODUCTION

In active signal detection systems, detection is performed by transmitting a signal over a communication channel, processing any received signal by a receiver, measuring the receiver output, and comparing the output to a predetermined threshold. The optimum receiver in Gaussian white noise is known to be a matched filter receiver, also known as a correlation receiver. It consists of a multiplier used to form the product between the received signal and processing signal, and an integrator to integrate the multiplier output.

Channel scattering having a delay extent greater than the average wavelength of the transmitted signal is said to be delay-spread. On the other hand, channels whose scattering properties vary rapidly in a time interval on the order of the signal time duration are said to be doppler-spread. Any communication channel exhibiting a combination of delay spreading and doppler spreading is said to be doubly-spread. Examples of doubly-spread sctterers are fish schools, volcanic plumes, storm cells, rotating planets, and asteroids.

A portion of the transmitted energy can also be scattered by the medium and is referred to as clutter or reverberation. Both clutter and reverberation, which may also be doubly-spread, represent interference and degrade the ability of the matched filter receiver to detect the channel output signal.

This thesis is concerned with the optimization of a matched filter receiver to detect a signal that has been transmitted through a doubly-spread communication channel whose scattering properties are

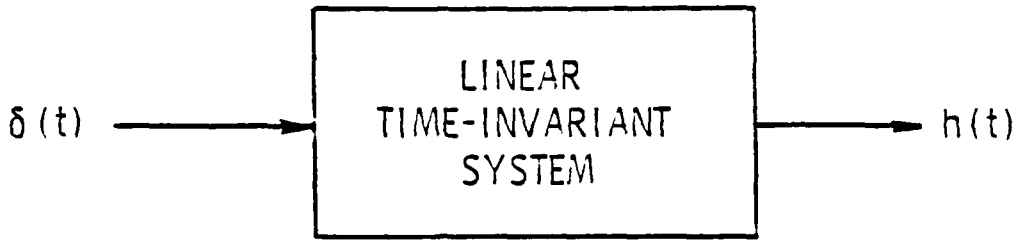

Figure 1. Block diagram of a linear time-varying system.

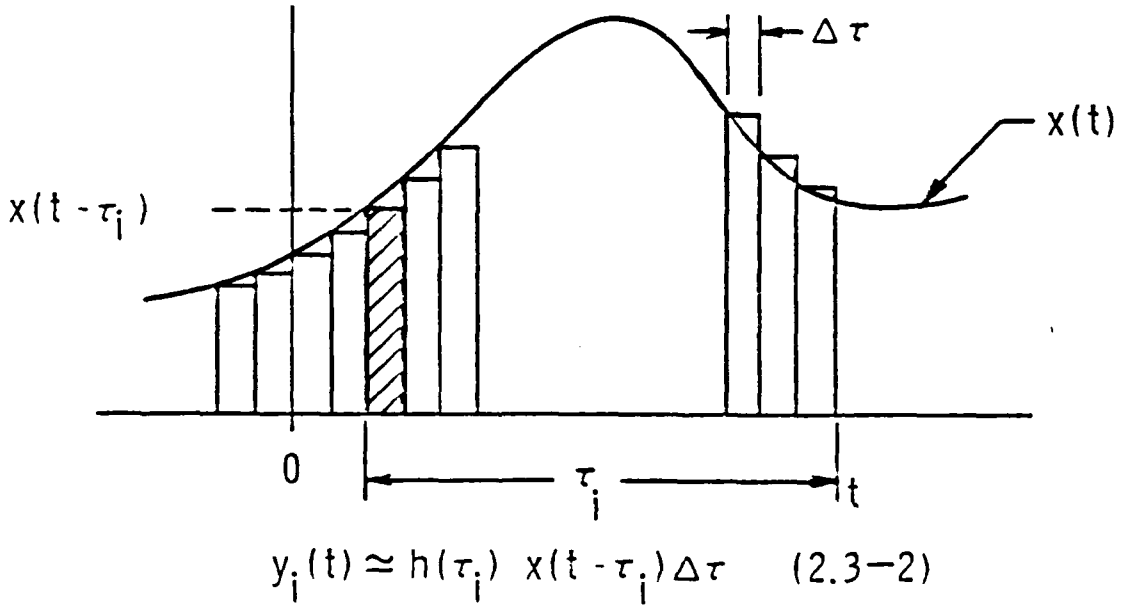

Figure 2. Derivation of (2.3-1). Input x(t) approximated by a pulse train. The response at time t due to the portion of the input approximated by the shaded panel.

then interpreted as an amplitude density function for the complex exponentials included in the continuous sum (integral) in (2.2-26). It is for this reason that the Fourier transform is also referred to as the 'spectrum' of the function x(t), since it gives a measure of the relative weighting of each complex exponential as a component of the function x(t). The terms Fourier transform and spectrum will be used interchangeably throughout this thesis.

2.3 Linear System Theory

2.3.1 Linear Time-Invariant and Time-Varying Systems

Linear time-invariant systems are often described by a function, h(t), referred to as the 'system impulse response function.' Its name decribes exactly what it does: it expresses the system output y(t) when the system input x(t) is an impulse function with unity weight. The impulse response does provide another service. It can be used to determine the system output for general inputs, and this is expressed by the convolution between h(t) and the input x(t), i.e.,

$$y(t) = \int_{-\infty}^{\infty} h(\tau)\, x(t-\tau)\, d\tau \ . \qquad (2.3\text{-}1)$$

The derivation of (2.3.1) can be developed in the time domain where the integral is considered to be a limit of a sum of responses to a square pulse train that approximates the input x(t). Figure 1 shows the linear time-invariant system as a block diagram and illustrates its interpretation in terms of the impulse response. Figure 2 shows how the input function is approximated by a series of square pulses with width $\Delta\tau$ and height $x(t-\tau_i)$. Note that the system response to the i-th pulse, $y_i(t)$, can be approximated by the response to an impulse applied at time $t-\tau_i$ whose weight is equal to $x(t-\tau_i)\ \Delta\tau$, therefore,

Theorem 2.7 Let $x(t) \in L^1(R^1)$ and be bounded ($|x(t)| < \infty$) for all $t \in R^1$. Then $x(t) \in L^2(R^1)$.

Proof Define the normalized function $\hat{x}$ by

$$\hat{x}(t) = \frac{x(t)}{\sup_t |x(t)|} . \tag{2.2-23}$$

Where $\sup_t |x(t)| < \infty$ because $x(t)$ is bounded by hypothesis. Then $|\hat{x}(t)| \leq 1$ for all $t \in R^1$. Moreover, $|\hat{x}(t)|^2 \leq |\hat{x}(t)|$ so

$$\|\hat{x}\|_2 = \int_{-\infty}^{\infty} |\hat{x}(t)|^2 \, dt \leq \int_{-\infty}^{\infty} |\hat{x}(t)| \, dt = \|\hat{x}\|_1 < \infty. \tag{2.2-24}$$

Therefore, $\hat{x}(t) \in L^2(R^1)$ and $x(t) = (\sup_t |x(t)|)\, \hat{x}(t) \in L^2(R^1)$ because $L^2(R^1)$ is a linear space. This proves the theorem.

It should be noted that the converse of this theorem is not true because there exist functions in both $L^1(R^1)$ and $L^2(R^1)$ that are not bounded. The following theorem will be particularly useful later when finite energy signals are discussed. Its proof can be found in any text on functional analysis.

Theorem 2.8 (Schwartz Inequality) If $x(t), y(t) \in L^2(R^1)$ then

$$|\langle x,y \rangle| \leq \|x\|_2 \, \|y\|_2. \tag{2.2-25}$$

Equality holds if and only if $y(t) = \lambda x(t)$ or $y = 0$ where λ is a real constant.

2.2.3 The Interpretation of the Fourier Transform

In engineering analysis, the inverse Fourier transform, given by

$$x(t) = \int_{-\infty}^{\infty} X(f) \, e^{j2\pi ft} \, df, \tag{2.2-26}$$

is often given the interpretation that it expresses the function $x(t)$ as a continuous sum of complex exponential functions. The function $X(\cdot)$ is

Theorem 2.5 Let $x(t) \in L^2(R^1)$ and define

$$X(f,a) = \int_{-a}^{a} x(t)\, e^{-j2\pi ft}\, dt. \tag{2.2-19}$$

then as $a \to \infty$, $X(f,a)$ converges in the mean over R^1 to a function $X(f)$ in $L^2(R^1)$. Conversely,

$$x(t,a) = \int_{-a}^{a} X(f)\, e^{j2\pi ft}\, df \tag{2.2-20}$$

converges in the mean to $x(t)$ almost everywhere over R^1 as $a \to \infty$.

From this theorem it is possible to prove another.

Theorem 2.6 The Fourier transform (2.2-19) defines a bounded linear transform of $L^2(R^1)$ to $L^2(R^1)$ which is norm preserving, i.e.,

$$\|X\|_2 = \|x\|_2. \tag{2.2-21}$$

This theorem states that Fourier transform maps $L^2(R^1)$ to $L^2(R^1)$, and so it defines an isomorphism of $L^2(R^1)$ onto itself. The symmetry between any element of $L^2(R^1)$ and its Fourier transform is not an unusual property for a Hilbert space. For example, it can be shown that in a Hilbert space χ all bounded linear functionals are of the form

$$f(x) = \langle x, \phi \rangle \tag{2.2-22}$$

for all $x \in \chi$ where ϕ is also in χ (a Hilbert space is its own algebraic dual)[2].

Before discussing the appliction of Fourier transforms and convolution to the analysis of systems in section 2.3, two theorems are stated that will be useful later.

By Fubini's theorem[5,6] it follows that

$$\int_{-\infty}^{\infty}\int |x(\tau)\, y(t-\tau)|\, d\tau dt$$

$$\leq \int_{-\infty}^{\infty} |x(\tau)|\, d\tau \int_{-\infty}^{\infty} |y(t-\tau)|\, dt$$

$$= \|x\|_1 \, \|y\|_1 \, . \qquad (2.2\text{-}17)$$

Therefore, from (2.2-16) and (2.2-17) it can be seen that

$$\|x*y\|_1 \leq \|x\|_1 \, \|y\|_1 < \infty \qquad (2.2\text{-}18)$$

and so $x*y \in L^1(R^1)$. Furthermore, since $\alpha(x(\tau)\, y(t-\tau)) = (\alpha x(\tau))\, y(t-\tau)$ $= x(\tau)\, (\alpha y(t-\tau))$ for all $\alpha \in R^1$ this establishes $L^1(R^1)$ as an algebra under convolution.

Since the convolution of two functions in $L^1(R^1)$ produces another function also in $L^1(R^1)$ it immediately follows that this function is Fourier transformable. The Fourier transform of a convolution is easily found if the transforms of the two original functions are known. This is shown in the following theorem.

Theorem 2.4 Let $x(t)$, $y(t) \in L^1(R^1)$, and let $X(f)$ and $Y(f)$ be the Fourier transforms of $x(t)$ and $y(t)$. Then $x*y \in L^1(R^1)$ and its transform is $X(f)\, Y(f)$.

For the space $L^2(R^1)$, the Fourier transform is defined to be a limit as shown in the following theorem whose proof can be found in the references.[3,4]

$$\int_{-\infty}^{\infty} \hat{\theta}(f)\, df = 1. \tag{2.2-12}$$

Then the inverse Fourier transform of X(f) is $\hat{\theta}$-summable almost everywhere to x(t), i.e.,

$$\lim_{\rho \to \infty} \int_{-\infty}^{\infty} \hat{\theta}\left(\frac{f}{\rho}\right) X(f)\, e^{j2\pi ft}\, df = x(t) \text{ a.e.} \tag{2.2-13}$$

In the case where both x(t) and X(f) are in $L^1(R^1)$, equation (2.2-11) can be used immediately. This is stated in the following theorem whose proof can be found in the references.

Theorem 2.3 If x(t) and X(f) are elements of $L^1(R^1)$ then

$$\int_{-\infty}^{\infty} X(f)\, e^{j2\pi ft}\, df = x(t) \text{ a.e.} \tag{2.2-14}$$

Therefore, x(t) is equal almost everywhere to a function in $L^1(R^1)$ and $C^0(R^1)$. If x(t) is continuous on R^1, then inversion formula (2.2-11) holds for all $t \in R^1$.

The space $L^1(R^1)$ has the property that it is an algebra under the operation of convolution with respect to the complex field. In other words, if the functions x(t) and y(t) are elements of $L^1(R^1)$ then the function given by

$$(x*y)(t) = \int_{-\infty}^{\infty} x(\tau)\, y(t-\tau)\, d\tau \tag{2.2-15}$$

is in $L^1(R^1)$ and $\alpha(x*y) = (\alpha x)*y = x*(\alpha y)$ for all α R^1 . Showing $x*y$ $L^1(R^1)$ is easy by considering the integral of its magnitude, i.e.,

$$\int_{-\infty}^{\infty} |x*y|\, dt = \int_{-\infty}^{\infty} \left| \int_{-\infty}^{\infty} x(\tau)\, y(t-\tau)\, d\tau \right| dt$$

$$\leq \iint_{-\infty}^{\infty} |x(\tau)\, y(t-\tau)|\, d\tau dt. \tag{2.2-16}$$

material for system and signal analysis in electrical engineering. It is left to the reader to find the proofs in a text on Fourier analysis since there exists a number of good books on the subject. Some of them are listed in the references.[3-6]

The Fourier transform of a function is defined to be

$$X(f) = \int_{-\infty}^{\infty} x(t)\, e^{-j2\pi ft}\, dt. \tag{2.2-9}$$

The Fourier transform is known to exist for all functions in $L^1(R^1)$ and by the following theorem, X(f) is shown to be an element of the normed linear space $C^0(R^1)$. $C^0(R^1)$ is the space of continuous bounded complex functions over R^1 that has as its norm

$$\|x\|_0 = \sup_t |x(t)|. \tag{2.2-10}$$

Theorem 2.1 Let $x(t) \in L^1(R^1)$. Then the Fourier transform exists and is given by

$$X(f) = \int_{-\infty}^{\infty} x(t)\, e^{-j2\pi ft}\, dt \tag{2.2-9}$$

and X(f) is an element of $C^0(R^1)$.

The inverse Fourier transform of X(f) is defined to be

$$\hat{x}(t) = \int_{-\infty}^{\infty} X(f)\, e^{j2\pi ft}\, df \tag{2.2-11}$$

and by the following two theorems is known to exist for all X(f) that are transforms of elements of $L^1(R^1)$.

Theorem 2.2 Let $x(t) \in L^1(R^1)$. Also, let $\hat{\theta}$ be a positive even function on R^1 and monotonically decreasing on $(0,\infty)$ where

x_o in X in the sense that $\| x_n - x_o \| \to 0$ as $n \to \infty$.

Finally, $L^2(R^1)$ has the additional property of being a Hilbert space which is a Banach space that has defined on it an inner product between two elements.[1,2] An inner product is an operation that associates a complex number to each pair of elements, x and y, in the space and is denoted by $\langle f,g \rangle$. It has the following properties for all elements x, y, and z in a Hilbert space and $\alpha \in R^1$:

i) $\langle x,y \rangle = \langle y,x \rangle^*$, where * denotes complex conjugation

ii) $\langle x+y,y \rangle = \langle x,y \rangle + \langle z,y \rangle$

iii) $\langle \alpha x,y \rangle = \alpha \langle x,y \rangle$

iv) $\langle x,x \rangle > 0$ with equality holding if and only if $x \equiv \theta$.

In the space $L^2(R^1)$ the inner product can be defined as

$$\langle x,y \rangle \triangleq \int_{-\infty}^{\infty} x(t)\, y^*(t)\, dt. \qquad (2.2\text{-}7)$$

It is easy to verify that this definition does obey the four properties of the inner product listed above.

Lastly, in a Hilbert space it can be shown that $\sqrt{\langle x,x \rangle}$ defines a suitable norm in that it obeys the four properties of the norm listed earlier. In the case of $L^2(R^1)$ the norm is given by

$$\| x \|_2 \triangleq \sqrt{\langle x,x \rangle} = \left[\int_{-\infty}^{\infty} x(t)\, x^*(t)\, dt \right]^{1/2} = \left[\int_{-\infty}^{\infty} |x(t)|^2 dt \right]^{1/2}, \qquad (2.2\text{-}8)$$

which coincides with (2.2-6).

2.2.2 The Fourier Transform and Convolution

Presented in this section are theorems concerning the Fourier transform and convolution of functions that are elements of the spaces $L^1(R^1)$ and $L^2(R^1)$. Most of these theorems are part of the foundational

Both $L^1(R^1)$ and $L^2(R^1)$ are normed linear spaces. In general, a normed linear space X is a space on which exists a function which maps elements of X to R^1. This function is called the norm, is denoted by $\|x\|$ where $x \in X$, and satisfies the following axioms when x, $y \in X$ and $\alpha \in R^1$:

i) $\|x\| \geq 0$ with equality holding if and only if $x \equiv \theta$.

ii) $\|x+y\| \leq \|x\| + \|y\|$

iii) $\|\alpha x\| = |\alpha| \|x\|$.

Property (ii) is often called the triangle inequality and is used to prove the inequality

$$\|x-y\| \geq \|x\| - \|y\|. \tag{2.2-4}$$

For the spaces $L^1(R^1)$ and $L^2(R^1)$ the norms are defined to be

$$\|x\|_1 \triangleq \int_{-\infty}^{\infty} |x(t)|\, dt \quad \text{for } x(t) \in L^1(R^1) \tag{2.2-5}$$

and

$$\|x\|_2 \triangleq \left[\int_{-\infty}^{\infty} |x(t)|^2\, dt\right]^{1/2} \quad \text{for } x(t) \quad L^2(R^1). \tag{2.2-6}$$

It can be verified that these definitions do satisfy the three properties of the norm listed above.

The norm is sometimes interpreted to be a measure of an element's distance from the zero element. More generally, if x and y are two elements in a normed space, $\|x-y\|$ is a measure of the distance between them. From property (i) of the norm it is seen that $\|x-y\| = 0$ if and only if $x \equiv y$.

Both $L^1(R^1)$ and $L^2(R^1)$ are Banach spaces because they are complete.[1,2] A Banach (complete) space is a space in which every Cauchy sequence has a limit. Thus if $\{x_n\}_{n=1}^{\infty}$ is a sequence in a Banach space X and $\|x_n-x_m\| \to 0$ as $n \to \infty$, then the sequence converges to some element

In either $L^1(R^1)$ or $L^2(R^1)$, two elements (functions), f and g, are considered to be identifiable if they differ from one another on a set of measure 0. In this case, it is customary to write $f \equiv g$ or $f = g$ a.e. which means f is equal to g 'almost everywhere.' For example, consider the function

$$f(t) = \begin{cases} 2 , & t \in Z \\ \exp(-|t|) , & t \in R^1/Z. \end{cases} \tag{2.2-3}$$

Here, the function f(t) maps R^1 to C through a symetric decaying exponential except when t is an integer. Since the set of integers Z is a countable set, it has measure 0, so $f \equiv \exp(-|\cdot|)$ or $f = \exp(-|\cdot|)$ a.e.

Both $L^1(R^1)$ and $L^2(R^1)$ are linear spaces.[1,2] In general, a linear space X is a set of elements that is closed under the operations of addition and multiplication with respect to elements in a scalar field. For example, if $x, y \in X$, then $(x + y) \in X$, and if α is a scalar then $\alpha x \in X$. Additionally, the linear space X satisfies the following axioms when $x, y, z \in X$ and $\alpha, \beta \in R^1$:

i) Commutivity: $x + y = y + x$

ii) Associativity under addition $(x + y) + z = x + (y + z)$

iii) The existence of a zero element θ such that $x + \theta = x$

iv) Associativity under multiplication: $\alpha(\beta x) = (\alpha\beta)x$

v) Distribution: $\alpha(x + y) = \alpha x + \beta y$

vi) The existence of the scalar 0 and 1 such that $0x = \theta$ and $1x = x$.

It should be noted that subtraction is done using the scalar $\alpha = -1$, which in the scalar field is the additive inverse of 1. The element $-1x$ is denoted $-x$ and so $x - x = x + (-1x) = (1-1)\,x = 0x = \theta$.

also show under what condition a linear time-varying system produces a stable output. Stating this statiblity criterion allows additional properties of linear time varying system functions to be discussed which were not developed in Ziomek's original work.

Readers with a background in mathematics, electrical engineering, or acoustics will probably find that sections 2.2 and 2.3 contain no material unfamiliar to them. Those already knowledgeable in the mathematical theory of doubly-spread communication channels (in the context of scattering functions) can proceed to Chapter 3.

2.2 Mathematical Background

2.2.1 The Spaces $L^1(R^1)$ and $L^2(R^1)$

In the mathematical development of the theory presented in this thesis all functions used to represent signals will be elements of the spaces $L^1(R^1)$ and $L^2(R^1)$. The space $L^1(R^1)$ is defined to be the class of all Lebesque measurable functions that map the field of real numbers R^1 (the real line), to the field of complex numbers C (the complex plane), and are magnitude integrable. A more compact notation for this class of functions is

$$L^1(R^1) = \{f: R^1 \to C \mid \int_{-\infty}^{\infty} |f(t)|\, dt < \infty\}. \qquad (2.2\text{-}1)$$

Similarly, the space $L^2(R^1)$ is defined to be the class of all Lebesque measurable complex functions that map R^1 to C and are square integrable. Again, a more compact notation for this class of functions is

$$L^2(R^1) = \{f: R^1 \to C \mid \left[\int_{-\infty}^{\infty} |f(t)|^2\, dt\right]^{1/2} < \infty\}. \qquad (2.2\text{-}2)$$

CHAPTER 2

TIME-VARYING SYSTEM THEORY

2.1 Introduction

The primary objective of this chapter is to introduce the mathematical fundamentals that will be used throughout this thesis. Section 2.2.1 presents a brief review of the properties of linear spaces. In particular, the spaces $L^1(R^1)$ and $L^2(R^1)$ will be discussed since their elements are functions that will be used to model signals. In section 2.2.2 the Fourier transform is introduced and several theorems are stated concerning the Fourier transforms of functions in $L^1(R^1)$ and $L^2(R^1)$. Section 2.3 presents a review of linear system theory for both time-varying and time-invariant systems. The chapter first presents the output of a deterministic linear time-invariant system as a convolution integral between the input waveform and the system impulse response function. This is then extended to find the output of a deterministic linear time-varying system which is described by a time-varying impulse response function. Finally, Section 2.4 describes four autocorrelation functions for time-varying systems for both deterministic and random cases. For random linear time-varying systems it is shown that the autocorrelation functions lead to the definition of the scattering function provided the system is used to model a wide sense stationary uncorrelated channel (WSSUS).

It should be mentioned that the derivation of the scattering function as developed from random linear time-varying system theory was originally done by Ziomek[10] in his Ph.D. dissertation. What has been done in this chapter is to not only present the same derivation but to

Finally, Chapter 4 introduces an iteration algorithm to optimize the expected matched filter receiver response to a signal transmitted through a channel having a known scattering function. The algorithm is derived using the calculus of variations and generates a series of processing signals which in turn produces a convergent monotonically increasing series of expected matched filter outputs. The chapter closes with several numerical examples of the optimization technique.

known. The optimization is accomplished by iteratively altering the processing signal of the matched filter given a fixed transmit signal and channel scattering function. Since the performance of a receiver is determined by the signal to noise ratio (SNR) of its output (in this case defined as the ratio of the receiver signal response to white Gaussian noise and clutter or reverberation response), increasing the receiver response to the channel output without significantly increasing the response to the interference will increase the SNR and imply an improved ability of the receiver to detect the channel output signal. If the only interfering signal is white Gaussian noise, then increasing the receiver signal response guarantees an increase in SNR.

It is important, however, to present the fundamental theory used to establish the properties of the communication channel and performance of the receiver. Therefore, Chapter 2 opens with a review for the properties of linear spaces and Fourier analysis. The remainder of the chapter presents the development of linear time-varying system theory for both the deterministic and stochastic cases. This eventually leads to the derivation of the scattering function which can be used to describe the time delay and frequency spreading characteristics of the communication channel.

Chapter 3 introduces the theory of matched filter receivers and shows their use in hypothesis testing for signal detection. The relationship between scattering function and receiver output is developed. This is used in the closing section of the chapter to show the conditions necessary for the matched filter to optimally detect a signal that has been transmitted through a channel whose scattering function is known.

$$y_i(t) \simeq h(\tau_i)\, x(t-\tau_i)\, \Delta\tau \,. \tag{2.3-2}$$

It follows that as $\Delta\tau$ becomes smaller the approximation of $y_i(t)$ by (2.3-2) becomes more accurate. Thus in the limit

$$y_i(t) = \lim_{\Delta\tau \to 0} h(\tau_i)\, x(t-\tau_i)\, \Delta\tau \,. \tag{2.3-3}$$

The desired system response, however, is the sum of all the responses to the approximating pulse train, so

$$y(t) \simeq \sum_i y_i(t) = \sum_i h(\tau_i)\, x(t-\tau_i)\, \Delta\tau \,. \tag{2.3-4}$$

Again, as $\Delta\tau$ becomes small it follows that the approximation of $y(t)$ by (2.3-4) becomes more accurate. Furthermore, the summation becomes an integral leading to (2.3-1).

It should be noted that from (2.3-1) it immediately follows that $h(t)$ is the system response to an impulse of unity weight, i.e.,

$$y(t) = \int_{-\infty}^{\infty} h(\tau)\, \delta(t-\tau)\, d\tau = h(t). \tag{2.3-5}$$

As mentioned earlier, (2.3-1) describes a system whose behavior is invariant with respect to time. A clearer statement of this can be made if one considers the response of the system to an impulse applied at some time $t_o \neq 0$ ($x(t) = \delta(t-t_o)$). Using (2.3-1), the system response is

$$y(t) = \int_{-\infty}^{\infty} h(\tau)\, \delta(t-t_o-\tau)\, d\tau = h(t-t_o), \tag{2.3-6}$$

which is just the system impulse response shifted forward in time an amount t_o. Outside of the fact that the response exhibits a time shift, it has the same form as the function $h(t)$. Therefore, the properties of the system remain the same regardless of when the input is applied.

In the real world, however, communication channels are never blessed with the property of time-invariance. Their responses change over a period of time depending on what mechanisms carry the signals in their respective mediums.

To account for the time-varying property of a linear system, the convolution integral determining the response can be rewritten as

$$y(t) = \int_{-\infty}^{\infty} h(\tau,t)\, x(t-\tau)\, d\tau \,, \tag{2.3-7}$$

where $h(\tau,t)$ describes the system response at time t to an impulse of unity weight applied at time $t - \tau$. In this case τ can be thought of as the variable that describes the 'antiquity' or 'age' of the impulse input.[9] By defining the impulse response in this way, it will be shown later that a symmetry will exist between $h(\tau,t)$ and its Fourier transform with respect to τ.

One restriction that will be placed on the system described by $h(\tau,t)$ is that every bounded input will produce a bounded response. Such systems are referred to as 'bounded input, bounded output' systems (BIBO). The conditions for a system to be a BIBO system are stated in terms of the impulse response and are given in the following theorem.

Theorem 2.9 Let a time-varying system be described by the impulse response $h(\tau,t)$. Then the system is a BIBO system if and only if

$$\int_{-\infty}^{\infty} |h(\tau,t)|\, d\tau < \infty \tag{2.3-8}$$

for all $t \in R^1$.

Proof. Proving the theorem in the reverse direction is easy. Suppose the system input $x(t)$ is bounded, i.e.,

$$|x(t)| \leq M \quad \text{for} \quad t \tag{2.3.9}$$

then for any t

$$|y(t)| = \left| \int_{-\infty}^{\infty} h(\tau,t)\, x(t-\tau)\, d\tau \right|$$

$$\leq \int_{-\infty}^{\infty} |h(\tau,t)|\, |x(t-\tau)|\, d\tau$$

$$\leq M \int_{-\infty}^{\infty} |h(\tau,t)|\, d\tau < \infty . \tag{2.3-10}$$

Hence, any bounded input produces a bounded output.

Proving the theorem in the forward direction is done by contradiction. Suppose, a system is a BIBO system but its impulse response does not satisfy (2.3-8). This can be stated as

$$\sup_t \int_{-\infty}^{\infty} |h(\tau,t)|\, d\tau = \infty . \tag{2.3-11}$$

Therefore, for any $M > 0$, there exists a t_M such that

$$\int_{-\infty}^{\infty} |h(\tau,t_M)|\, d\tau > M . \tag{2.3-12}$$

Now define the bounded input function

$$x_M(t) = \text{sgn}[h(t_M - t, t_M)] \tag{2.3-13}$$

which is equal to the sign of the system response at time t_M to an impulse of unity weight applied to the system input at time t. The response to $x_M(t)$ at time t_M is

$$y(t_M) = \int_{-\infty}^{\infty} h(\tau,t_M)\, \text{sgn}[h(t_M - t_M + \tau, t_M)]\, d\tau$$

$$= \int_{-\infty}^{\infty} |h(\tau,t_M)|\, d\tau > M \tag{2.3-14}$$

Therefore, given any $M > 0$, however large, we can construct a bounded

input which will produce an output that at some time is larger than M. This contradicts the hypothesis that the system is a BIBO system, and so the theorem is proved.

For linear time-invariant systems $h(\tau,t)$ reduces to $h(\tau)$ and by (2.3-8)

$$\|h\|_1 = \int_{-\infty}^{\infty} |h(\tau)|\, d\tau < \infty . \tag{2.3-15}$$

Thus, $h(\tau)$ is an element of $L^1(R^1)$ which proves the following corollary:

Corollary 2.10 Let a time-invariant system be described by the impulse response $h(t)$. Then the system is a BIBO sytem if and only if $h(t)$ is an element of $L^1(R^1)$.

It is now possible to solve for the response of a time-varying system using Fourier analysis. Since the input $x(t)$ is assumed to be an element of $L^1(R^1)$ and $L^2(R^1)$, its Fourier transform exists because the transform exists for all functions in either space. Therefore, using (2.2-11) and (2.3-7),

$$y(t) = \int_{-\infty}^{\infty} h(\tau,t)\, x(t-\tau)\, d\tau = \int_{-\infty}^{\infty} h(\tau,t) \left[\int_{-\infty}^{\infty} X(f)\, e^{j2\pi f(t-\tau)}\, df \right] d\tau$$

$$= \int_{-\infty}^{\infty} \left[\int_{-\infty}^{\infty} h(\tau,t)\, e^{-j2\pi f\tau}\, d\tau \right] X(f)\, e^{j2\pi ft}\, df. \tag{2.3-16}$$

Notice that the bracketed term in the integrand of (2.3-16) is of the same form as a Fourier transform of a function of a single variable. It is, in fact, the Fourier transform of $h(\tau,t)$ with respect to τ if one is allowed to define the transform of a multivariable function with respect to a single variable. Here, the bracketed term will be defined as

$$H(f,t) \triangleq \int_{-\infty}^{\infty} h(\tau,t)\, e^{-j2\pi f\tau}\, d\tau\ . \tag{2.3-17}$$

Furthermore, H(f,t) exists and is bounded because by (2.3-8)

$$\begin{aligned} |H(f,t)| &= \left| \int_{-\infty}^{\infty} h(\tau,t)\, e^{-j2\pi f\tau}\, d\tau \right| \\ &\leq \int_{-\infty}^{\infty} |h(\tau,t)|\, d\tau < \infty\ . \end{aligned} \tag{2.3-18}$$

Now (2.3-16) can be rewritten as

$$y(t) = \int_{-\infty}^{\infty} h(\tau,t)\, x(\tau-t)\, d\tau = \int_{-\infty}^{\infty} H(f,t)\, X(f)\, e^{j2\pi ft}\, df. \tag{2.3-19}$$

It appears that the system response is the inverse Fourier transform of the function H(f,t) X(f). This is not, in fact, true, because the Fourier transform of the response y(t) regardless of whether the system is time-varying or time-invariant is

$$Y(f) = \int_{-\infty}^{\infty} y(t)\, e^{-j2\pi ft}\, dt \tag{2.3-20}$$

which is not a function of both f and t. The only time Y(f) = H(f,t) X(f) is when the system is time-invariant. In this case, $h(\tau,t) \to h(\tau)$ which means $H(f,t) \to H(f)$, so (2.3-19) reduces to

$$y(t) = \int_{-\infty}^{\infty} h(\tau)\, x(\tau-t)\, d\tau = \int_{-\infty}^{\infty} H(f)\, X(f)\, e^{j2\pi ft}\, df. \tag{2.3-21}$$

This also follows from Theorem 2.4 which states that the convolution of two functions is equal to the inverse Fourier transform of the product of the Fourier transforms of the two functions. Because y(t) is given by

$$y(t) = \int_{-\infty}^{\infty} Y(f)\, e^{j2\pi ft}\, df, \tag{2.3-22}$$

and because of the uniqueness of the Fourier transform, Y(f) = H(f) X(f).

It must be stressed, however, this is only guaranteed for time-invariant systems.

The function H(f,t) can be interpreted to be the modulation of a single frequency (monochromatic) signal applied to the system. This can be seen by finding the response to the signal $x(t) = e^{j2\pi f_o t}$. From (2.3-7) and (2.3-17),

$$y(t) = \int_{-\infty}^{\infty} h(\tau,t)\, e^{j2\pi f_o(t-\tau)}\, d\tau$$

$$= \left[\int_{-\infty}^{\infty} h(\tau,t)\, e^{-j2\pi f_o \tau}\, d\tau\right] e^{j2\pi f_o t}$$

$$= H(f_o,t)\, e^{j2\pi f_o t} . \qquad (2.3\text{-}23)$$

If $H(f_o,t)$ changes with respect to t (time), it follows that the amplitude of the input signal is modulated. Since H(f,t) can be used directly to find the response to a monochromatic signal, it is often referred to as the time-varying transfer function or the time-varying spectrum of the system impulse response.

2.3.2 The Space $L^1(R^2)$ and the Time-Varying System Functions

It was shown in the last section that if the time-varying system impulse response $h(\tau,t)$ has the property

$$\int_{-\infty}^{\infty} |h(\tau,t)|\, d\tau < \infty \quad \text{for all } t \in R^1 \qquad (2.3\text{-}8)$$

then it describes a BIBO system and the time-varying transfer function is defined as

$$H(f,t) \triangleq \int_{-\infty}^{\infty} h(\tau,t)\, e^{-j2\pi f\tau}\, d\tau . \qquad (2.3\text{-}17)$$

A question that naturally arises is: Can the Fourier transform of $h(\tau,t)$ with respect to t be found and what is its interpretation? Also, is it

possible to find the two-dimensional Fourier transform of $h(\tau,t)$? An affirmative answer to these questions requires an additional restriction on $h(\tau,t)$.

It will be assumed that the time-varying impulse response $h(\tau,t)$ is an element of the normed linear space $L^1(R^2)$. The space $L^1(R^2)$ is the class of all Lebeque measurable functions that map the set of real ordered pairs R^2 to the complex field C, and are magnitude integrable, i.e.,

$$L^1(R^2) = \{x: R^2 \to C \mid \int_{-\infty}^{\infty}\int |x(\tau,t)|\, d\tau dt < \infty\} . \tag{2.3-24}$$

The norm of any element $x(t)$ in $L^1(R^2)$ is defined as

$$\|x\|_1 = \int_{-\infty}^{\infty}\int |x(\tau,t)|\, d\tau dt . \tag{2.3-25}$$

The two-dimensional Fourier transform of any element $x(t)$ in $L^1(R^2)$ is given by

$$X(f,\phi) = \int_{-\infty}^{\infty}\int x(\tau,t)\, e^{-j2\pi(f\tau+\phi t)}\, d\tau dt \tag{2.3-26}$$

and is bounded because

$$|X(f,\phi)| = \left|\int_{-\infty}^{\infty}\int x(\tau,t)\, e^{-j2\pi(f\tau+\phi t)}\, d\tau dt\right|$$

$$\leq \int_{-\infty}^{\infty}\int |x(\tau,t)|\, d\tau dt = \|x\|_1 < \infty . \tag{2.3-27}$$

An interesting and useful property of the space $L^1(R^2)$ is that if $h(\tau,t)$ is an element of $L^1(R^2)$ then

$$\int_{-\infty}^{\infty} |h(\tau,t)|\, d\tau < \infty \quad \text{and} \quad \int_{-\infty}^{\infty} |h(\tau,t)|\, dt < \infty . \tag{2.3-28}$$

This property arises from Fubini's reduction theorem for double

integrals[1], and it should be noted that its converse is not true. A consequence of this property is that it is possible to find the one-dimensional Fourier transform of $h(\tau,t)$ with respect to either τ or t.

The Fourier transform of $h(\tau,t)$ with respect to t exists, is given by

$$S(\tau,\phi) \triangleq \int_{-\infty}^{\infty} h(\tau,t)\, e^{-j2\pi\phi t}\, dt \tag{2.3-29}$$

and is bounded for all τ and ϕ because by (2.3-8) it is easily seen that

$$\begin{aligned} |S(\tau,\phi)| &= \left| \int_{-\infty}^{\infty} h(\tau,t)\, e^{-j2\pi\phi t}\, dt \right| \\ &\leq \int_{-\infty}^{\infty} |h(\tau,t)|\, dt < \infty . \end{aligned} \tag{2.3-30}$$

The function $S(\tau,\phi)$ is referred to as the spreading function[10] and can be interpreted as a measure of the system time variation. It follows that if $S(\tau,\phi)$ is significantly large over a wide range of ϕ, then the system is rapidly time varying. Otherwise, if $S(\tau,\phi)$ is significant only over a small range of ϕ centered around $\phi = 0$, then the system changes slowly with time.

Another description of a time-varying system can be given by finding the Fourier transform of the time-varying transfer function $H(f,t)$ with respect to t, i.e.,

$$B(f,\phi) \triangleq \int_{-\infty}^{\infty} H(f,t)\, e^{-j2\pi\phi t}\, dt . \tag{2.3-31}$$

This is also equivalent to finding the two-dimensional Fourier transform of $h(\tau,t)$, because if $H(f,t)$ is replaced by (2.3-17) then

$$B(f,\phi) = \iint_{-\infty}^{\infty} h(\tau,t)\, e^{-j2\pi(f\tau+\phi t)}\, d\tau dt . \tag{2.3-32}$$

Furthermore, $B(f,\phi)$ is bounded because

$$|B(f,\phi)| = \left| \int_{-\infty}^{\infty}\int h(\tau,t)\, e^{-j2\pi(f\tau+\phi t)}\, d\tau dt \right|$$

$$\leq \int_{-\infty}^{\infty}\int |h(\tau,t)|\, d\tau dt < \infty . \qquad (2.3\text{-}33)$$

The function $B(f,\phi)$ is referred to as the bi-frequency function[10] and can be interpreted as a measure of the amount of modulation the system output exhibits when the input is a monochromatic signal. For example, in section 2.3.1 it was shown that if the system input is $e^{j2\pi f_o t}$ then the output is

$$y(t) = H(f_o,t)\, e^{j2\pi f_o t} . \qquad (2.3\text{-}34)$$

Therefore, $H(f_o t)$, the system transfer function evaluated at f_o, is the modulation function of the output signal. The Fourier transform of the modulation signal with respect to t is then

$$\int_{-\infty}^{\infty} H(f_o,t)\, e^{-j2\pi\phi t}\, dt = B(f_o,\phi) \qquad (2.3\text{-}35)$$

which is just the bi-frequency function evaluated at f_o with ϕ left as a free parameter. At this point the interpretation of the bi-frequency function is clear. If the modulation of output signal changes rapidly with time, then $B(f_o,\phi)$ is significant over a wide range of ϕ. On the other hand, if the modulation changes slowly with time as a result of the system varying slowly with time, then $B(f_o,\phi)$ is significant for a small range of ϕ centered about $\phi = 0$.

The bi-frequency function can also be found by determining the one-dimensional Fourier transform of $S(\tau,\phi)$ with respect to τ. This can be seen by finding the Fourier transform of (2.3-29)

$$\int_{-\infty}^{\infty} S(\tau,\phi)\, e^{-j2\pi f\tau}\, d\tau$$

$$= \int_{-\infty}^{\infty} \left[\int_{-\infty}^{\infty} h(\tau,t)\, e^{-j2\pi\phi t}\, dt\right] e^{-j2\pi f\tau}\, d\tau$$

$$\iint_{-\infty}^{\infty} h(\tau,t)\, e^{-j2\pi(f\tau+\phi t)}\, d\tau dt \qquad (2.3\text{-}36)$$

which is the same as (2.3-32).

Figure 3 shows the relationship among the four time-varying system functions. Each function can be used to characterize the system because if any one of the functions is known then it is only a matter of Fourier transforming (or inverse Fourier transforming) with respect to the correct variables to find any of the remaining three system functions.

The bi-frequency function can be used to find the Fourier transform of the output signal y(t). From (2.3-19), (2.3-31), and the definition of the Fourier transform,

$$Y(\eta) = \int_{-\infty}^{\infty} y(t)\, e^{-j2\pi\eta t}\, dt$$

$$= \iint_{-\infty}^{\infty} X(f)\, H(f,t)\, e^{-j2\pi(\eta-f)t}\, df dt$$

$$= \int_{-\infty}^{\infty} X(f) \left[\int_{-\infty}^{\infty} H(f,t)\, e^{-j2\pi(\eta-f)t}\, dt\right] df$$

$$= \int_{-\infty}^{\infty} X(f)\, B(f,\eta-f)\, df \qquad (2.3\text{-}37)$$

Thus $Y(\eta)$ can be found by convolving $X(f)$, the Fourier transform of the input $x(t)$, with the function $B(f,\eta-f)$. The function $B(f,\eta-f)$ is the projection of $B(f,\phi)$ on the line $\phi = \eta-f$ to the line $\phi = 0$. This is shown in Figure 4.

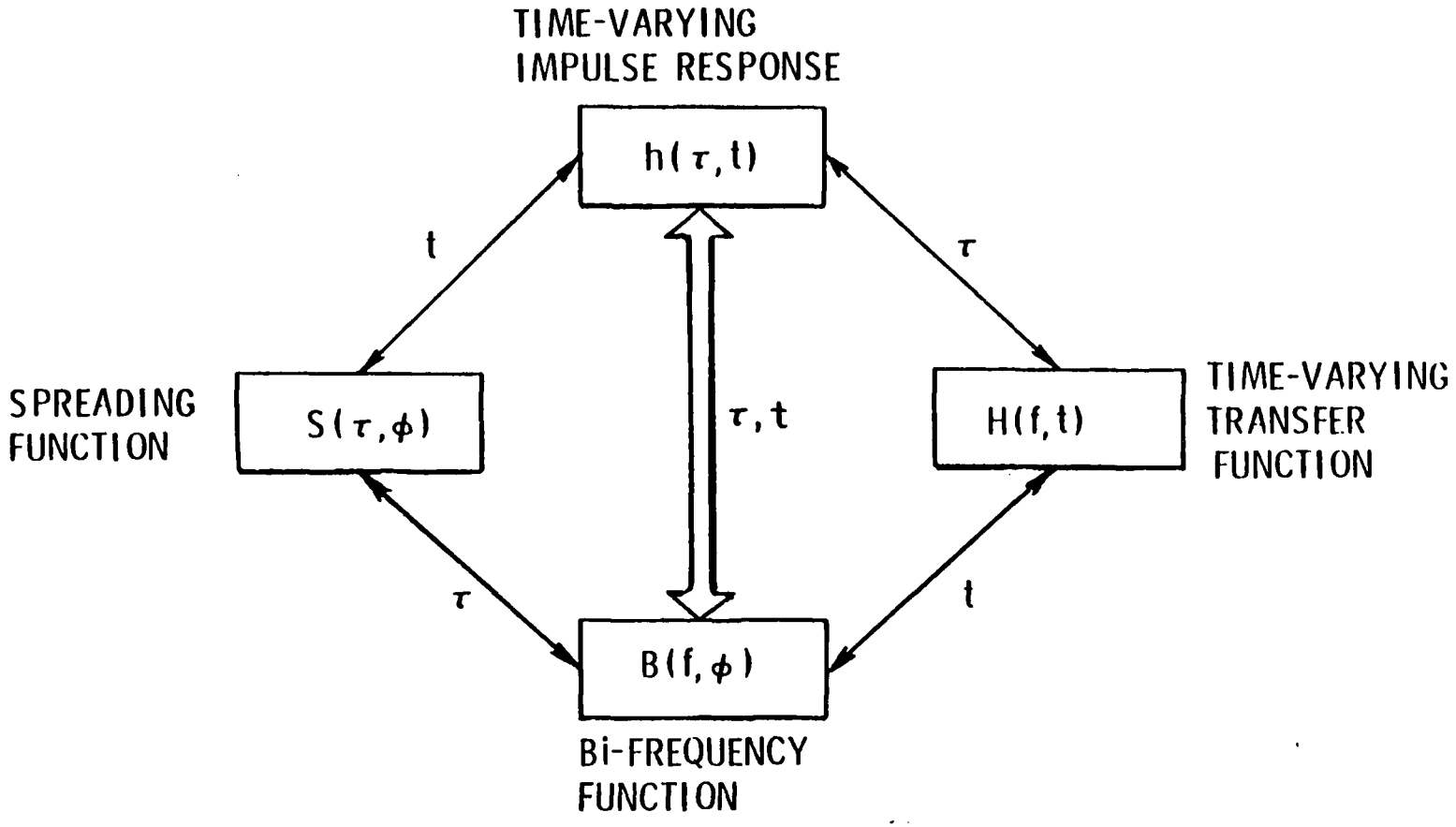

Figure 3. The relationship between the four time-varying system functions. Each arrow is labeled with its respective forward Fourier transformation variable.

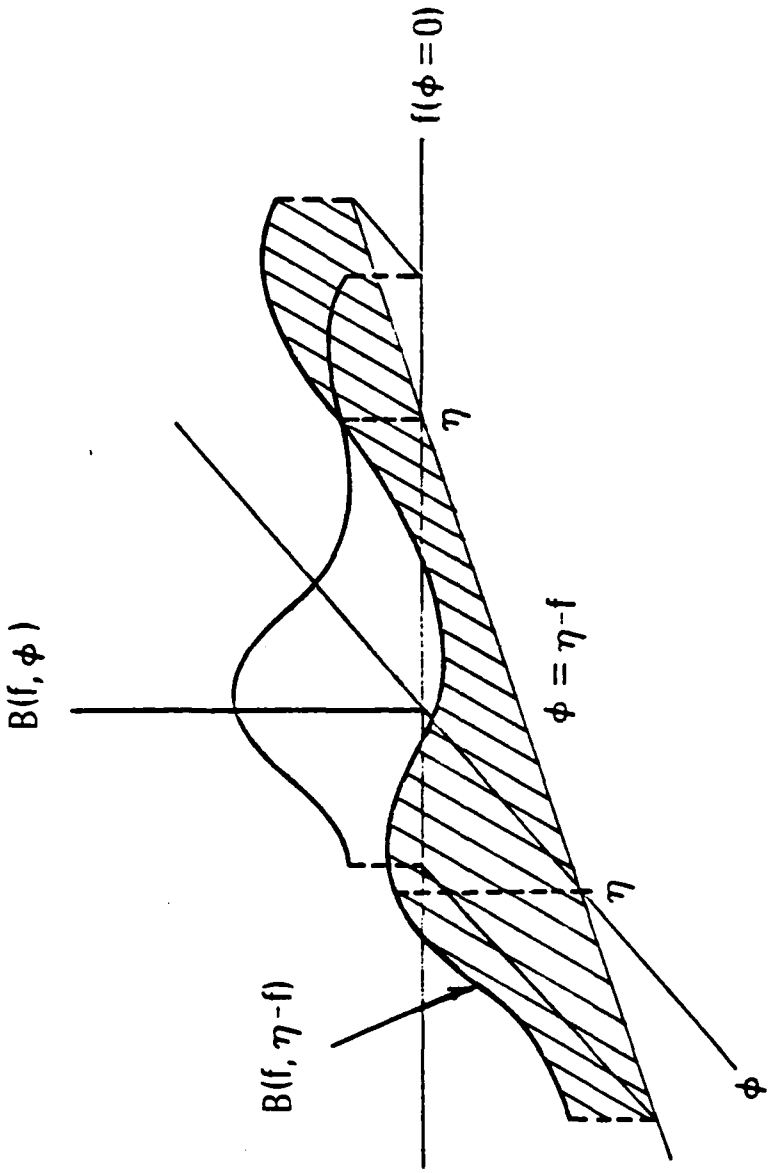

Figure 4. The function B(f,φ-f) and its projection into the line $\phi = 0$.

2.4 Random Time-Varying System Theory

2.4.1 System Autocorrelation Functions

To this point the time-varying system described by the time-varying impulse response $h(\tau,t)$ has been deterministic. In other words, $h(\tau,t)$ is known precisely for all τ and t. For real world systems this is never the case, so the behavior of $h(\tau,t)$ and the three other time-varying system functions must be described by their statistical properties. This is done by considering the autocorrelation functions of all the time-varying system functions. They are

$$R_h(\tau,\tau',t,t') = E\{h(\tau,t)\ h^*(\tau',t')\} \tag{2.4-1}$$

$$R_H(f,f',t,t') = E\{H(f,t)\ H^*(f',t')\} \tag{2.4-2}$$

$$R_S(\tau,\tau',\nu,\nu') = E\{S(\tau,\nu)\ S^*(\tau',\nu')\} \tag{2.4-3}$$

$$R_B(f,f',\phi,\phi') = E\{B(f,\phi)\ B^*(f',\phi')\} \tag{2.4-4}$$

Ziomek[10] has shown that with the correct interpretation the four time-varying filter functions are related through two-dimensional Fourier transforms. For example, consider the spreading function autocorrelation function which by (2.3-29) and (2.4-3) is

$$\begin{aligned} R_S(\tau,\tau',\nu,\nu) &= E\{\int_{-\infty}^{\infty} h(\tau,t)\ e^{-j2\pi\nu t}\ dt \int_{-\infty}^{\infty} h^*(\tau',t')\ e^{j2\pi\nu' t'}\ dt'\} \\ &= E\{\iint_{-\infty}^{\infty} h(\tau,t)\ h^*(\tau',t')\ e^{-j2\pi(\nu t-\nu' t')}\ dtdt'\} \end{aligned} \tag{2.4-5}$$

Because the expectation operator and integration are linear operations, (2.4-5) can be rewritten as

$$\begin{aligned} R_S(\tau,\tau',\nu,\nu') &= \iint_{-\infty}^{\infty} E\{h(\tau,t)\ h^*(\tau',t')\}\ e^{-j2\pi(\nu t-\nu' t')}\ dtdt' \\ &= \iint_{-\infty}^{\infty} R_h(\tau,\tau',t,t')\ e^{-j2\pi(\nu t-\nu' t')}\ dtdt'. \end{aligned} \tag{2.4-6}$$

Note that (2.4-6) does not express $R_S(\epsilon,\tau',\phi,\phi')$ as a two-dimensional Fourier transform of $R_h(\tau,\tau',t,t')$, even though it has a similar form. This is because the two-dimensional Fourier transform of $R_h(\tau,\tau',t,t')$ is actually given by

$$\int_{-\infty}^{\infty}\int R_h(\tau,\tau',t,t')\, e^{-j2\pi(\phi t+\phi' t')}\, dtdt'. \tag{2.4-7}$$

The difference between (2.4-6) and (2.4-7) can be seen in the argument of the exponential function in the integrand.

The discrepancy can be cleared up redefining the Fourier transform with respect to τ' and t' as

$$\int_{-\infty}^{\infty} h(\tau',t')\, e^{j2\pi f'\tau'}\, d\tau' , \tag{2.4-8}$$

$$\int_{-\infty}^{\infty} h(\tau',t')\, e^{j2\pi\phi' t'}\, dt' . \tag{2.4-9}$$

Thus, by using (2.4-9), (2.4-6) is the two-dimensional Fourier transform of $R_h(\tau,\tau',t,t')$ which can be written as

$$R_h(\tau,\tau',t,t') \underset{t,t'}{\Longleftrightarrow} R_S(\tau,\tau',\phi,\phi'). \tag{2.4-10}$$

Similarly, using (2.4-8) and (2.4-9) the relationships between all the system autocorrelation functions are

$$R_h(\tau,\tau',t,t') \underset{\tau,\tau'}{\Longleftrightarrow} R_H(f,f',t,t') \tag{2.4-11}$$

$$R_h(\tau,\tau',t,t') \underset{\tau,\tau',t,t'}{\Longleftrightarrow} R_B(f,f',\phi,\phi') \tag{2.4-12}$$

$$R_S(\tau,\tau',\phi,\phi') \underset{\tau,\tau'}{\Longleftrightarrow} R_B(f,f',\phi,\phi') \tag{2.4-13}$$

$$R_H(f,f',t,t') \underset{t,t'}{\Longleftrightarrow} R_B(f,f',\phi,\phi'). \tag{2.4-14}$$

Figure 5 illustrates the relationships among all four autocorrelation functions.

where C_T is the radial speed referenced away from the scatterer and C is propagation speed of the medium. It can be shown that the Fourier transform of (3.2-11) is given by

$$Y(f) = \frac{b}{|s|} X(\frac{f}{s}) e^{j2\pi f\tau}. \qquad (3.2\text{-}14)$$

The effect the doppler variable has on the spectrum of the input signal is illustrated in Figure 8. For a scatterer traveling away from the receiver, the doppler variable is less than one, causing the spectrum to move toward lower values of f. This occurs because the point scatterer is traveling with the expanding wavefront of the transmitted signal, so it is irradiated by the wavefront for a period of time longer than the duration of the signal. This causes the reflected signal to be a time stretched version of the transmit signal changing slower in time and consequently composed of exponential signals of lower frequency. A similar analysis holds when the point scatterer moves toward the receiver. In this case the scatterer is irradiated by the expanding transmitted wavefront for a period of time less than the transmit signal time duration. Consequently, the signal is compressed in time, changes more rapidly than the transmit signal and so is composed of higher frequency exponential signals. This is also seen from Figure 8, where the doppler variable is greater than one causing the spectrum to shift to higher values of f.

Another phenomenon induced by the doppler variable s is a change in bandwidth for bandpass transmit signals. If the spectrum of the transmit signal is significant only in the interval (f_1,f_2) then the spectrum of the received signal is significant in the interval (sf_1,sf_2). This occurs because the spectrum of the transmit signal is either stretched or

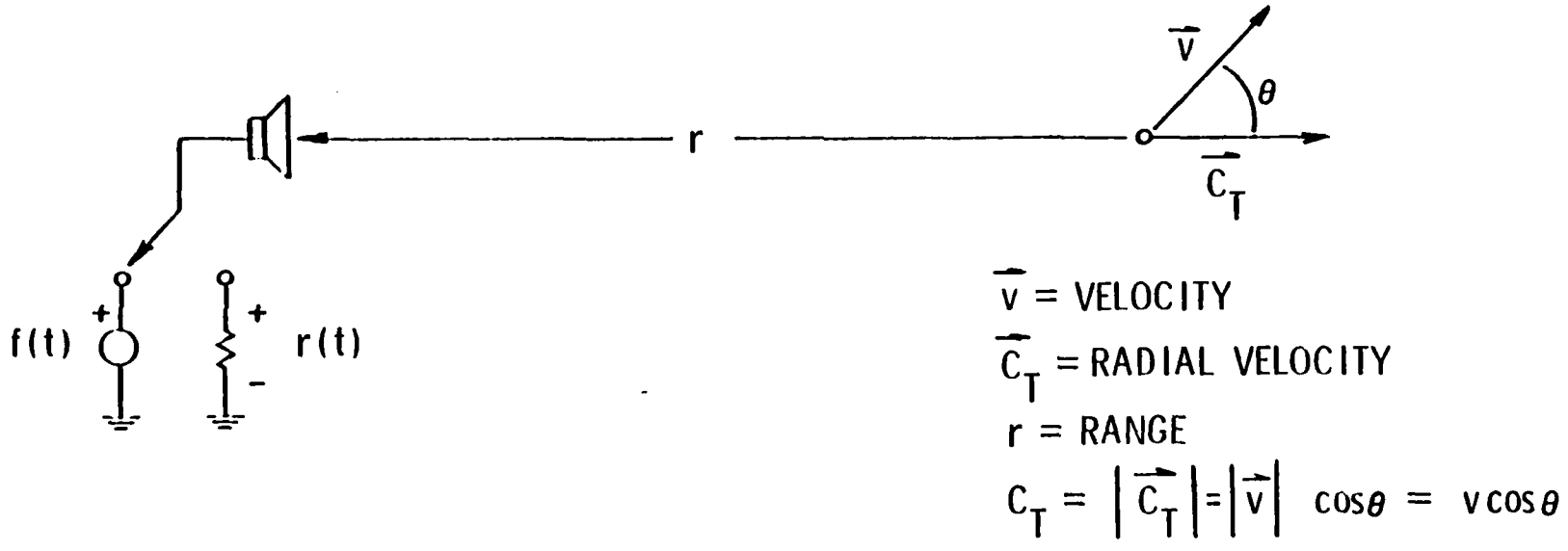

Figure 7. The geometry of a monostatic detection system with a point scatterer.

constant b in (3.2-9) is not a random variable. In either the random or deterministic case the idea is the same; if spreading or scattering occurs at only one τ and ϕ then the system output is a scaled time and frequency shifted replica of the input signal. The time shift $\hat{\tau}$ is evident by examining the argument of (3.2-5) and (3.2-9). Finding the Fourier transform of (3.2-5) or (3.2-9) gives the spectrum of the channel output signal as

$$Y(f) = b\, X(f-\hat{\phi})\, e^{j2\pi f\hat{\tau}} \tag{3.2-10}$$

where X(f) is the spectrum of the transmit signal. Examination of the right side of (3.2-10) shows the frequency shifting of the transmit signal spectrum by the amount $\hat{\phi}$.

The reflection from a point scatterer that has a given range and velocity can, under certain conditions, be modeled by a random linear time-varying system whose output is a scaled version of its input having a specific time shift $\hat{\tau}$ and frequency shift $\hat{\phi}$. This is why the scattering function described by (3.2-1) was considered. A more accurate modeling of the point scatterer reflection can be found by considering Figure 7 where the geometry of a monostatic signal detection system is shown. Here the reflection of the transmit signal is given by

$$y(t) = b\, x(s(t-\tau)) \tag{3.2-11}$$

where τ is the range delay, s is the doppler variable, and b is a random variable. Applying simple physics to the geometry it can be shown that[14,15]

$$\tau = \frac{2r}{C_T} \tag{3.2-12}$$

$$s = \frac{1 - C_T/C}{1 + C_T/C} \tag{3.2-13}$$

$$R_y(t,t') = E\{\left[b\ x(t-\hat{\tau})\ e^{j2\pi\hat{\phi}t}\right]\ \left[b\ x(t'-\hat{\tau})\ e^{j2\pi\hat{\phi}t'}\right]^*\}. \qquad (3.2\text{-}4)$$

Thus the system output can be interpreted as

$$y(t) = b\ x(t-\hat{\tau})\ e^{j2\pi\hat{\phi}t}. \qquad (3.2\text{-}5)$$

Time-varying systems whose outputs are of the form of (3.2-5) are used to model a non-dispersive communication channel.[11,12]

A similar result can be derived by considering a time-varying system for which the spreading function $S(\tau,\phi)$ is known. It was shown in section 2.3.1 that the system output is given by

$$y(t) = \int_{-\infty}^{\infty} h(\tau,t)\ x(t-\tau)\ d\tau. \qquad (2.3\text{-}7)$$

Also, from section 2.3.2 the time-varying impulse response is related to the spreading function by

$$h(\tau,t) = \int_{-\infty}^{\infty} S(\tau,\phi)\ e^{j2\pi\phi t}\ d\phi. \qquad (3.2\text{-}6)$$

Combining (2.3-7) and (3.2-6) gives the output as

$$y(t) = \int\int_{-\infty}^{\infty} S(\tau,\phi)\ x(t-\tau)\ e^{j2\pi\phi t}\ d\phi d\tau. \qquad (3.2\text{-}7)$$

If the spreading function is of the form

$$S(\tau,\phi) = b\ \delta(\tau-\hat{\tau})\ \delta(\phi-\hat{\phi}) \qquad (3.2\text{-}8)$$

then the system output is

$$\begin{aligned} y(t) &= \int\int_{-\infty}^{\infty} b\ \delta(\tau-\hat{\tau})\ \delta(\phi-\hat{\phi})\ x(t-\tau)\ e^{j2\pi\phi t}\ d\phi d\tau \\ &= b \int_{-\infty}^{\infty} \delta(\phi-\hat{\phi})\ x(t-\hat{\tau})\ e^{j2\pi\phi t}\ d\phi \\ &= b\ x(t-\hat{\tau})\ e^{j2\pi\hat{\phi}t}. \end{aligned} \qquad (3.2\text{-}9)$$

Notice that (3.2-5) and (3.2-9) are of the same form except that the

Finally, in section 3.3 it is shown that the expected matched filter receiver output is maximized for a given communication channel if the cross-ambiguity function and the channel scattering function are in constant proportion.

3.2 Signal Detection

3.2.1 Propagation Modeling

Consider a linear random time-varying system which models a WSSUS channel and has a scattering function of the form

$$R_S(\tau,\phi) = K\ \delta(\tau-\tau)\ \delta(\phi-\phi)\ . \tag{3.2-1}$$

In section 2.4.2, the scattering function was interpreted as a density function which determines the amount of delay τ and frequency shift ϕ an input signal will exhibit at the output of the system. If the scattering function has the same form as (3.2-1), then it implies that the system output will be a replica of the input having time shift $\hat{\tau}$ and frequency shift $\hat{\phi}$. This can also be implied by determining the system output correlation using (2.4-33) and (3.2-1), i.e.,

$$\begin{aligned} R_y(t,t') &= K \int_{-\infty}^{\infty}\int x(t-\tau)\ \delta(\tau-\hat{\tau})\ \delta(\phi-\hat{\phi})\ x^*(t'-\tau)\ e^{j2\pi\phi(\Delta t)}\ d\tau d\phi \\ &= K \int_{-\infty}^{\infty} x(t-\hat{\tau})\ \delta(\phi-\hat{\phi})\ x^*(t'-\hat{\tau})\ e^{j2\pi\phi(\Delta t)}\ d\phi \\ &= K\ x(t-\hat{\tau})\ x^*(t'-\hat{\tau})\ e^{j2\pi\hat{\phi}(\Delta t)} \\ &= K \left[x(t-\hat{\tau})\ e^{j2\pi\hat{\phi}t}\right]\ \left[x(t'-\hat{\tau})\ e^{j2\pi\hat{\phi}t'}\right]^*. \end{aligned} \tag{3.2-2}$$

Defining the constant K as

$$K = E\{|b|^2\} = E\{b\ b^*\} \tag{3.2-3}$$

then (3.2-2) can be rewritten as

CHAPTER 3

MATCHED FILTERING IN SIGNAL DETECTION

3.1 Introduction

In this chapter, the detection of a signal that has been transmitted through a communication channel whose scattering properties are known is developed. Detection will be performed by examining the output of a matched filter receiver. In this receiver structure, the channel output signal is multiplied by a processing signal, the product integrated, and the square of the magnitude of the integrator output is used as the receiver output. If the receiver output exceeds a predetermined threshold, then it is assumed that a portion of the channel output contains a transmitted signal; otherwise, if the threshold is not exceeded then it is assumed that no signal is present. This is also referred to as a likelihood ratio test. It will be shown that the expected value of the matched filter response to a channel output containing a response to a transmitted signal can be written in terms of the channel scattering function.

In section 3.2.1, the modeling of a signal transmitted through a non-dispersive channel (point scatterer) as a time and frequency shifted version of the original transmit signal is presented, and the conditions necessary for this modeling to be valid are also discussed. Next, hypothesis testing, the matched filter receiver, and the derivation of its expected output are presented in section 3.2.2, followed by the derivation of the expected energy of the channel output is section 3.2.3. In section 3.2.4 the finite volume property of the cross-ambiguity function is derived, and it is also shown that the function is bounded.

Thus, (2.4-31) can be rewritten as

$$R_y(t,t') = \iint_{-\infty}^{\infty} x(t-\tau)\, R_S(\tau,\phi)\, x^*(t'-\tau)\, e^{j2\pi\phi(\Delta t)}\, d\tau d\phi \qquad (2.4\text{-}33)$$

$$R_y(t,t') = E\{\int_{-\infty}^{\infty} X(f)\, H(f,t)\, e^{j2\pi ft}\, df \int_{-\infty}^{\infty} X^*(f')\, H^*(f',t')\, e^{-j2\pi f't'}\, df'\}$$

$$= E\{\iint_{-\infty}^{\infty} X(f)\, X^*(f')\, H(f,t)\, H^*(f',t')\, e^{j2\pi(ft-f't')}\, dfdf'\}$$

$$= \iint_{-\infty}^{\infty} X(f)\, X^*(f')\, E\{H(f,t)\, H^*(f',t')\}\, e^{j2\pi(ft-f't')}\, dfdf'$$

$$= \iint_{-\infty}^{\infty} X(f)\, X^*(f')\, R_H(f,f',t,t')\, e^{j2\pi(ft-ft')}\, dfdf'. \qquad (2.4\text{-}28)$$

Under the WSSUS assumption $R_H(f,f',t,t') = R_H(\Delta f, \Delta t)$ where $\Delta f \triangleq f - f'$ and $\Delta t \triangleq t - t'$, so (2.4-28) becomes

$$R_y(t,t') = \iint_{-\infty}^{\infty} X(f)\, X^*(f')\, R_H(\Delta f, \Delta t)\, e^{j2\pi(ft-f't')}\, dfdf'. \qquad (2.4.\text{-}29)$$

From (2.4-26), $R_H(\Delta f, \Delta t)$ can be replaced by its Fourier transform relationship to the scattering function $R_S(\tau,\phi)$, so (2.4-29) can be restated as

$$R_y(t,t') =$$

$$\int\int\int\int_{-\infty}^{\infty} X(f)\, R_S(\tau,\phi)\, X^*(f)\, e^{j2\pi(ft-f't')}\, e^{\,j2\pi(\phi(\Delta t)-(\Delta f)\tau)}\, d\tau d\phi dfdf'. \qquad (2.4\text{-}30)$$

This multiple integral can be rewritten as the multiple iterated integral

$$R_y(t,t') = \iint_{-\infty}^{\infty} \left[\int_{-\infty}^{\infty} X(f)\, e^{j2\pi f(t-\tau)}\, df\right] R_S(\tau,\phi)$$

$$\times \left[\int_{-\infty}^{\infty} X(f')\, e^{\,j2\pi f'(t'-\tau)}\, df'\right]^* e^{j2\pi\phi(\Delta t)}\, d\tau d\phi. \qquad (2.4\text{-}31)$$

By (2.2-11) the bracketed terms in the integrand of (2.3-31) become

$$\int_{-\infty}^{\infty} X(f)\, e^{\,j2\pi f(t-\tau)}\, df = x(t-\tau)\,. \qquad (2.4\text{-}32)$$

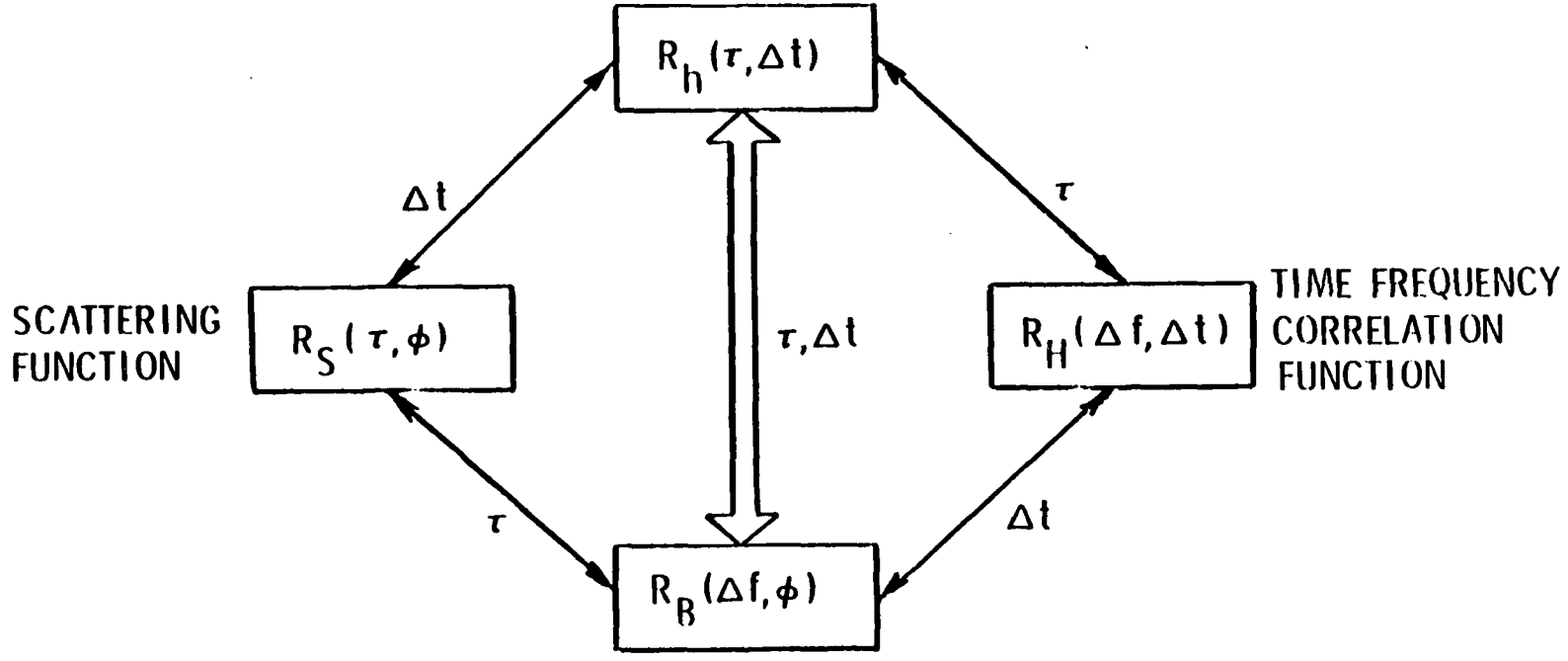

Figure 6. The scattering function and its three Fourier transforms. Each arrow is labeled with its respective forward Fourier transformation variable.

uncorrelated with the value for all f greater than $f_o + B$ or less than $f_o - B$.

The important result of this section is that under the assumption of uncorrelated spreading, the scattering function can be defined as well as other system functions based on the original system autocorrelation functions. These other system functions described by (2.4-20), (2.4-23), and (2.4-25) are related to the scattering function as either forward or inverse Fourier transforms. This is illustrated in Figure 6. From the figure it can be seen that

$$R_H(\Delta f, \Delta t) = \int\int_{-\infty}^{\infty} R_S(\tau, \phi)\, e^{j2\pi(\phi(\Delta t)-(\Delta f)\tau)}\, d\tau d\phi \qquad (2.4\text{-}26)$$

which can be verified by using (2.4-20) and (2.4-25).

2.4.3 The System Output Correlation Function

In this section the correlation function of the linear time-varying system output under the WSSUS assumption is derived. It will be useful in the development presented in the next chapter where random time-varying system theory is applied to signal detection.

By definition, the output correlation function is[13]

$$R_y(t,t') = E\{y(t)\, y^*(t')\} \qquad (2.4\text{-}27)$$

Replacing y(t) by (2.3-19) the correlation function in (2.4-27) becomes

$$R_B(f,f',\phi,\phi') = R_B(\Delta f,\phi)\ \delta(\phi-\phi') \tag{2.4-22}$$

where

$$R_B(\Delta f,\phi) = \int_{-\infty}^{\infty} R_S(\tau,\phi)\ e^{-j2\pi(\Delta f)\tau}\ d\tau. \tag{2.4-23}$$

Thus, $R_B(\Delta f,\phi)$ is the Fourier transform of the scattering function $R_S(\tau,\phi)$ with respect to τ.

Finally, an expression for $R_H(f,f',t,t')$ under the WSSUS assumption can be found. From (2.4-11) and (2.4-19)

$$\begin{aligned} R_H(f,f',t,t') &= \iint_{-\infty}^{\infty} R_h(\tau,\tau',t,t')\ e^{-j2\pi(f\tau-f'\tau')}\ d\tau d\tau' \\ &= \iint_{-\infty}^{\infty} R_h(\tau,\Delta t)\ \delta(\tau-\tau')\ e^{-j2\pi(f\tau-f'\tau')}\ d\tau d\tau' \\ &= \int_{-\infty}^{\infty} R_h(\tau,\Delta t) \left[\int_{-\infty}^{\infty} \delta(\tau-\tau')\ e^{-j2\pi(f\tau-f'\tau')}\ d\tau'\right] d\tau. \end{aligned} \tag{2.4-24}$$

Evaluating the inner integral gives

$$\begin{aligned} R_H(f,f',t,t') &= \int_{-\infty}^{\infty} R_h(\tau,\Delta t)\ e^{-j2\pi(\Delta f)\tau}\ d\tau \\ &\triangleq R_H(\Delta f,\Delta t). \end{aligned} \tag{2.4-25}$$

Equation (2.4-25) is referred to as the time-frequency correlation function.[10] If $R_H(\Delta f,\Delta t)$ is significant only on a region centered at $(\Delta f,\Delta t) = (0,0)$, then it indicates that little statistical correlation exists in the systems behavior for either time separation or frequency separation. For example, if $R_H(\Delta f,\Delta t) = 0$ for all $|\Delta t| > T$, then the implication is that the system transfer function at time t is in no way dependent upon the form of the system transfer function for all time greater than $t + T$ or less than $t - T$. Similarly, if $R_H(\Delta f,\Delta t) = 0$ for all $|\Delta f| > B$, then the value of the system transfer function at any f_o is

$$R_h(\tau,\tau',t,t') = \iint_{-\infty}^{\infty} R_S(\tau,\tau',\phi,\phi')\, e^{j2\pi(\phi t-\phi' t')}\, d\phi d\phi'$$

$$= \iint_{-\infty}^{\infty} R_S(\tau,\phi)\, \delta(\tau-\tau')\, \delta(\phi-\phi')\, e^{j2\pi(\phi t-\phi' t')}\, d\phi d\phi'$$

$$= \int_{-\infty}^{\infty} R_S(\tau,\phi) \left[\int_{-\infty}^{\infty} \delta(\phi-\phi')\, e^{j2\pi(\phi t-\phi' t')}\, d\phi'\right] d\phi\ \delta(\tau-\tau'). \tag{2.4-18}$$

The inner integral, due to the properties of the impulse function, is equal to $e^{j2\pi\phi(t-t')}$. If the notation $t - t' = \Delta t$ is adopted, then (2.4-18) can be rewritten as

$$R_h(\tau,\tau',t,t') = R_h(\tau,\Delta t)\, \delta(\tau-\tau') \tag{2.4-19}$$

where

$$R_h(\tau,\Delta t) = \int_{-\infty}^{\infty} R_S(\tau,\phi)\, e^{j2\pi\phi(\Delta t)}\, d\phi. \tag{2.4-20}$$

Notice that $R_h(\tau,\Delta t)$ is inverse Fourier transform of the scattering function $R_S(\tau,\phi)$ with respect to ϕ.

A similar result occurs for the autocorrelation function $R_B(f,f',\phi,\phi')$. From (2.4-13) and (2.4-16) it follows that

$$R_B(f,f',\phi,\phi') = \iint_{-\infty}^{\infty} R_S(\tau,\tau',\phi,\phi')\, e^{-j2\pi(f\tau-f'\tau')}\, d\tau d\tau'$$

$$= \iint_{-\infty}^{\infty} R_S(\tau,\phi)\, \delta(\tau-\tau')\, \delta(\phi-\phi')\, e^{-j2\pi(f\tau-f'\tau')}\, d\tau d\tau'$$

$$= \int_{-\infty}^{\infty} R_S(\tau,\phi) \left[\int_{-\infty}^{\infty} \delta(\tau-\tau')\, e^{-j2\pi(f\tau-f'\tau')}\, d\tau'\right] d\tau\ \delta(\phi-\phi'). \tag{2.4-21}$$

Again, due to the properties of the impulse function, the inner integral is equal to $e^{-j2\pi(f-f')\tau}$. Adopting the notation $\Delta f = f - f'$, (2.9-21) can be rewritten as

2.4.2 Uncorrelated Spreading

In their present form, the four autocorrelation functions, (2.4-1) to (2.4-4), are of little utility for communication channel description. The additional assumption required is that the spreading function is essentially uncorrelated with itself for different values of τ and ϕ. This is equivalent to expressing the spreading function autocorrelation function as

$$R_S(\tau,\tau',\phi,\phi') = R_S(\tau,\phi)\ \delta(\tau-\tau')\ \delta(\phi-\phi') - m_S(\tau,\phi)\ m_S^*(\tau',\phi') \qquad (2.4\text{-}15)$$

where $m_S(\tau,\phi) = E\{S(\tau,\phi)\}$. Assuming that $m_S(\tau,\phi) = 0$ then (2.4-15) reduces to

$$R_S(\tau,\tau',\phi,\phi') = R_S(\tau,\phi)\ \delta(\tau-\tau')\ \delta(\phi-\phi') \qquad (2.4\text{-}16)$$

where

$$R_S(\tau,\phi) = E\{|S(\tau,\phi)|^2\} \geq 0\ . \qquad (2.4\text{-}17)$$

The positive semidefinite function $R_S(\tau,\phi)$ is referred to as the scattering function[10,11,12] and, according to Ziomek[10], can be interpreted as a density function which determines the amount of delay τ and frequency shift ϕ an input signal will exhibit at the output of a random linear time-varying system with uncorrelated spreading. Communication channels that can be modeled using scattering functions are commonly referred to as wide sense stationary uncorrelated scattering (WSSUS) channels.[10,11]

The WSSUS assumption not only effects the form of $R_S(\tau,\tau',\phi,\phi')$ but also the remaining three system autocorrelation functions. Consider $R_h(\tau,\tau',t,t')$ and its relationship to $R_S(\tau,\tau',\phi,\phi')$ via the Fourier transform. Using (2.4-10) and (2.4-16) it follows that

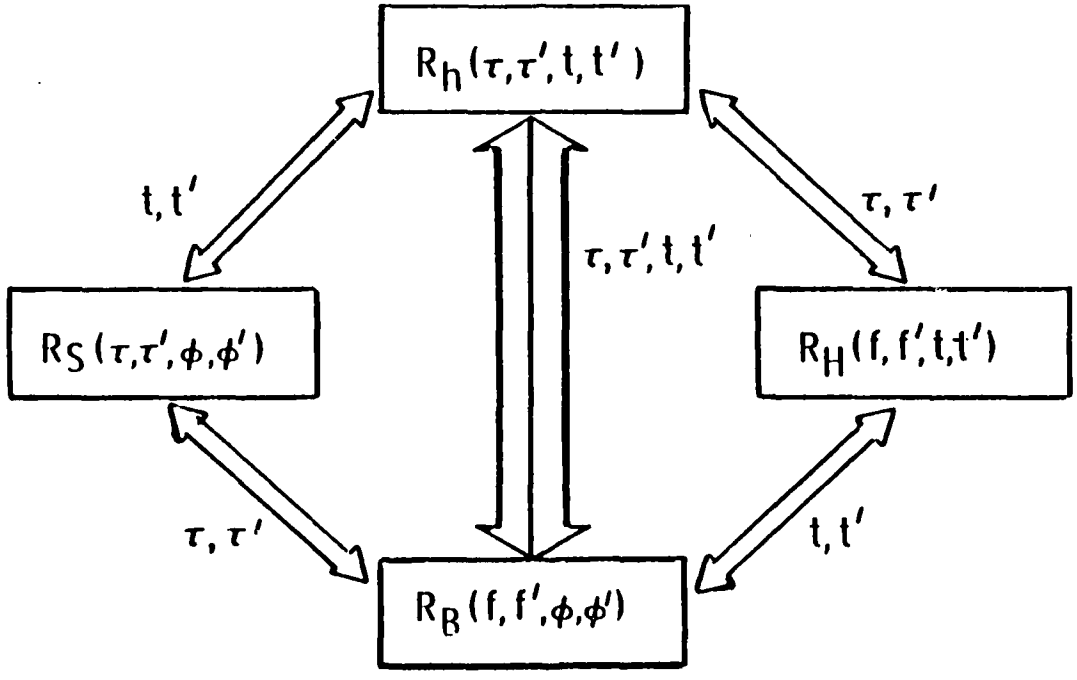

Figure 5. The relationship between the four autocorrelation functions. Each arrow is labeled with its respective forward Fourier transformation variable.

compressed due to the doppler variable s. Therefore, it follows that if the signal bandwidth is defined as

$$BW_{TRANS} = f_2 - f_1 \tag{3.2-15}$$

then the bandwidth of the received signal is

$$BW_{REC} = s\, f_2 - s\, f_1 = s\,(f_2 - f_1) = s\, BW_{TRANS}. \tag{3.2-16}$$

This change in bandwidth can be related to the received signal carrier frequency defined to be the spectral centroid. Since all signals are considered to be elements of $L^1(R^1)$ and $L^2(R^1)$ their spectrums are magnitude integrable by Theorem 2.6, so the spectral centroid is defined as

$$f_{o_{TRANS}} = \frac{\int_{-\infty}^{\infty} f|X(f)|\, df}{\int_{-\infty}^{\infty} |X(f)|\, df}. \tag{3.2-17}$$

If the spectrum of the received signal is given by (3.2-14), then the carrier frequency becomes

$$\begin{aligned} f_{o_{REC}} &= \frac{\int_{-\infty}^{\infty} f\, \left|\frac{1}{s} X(\frac{f}{s})\right| df}{\int_{-\infty}^{\infty} \left|\frac{f}{s} X(\frac{f}{s})\right| df} \\ &= s\, \frac{\int_{-\infty}^{\infty} f|X(f)|\, df}{\int_{-\infty}^{\infty} |X(f)|\, df} \\ &= s\, f_{o_{TRANS}}. \end{aligned} \tag{3.2-18}$$

Combining (3.2-16) and (3.2-18), the received signal bandwidth becomes

$$BW_{REC} = \frac{f_{o_{REC}}}{f_{o_{TRANS}}} BW_{TRANS} \tag{3.2-19}$$

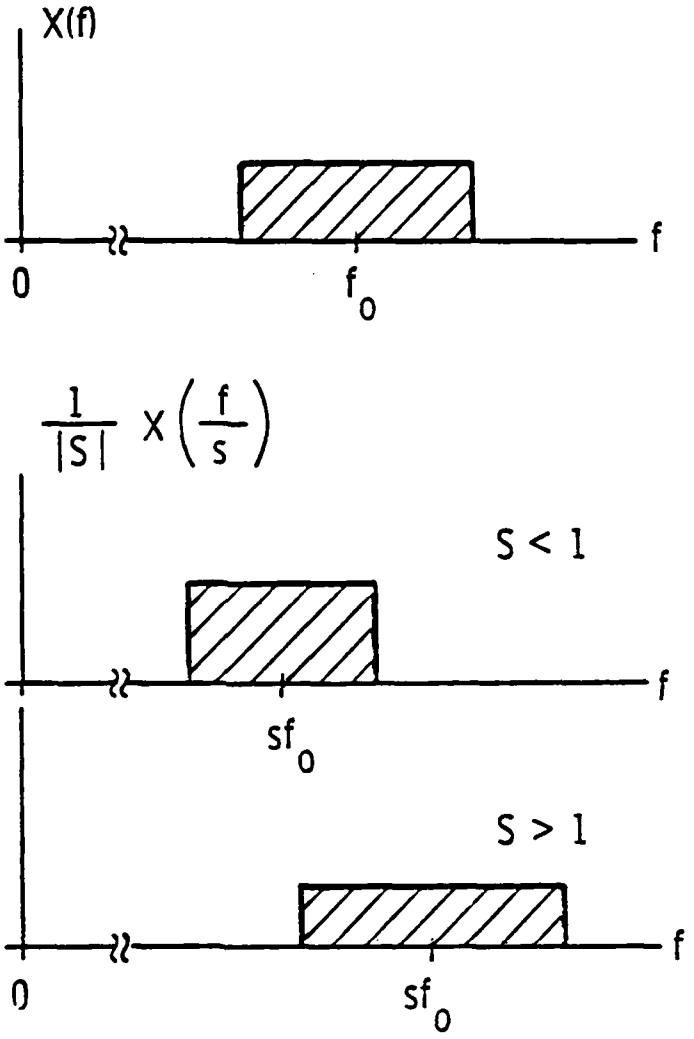

Figure 8. The shifting of spectra due to the Doppler variable s.

thus the change in bandwidth is

$$\begin{aligned}\Delta BW &= BW_{REC} - BW_{TRANS} \\ &= (s-1)\, BW_{TRANS} \\ &= \frac{f_{o_{REC}} - f_{o_{TRANS}}}{f_{o_{TRANS}}} BW_{TRANS} \\ &= \frac{\phi}{f_{o_{TRANS}}} BW_{TRANS} \end{aligned} \tag{3.2-20}$$

where $\phi = f_{o_{REC}} - f_{o_{TRANS}}$ is the doppler frequency shift. Furthermore, from (3.2-20) this frequency shift is also given by

$$\phi = (s-1)\, f_{o_{TRANS}}. \tag{3.2-21}$$

It is easily seen that if the carrier frequency is substantially larger than the transmit signal bandwidth, the change in bandwidth due to the doppler shift ϕ is small. If a transmit signal in a communication system is a bandpass signal and possesses a bandwidth much smaller than the carrier frequency, then for an adequately small range of doppler frequency shift, the return signal spectrum given by (3.2-14) can be approximated by (3.2-10), i.e.,

$$\frac{1}{|s|} X(\tfrac{f}{s})\, e^{j2\pi f\tau} \approx X(f-\phi)\, e^{j2\pi f\tau}. \tag{3.2-22}$$

The term 'adequately small doppler frequency shift' means that the doppler variable s is never large enough to cause the change in bandwidth to be a significant percentage of the transmit signal bandwidth.

3.2.2 The Matched Filter Receiver

From this point forward all system input signals are assumed to be bandpass signals with bandwidths sufficiently small to allow the communication channel to be accurately modeled as a random linear time-varying system. The communication channel outputs will be considered to be the sum of the responses to two random linear time-varying systems and a noise process. The first system models the channel scattering; the second system models the medium scattering. Detecting the presence of a signal is reduced to the hypothesis test:

$$H_0 : \quad r(t) = y_{REV}(t) + n(t) \tag{3.2-23}$$

$$H_1 : \quad r(t) = y_{CHN}(t) + y_{REV}(t) + n(t) \tag{2.3-24}$$

where $r(t)$ is the channel output, $y_{REV}(t)$ is the reverberation or clutter response, $y_{CHN}(t)$ is the response to channel scattering, and $n(t)$ is noise. It will be assumed that the noise term is white and uncorrelated with both $y_{CHN}(t)$ and $y_{REV}(t)$. Furthermore, it will be assumed that $y_{CHN}(t)$ and $y_{REV}(t)$ are uncorrelated. The individual responses due to the channel scattering and reverberation are given by

$$y_{CHN}(t) = \int_{-\infty}^{\infty} h_{CHN}(\tau,t)\, x(t-\tau)\, dt \ , \tag{3.2-25}$$

$$y_{REV}(t) = \int_{-\infty}^{\infty} h_{REV}(\tau,t)\, x(t-\tau)\, dt \ . \tag{3.2-26}$$

The hypothesis test will be implemented by testing the output of a matched filter given by

$$|\ell|^2 = \left| \int_{-\infty}^{\infty} r(t)\, g^*(t)\, dt \right|^2 \tag{3.2-27}$$

where $g(t)$ is called the processing waveform. If the output $|\ell|^2$ exceeds a threshold γ then hypothesis H_1 is assumed and a signal has been

detected. The threshold γ is determined to maximize the probability of detection for given probability of false alarm (Neyman-Pearson test). The performance of the matched filter receiver for different threshold settings is presented in Van-Trees[11], so it will not be discussed here. The entire channel model and receiver structure is shown in Figure 9.

Since the communication channel is stochastic, the expected matched filter output is used to describe the performance of the receiver. For the response to channel scattering, the expected output is

$$\begin{aligned} E\{|\ell_{CHN}|^2\} &= E\{\ell_{CHN}\ \ell_{CHN}^*\} \\ &= E\{\int_{-\infty}^{\infty} y_{CHN}(t)\ g^*(t)\ dt \int_{-\infty}^{\infty} y_{CHN}^*(t')\ g(t')\ dt'\} \\ &= \int\int_{-\infty}^{\infty} g^*(t)\ E\{y_{CHN}(t)\ y_{CHN}^*(t')\}\ g(t')\ dtdt' \\ &= \int\int_{-\infty}^{\infty} g^*(t)\ R_{y_{CHN}}(t,t')\ g(t')\ dtdt'. \end{aligned} \tag{3.2-28}$$

A similar result holds for the reverberation response, i.e.

$$E\{|\ell_{REV}|^2\} = \int\int_{-\infty}^{\infty} g^*(t)\ R_{y_{REV}}(t,t')\ g(t')\ dtdt'. \tag{3.2-29}$$

Because it is assumed that the noise is white, its autocorrelation function is

$$R_n(t,t') = N_o\ \delta(t-t'), \tag{3.2-30}$$

so the expected value of the receiver output due to the noise term is

$$\begin{aligned} E\{|\ell_n|^2\} &= \int\int_{-\infty}^{\infty} g^*(t)\ R_n(t,t')\ g(t)\ dtdt' \\ &= N_o \int\int_{-\infty}^{\infty} g^*(t)\ \delta(t-t')\ g(t')\ dtdt' \\ &= N_o \int_{-\infty}^{\infty} |g(t)|^2\ dt\ . \end{aligned} \tag{3.2-31}$$

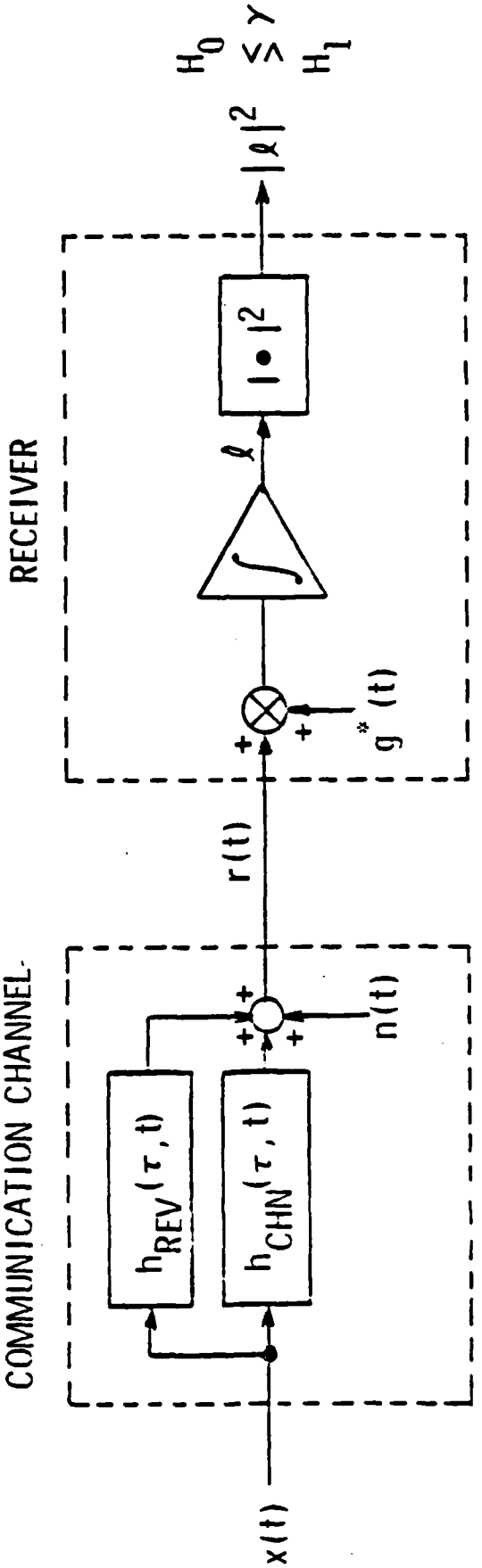

Figure 9. The communication channel model and the matched filter receiver.

A figure of merit used to judge the performance of the matched filter receiver is the signal-to-noise ratio defined as

$$SNR = \frac{E\{|\ell_{CHN}|^2\}}{E\{|\ell_{REV}+\ell_n|^2\}}, \tag{3.2-32}$$

where $|\ell_{REV} + \ell_n|^2$ is the receiver output response to both reverberation and noise. Because it has been assumed that the noise is uncorrelated with the reverberation response, the denominator of (3.2-32) can be written as

$$\begin{aligned} E\{|\ell_{REV}+\ell_n|^2\} &= E\{|\ell_{REV}|^2\} + 2\,\mathrm{Re}[E\{\ell_{REV}\,\ell_n^*\}] + E\{|\ell_n|^2\} \\ &= E\{|\ell_{REV}|^2\} + E\{|\ell_n|^2\}. \end{aligned} \tag{3.2-33}$$

The cross-correlation term vanishes in (3.2-33) because

$$E\{\ell_{REV}\,\ell_n^*\} = \int_{-\infty}^{\infty}\int g^*(t)\,E\{y_{REV}(t)\,n^*(t)\}\,g(t')\,dtdt' \tag{3.2-34}$$

and $E\{y_{REV}(t)\,n^*(t)\}$ is assumed to be zero. Thus, the SNR in (3.2-32) can be rewritten as

$$\begin{aligned} SNR &= \frac{E\{|\ell_{CHN}|^2\}}{E\{|\ell_{REV}|^2\} + E\{|\ell_n|^2\}} \\ &= \frac{\int_{-\infty}^{\infty}\int g^*(t)\,R_{y_{CHN}}(t,t')\,g(t')\,dtdt'}{\int_{-\infty}^{\infty}\int g^*(t)\,R_{y_{REV}}(t,t')\,g(t')\,dtdt' + N_o\int_{-\infty}^{\infty}|g(t)|^2\,dt}. \end{aligned} \tag{3.2-35}$$

Although the SNR has been somewhat simplified in (3.2-35) both the numerator and denominator can be reformulated in terms of the scattering functions for both the channel scattering and reverberation. Consider the numerator in (3.2-35), using (2.4-33) and expressing the channel scattering function as $R_{S_{CHN}}(\tau,\phi)$, the expected matched filter output is

$$E\{|\ell_{CHN}|^2\} =$$

$$\int_{-\infty}^{\infty}\int g^*(t)\left[\int_{-\infty}^{\infty}\int x(t-\tau)\, R_{S_{CHN}}(\tau,\phi)\, x^*(t'-\tau)\, e^{j2\pi\phi(\Delta t)}\, d\tau d\phi\right] g(t')\, dtdt'$$

$$= \int_{-\infty}^{\infty}\int\left[\int_{-\infty}^{\infty} x(t-\tau)\, g^*(t)\, e^{j2\pi\phi(t-\tau/2)}\, dt\right] R_{S_{CHN}}(\tau,\phi)$$

$$\times\left[\int_{-\infty}^{\infty} x(t'-\tau)\, g^*(t')\, e^{j2\pi\phi(t'-\tau/2)}\, dt'\right]^* d\tau d\phi$$

$$= \int_{-\infty}^{\infty}\int\left[\int_{-\infty}^{\infty} x(t-\tau/2)\, g^*(t+\tau/2)\, e^{j2\pi\phi t}\, dt\right] R_{S_{CHN}}(\tau,\phi)$$

$$\times\left[\int_{-\infty}^{\infty} x(t'-\tau/2)\, g^*(t'+\tau/2)\, e^{j2\pi\phi t'}\, dt'\right]^* d\tau d\phi. \qquad (3.2\text{-}36)$$

The bracketed terms in the integrand of the last equation of (3.2-36) is called the uncertainty function and is written as

$$\chi_{x,g}(\tau,\phi) \triangleq \int_{-\infty}^{\infty} x(t-\tau/2)\, g^*(t+\tau/2)\, e^{j2\pi\phi t}\, dt. \qquad (3.2\text{-}37)$$

Using this definition, (3.2-36) can be restated as

$$E\{|\ell_{CHN}|^2\} = \int_{-\infty}^{\infty}\int |\chi_{x,g}(\tau,\phi)|^2\, R_{S_{CHN}}(\tau,\phi)\, d\tau d\phi \qquad (3.2\text{-}38)$$

where the function $|\chi_{x,g}(\tau,\phi)|^2$ is referred to as the cross-ambiguity function. The same reformulation can also be applied to the denominator, so if $R_{S_{REV}}(\tau,\phi)$ is the reverberation scattering function, the SNR can be written as

$$SNR = \frac{\int_{-\infty}^{\infty}\int |\chi_{x,g}(\tau,\phi)|^2\, R_{S_{CHN}}(\tau,\phi)\, d\tau d\phi}{\int_{-\infty}^{\infty}\int |\chi_{x,g}(\tau,\phi)|^2\, R_{S_{REV}}(\tau,\phi)\, d\tau d\phi + N_o \int_{-\infty}^{\infty} |g(t)|^2\, dt}. \qquad (3.2\text{-}39)$$

If the SNR is used as a performance measure for the matched filter receiver, then optimization (increasing the SNR) can be accomplished by either attempting to decrease the reverberation response without significantly decreasing the channel response or increasing the channel response without significantly increasing the reverberation response. Stutt[16], and Spafford[16,17], have been successful in optimizing the SNR for a point scatterer embedded in doubly spread reverberation by altering the processing waveform so as to minimize the denominator of (3.2-39). In this thesis, the numerator will be increased by altering the processing signal. This will imply an increase in SNR if the denominator of (3.2-39) does not also significantly increase. If the only interfering signal is the white noise process, then the first term in the denominator is zero (no reverberation response). In this case, increasing the numerator guarantees an increase in SNR.

3.2.3 Return Energy and the Scattering Function

Using a result from the last chapter, the expected value of the energy of the system response y(t) can be found. From (2.4-33) the system output correlation function is

$$E\{y(t)\ y^*(t')\} = R_y(t,t')$$
$$= \int_{-\infty}^{\infty}\int x(t-\tau)\ R_S(\tau,\phi)\ x^*(t'-\tau)\ e^{j2\pi\phi(\Delta t)}\ d\tau d\phi, \qquad (3.2\text{-}40)$$

where $\Delta t = t - t'$. Setting $t = t'$ gives the expected system output power as

$$E\{|y(t)|^2\} = \int_{-\infty}^{\infty}\int |x(t-\tau)|^2\ R_S(\tau,\phi)\ d\tau d\phi\ . \qquad (3.2\text{-}41)$$

Now the expected system output energy, called the return energy, is

defined as

$$E_r = E\{\int_{-\infty}^{\infty} |y(t)|^2 \, dt\} = \int_{-\infty}^{\infty} E\{|y(t)|^2\} \, dt. \tag{3.2-42}$$

Substituting (3.2-41) into (3.2-42) gives

$$\begin{aligned} E_r &= \iiint_{-\infty}^{\infty} |x(t-\tau)|^2 \, R_S(\tau,\phi) \, d\tau d\phi dt \\ &= \iint_{-\infty}^{\infty} \left[\int_{-\infty}^{\infty} |x(t-\tau)|^2 \, dt\right] R_S(\tau,\phi) \, d\tau d\phi \\ &= E_t \iint_{-\infty}^{\infty} R_S(\tau,\phi) \, d\tau d\phi \end{aligned} \tag{3.2-43}$$

where

$$E_t = \int_{-\infty}^{\infty} |x(t-\tau)|^2 \, dt = \int_{-\infty}^{\infty} |x(t)|^2 \, dt \tag{3.2-44}$$

is the system input energy or transmit energy.

At this point several statements can be made. First, in any practical communication channel it can be assumed that the return energy will be finite. Second, the return energy can be expected to be less than that of the transmitted energy. This occurs because a scatterer can subtend only a small portion of the transmitted wavefront, thus it reflects only a fraction of E_t. Furthermore, some of the transmitted energy is lost due to absorption loss of the medium and spherical spreading of the transmitted and reflected wavefronts. Therefore it can be concluded that

$$\iint_{-\infty}^{\infty} R_S(\tau,\phi) \, d\tau d\phi = \frac{E_r}{E_t} < 1 \, . \tag{3.2-45}$$

Furthermore, because the scattering function is positive definite

$$\iint_{-\infty}^{\infty} R_S(\tau,\phi) \, d\tau d\phi = \iint_{-\infty}^{\infty} |R_S(\tau,\phi)| \, d\tau d\phi \tag{3.2-46}$$

and so it is an element of $L^1(R^2)$.

Scattering functions that are significant over a region of the (τ, ϕ) plane are said to describe doubly-spread or doubly-dispersive communication channels. Such scattering functions will be considered in this thesis, and in Chapter 4 a method for optimizing a receiver to detect a signal that has been transmitted through a doubly-spread communication channel is presented.

3.2.4 Properties of the Cross-ambiguity Function

From the SNR equation (3.2-39) it is easily seen that the cross-ambiguity function in part determines the performance of the receiver. Since the channel and reverberation scattering functions are not free parameters, optimization of the receiver response to a signal can only be done by altering either the transmit signal x(t), the processing signal g(t), or both. Since these signals are related to receiver response through the cross-ambiguity function, it will play a major role in the optimization procedure developed in Chapter 4. Since the cross-ambiguity function is significant to the theory developed in this thesis, it is appropriate to discuss some of its properties.

The most important property of the cross-ambiguity function is that its volume is finite. To prove this it is necessary to find a new form of the uncertainty function. From (3.2-37), and by expressing the waveforms x(t) and g(t) as inverse Fourier transforms gives

$$\chi_{x,g}(\tau,\phi) = \int_{-\infty}^{\infty} x(t-\tau/2)\, g^*(t+\tau/2)\, e^{j2\pi\phi t}\, dt$$

$$= \int_{-\infty}^{\infty} \left[\int_{-\infty}^{\infty} X(f)\, e^{j2\pi f(t-\tau/2)}\, df\right] \left[\int_{-\infty}^{\infty} G(\eta)\, e^{j2\pi\eta(t+\tau/2)}\, d\eta\right]^* e^{j2\pi\phi t}\, dt$$

$$= \iint_{-\infty}^{\infty} X(f)\, G^*(\eta) \left[\int_{-\infty}^{\infty} e^{j2\pi(f-\eta+\phi)t}\, dt\right] e^{-j2\pi(f+\eta)\tau/2}\, df d\eta. \quad (3.2\text{-}47)$$

The bracketed term in the integrand of (3.2-47) can be replaced by a delta function, i.e.,

$$\int_{-\infty}^{\infty} e^{j2\pi(f-\eta+\phi)t}\, dt = \delta(\eta-f-\phi) \tag{3.2-48}$$

Replacing (3.2-48) in (3.2-47) gives

$$\begin{aligned}\chi_{x,g}(\tau,\phi) &= \iint_{-\infty}^{\infty} X(f)\, G^*(\eta)\, \delta(\eta-f-\phi)\, e^{-j2\pi(f+\eta)\tau/2}\, df d\eta \\ &= \iint_{-\infty}^{\infty} X(f)\, G^*(f+\phi)\, e^{-j2\pi(f+\phi/2)\tau}\, df. \end{aligned} \tag{3.2-49}$$

Equation (3.2-49) now expresses the uncertainty function in a useable form.

The volume of the cross-ambiguity function can now be found. From the definition of the cross-ambiguity function in (3.2-49), the volume is given by

$$\begin{aligned} V &= \iint_{-\infty}^{\infty} |\chi_{x,g}(\tau,\phi)|^2\, d\tau d\phi = \iint_{-\infty}^{\infty} \chi_{x,g}(\tau,\phi)\, \chi^*_{x,g}(\tau,\phi)\, d\tau d\phi \\ &= \iint_{-\infty}^{\infty} \left[\int_{-\infty}^{\infty} X(f)\, G^*(f+\phi)\, e^{-j2\pi(f+\phi/2)\tau}\, df\right] \\ &\quad \times \left[\int_{-\infty}^{\infty} X(\eta)\, G^*(\eta+\phi)\, e^{-j2\pi(\eta+\phi/2)\tau}\, d\eta\right]^* d\tau d\phi \\ &= \iiint_{-\infty}^{\infty} X(f)\, X^*(\eta)\, G^*(f+\phi)\, G(\eta+\phi) \left[\int_{-\infty}^{\infty} e^{-j2\pi(f-\eta)\tau}\, d\tau\right] d\eta df d\phi. \end{aligned} \tag{3.2-50}$$

As in (3.2-47), the bracketed term in the (3.2-50) can be replaced by an impulse function thus reducing (3.2-50) to

$$V = \int_{-\infty}^{\infty}\int\int X(f)\, X^*(n)\, G^*(f+\phi)\, G(n+\phi)\, \delta(f-n)\, dn df d\phi$$

$$= \int_{-\infty}^{\infty}\int X(f)\, X^*(f)\, G^*(f+\phi)\, G(f+\phi)\, df d\phi$$

$$= \int_{-\infty}^{\infty}\int |X(f)|^2\, |G(f+\phi)|^2\, df d\phi. \qquad (3.2\text{-}51)$$

Because it is assumed that both the transmit waveform x(t) and the processing waveform g(t) are elements of $L^1(R^1)$ and $L^2(R^1)$, by Theorem 2.6 the integral of the squares of their respective Fourier transforms are finite and by convention are equal to the energies of each signal, i.e.,

$$\int_{-\infty}^{\infty} |X(f)|^2\, df = E_x < \infty \qquad (3.2\text{-}52)$$

$$\int_{-\infty}^{\infty} |G(f)|^2\, df = E_g < \infty \qquad (3.2\text{-}53)$$

Therefore, from (3.2-51)

$$V = \int_{-\infty}^{\infty} |X(f)|^2 \left[\int_{-\infty}^{\infty} |G(f+\phi)|^2\, d\phi\right] df$$

$$= E_g \int_{-\infty}^{\infty} |X(f)|^2\, df$$

$$= E_g\, E_x < \infty\,. \qquad (3.2\text{-}54)$$

Thus, the volume of the cross-ambiguity function is finite and is equal to the product of the energies of the transmit and processing waveforms.

By convention, the value of the processing signal is dimensionless as opposed to the transmit signal which may have units of either volts or amperes. Therefore, E_g is a dimensionless number and the volume of the cross-ambiguity function is in units of energy.

Another property of the cross-ambiguity function is that it is bounded. This can be shown by applying the Schwartz inequality, i.e.,

$$|\chi_{x,g}(\tau,\phi)|^2 = \left[\int_{-\infty}^{\infty} x(t-\tau/2)\, g^*(t+\tau/2)\, e^{j2\pi\phi t}\, dt\right]^2$$

$$\leq \int_{-\infty}^{\infty} |x(t-\tau/2)|^2\, dt \int_{-\infty}^{\infty} |g(t+\tau/2)|^2\, dt\ . \qquad (3.2\text{-}55)$$

By definition, the integrals on the right side of the inequality in (3.2-55) are the energies of the transmit and processing signals, so

$$|\chi_{x,g}(\tau,\phi)|^2 \leq E_x E_g < \infty\ . \qquad (3.2\text{-}56)$$

Thus the cross-ambiguity function is bounded.

3.3 Principles of Matched Filter Receiver Optimization

From this point forward it will be assumed that the transmit signal x(t) and processing signal g(t) are unit energy waveforms, i.e.,

$$\int_{-\infty}^{\infty} |x(t)|^2\, dt = 1, \qquad (3.3\text{-}1)$$

$$\int_{-\infty}^{\infty} |g(t)|^2\, dt = 1. \qquad (3.3\text{-}2)$$

These assumptions will cause no loss of generality in any of the theory developed in this thesis. A consequence of (3.3-1) and (3.3-2) is

$$\iint_{-\infty}^{\infty} |\chi_{x,g}(\tau,\phi)|^2\, d\tau d\phi = E_x\, E_g = 1 \qquad (3.3\text{-}3)$$

and

$$|\chi_{x,g}(\tau,\phi)|^2 \leq E_x\, E_g = 1. \qquad (3.3\text{-}4)$$

Thus, the cross-ambiguity function has unity volume and is bounded by one.

$$J(g+\eta) = J(g) + \delta J(g,\eta) + \frac{1}{2}\,\delta^2 J(g,\eta) + \ldots + \frac{1}{m!}\,\delta^{(m)} J(g,\eta) + \ldots \tag{4.3-21}$$

where

$$\delta^{(m)} J(g,\eta) = \lim_{\varepsilon \to 0} \frac{d^m}{d\varepsilon^m} J(g+\varepsilon\eta) \tag{4.3-22}$$

and is referred to as the m-th Gateaux derivative of J(g) at g(t) with increment η(t). In section 4.3.1, it was shown that J(g+εη) is a second degree polynomial in ε (see equation (4.3-5)); therefore, by examination of (4.3-22) all Gateaux derivatives of order three or higher are equal to zero. Thus,

$$\begin{aligned} J(g+\eta) &= J(g) + \delta J(g,\eta) + \frac{1}{2}\,\delta^2 J(g,\eta) + \ldots \\ &= J(g) + 2\,\mathrm{Re}\{\int_{-\infty}^{\infty} \eta(t)\,\phi^*(t)\,dt\} + J(\eta), \end{aligned} \tag{4.3-23}$$

by (4.3-8), (4.3-19), and (4.3-21). It is fortunate that the Taylor series can be truncated to only three terms since this will allow for an accurate analysis of the optimization procedure developed later.

4.3.4 Properties of the Gradient Function

In section 4.3.1, the gradient function, given by

$$\Phi(t) = \iint_{-\infty}^{\infty} \chi^*_{x,g}(\tau,\phi)\, R_S(\tau,\phi)\, x(t-\tau)\, e^{j2\pi\phi(t-\tau/2)}\, d\tau d\phi, \tag{4.3-9}$$

arose from rearranging the integral that defined the first Gateaux differential of the cost functional J(g). As with the cross-ambiguity function, since the gradient function is significant to the theory developed in this thesis, it is appropriate to discuss some of its properties.

Therefore,

$$\lim_{\|\beta\|_2 \to 0} \frac{|\delta^2 J(g,\eta,\beta) - \delta^2 J(g,\eta,\beta)|}{\|\beta\|_2} = \lim_{\|\beta\|_2 \to 0} \frac{0}{\|\beta\|_2} = 0. \qquad (4.3\text{-}17)$$

Thus, (4.3-15) holds for $\delta J(g,\eta)$ as given by (4.3-6) so $J(g)$ is twice Frechet differentiable and $\delta J(g,\eta,\beta)$ describes a unique and continuous linear mapping of all $\beta(t)$ in $L^2(R^1)$ to R^1.

For the purposes of analyzing the behavior of $J(g)$ as $g(t)$ changes to $g(t) + \beta(t)$, the second Frechet derivative must be evaluated with $\eta(t) = \beta(t)$. In this case, the second Frechet derivative is written as

$$\delta^2 J(g,\eta,\eta) = \delta^2 J(g,\eta). \qquad (4.3\text{-}18)$$

From (4.3-18) it follows that for the cost functional given by (4.1-1), the second Frechet differential is

$$\delta^2 J(g,\eta) = 2 \int_{-\infty}^{\infty}\int |\chi_{g,\eta}(\tau,\phi)|^2 R_S(\tau,\phi)\, d\tau d\phi = 2\, J(\eta). \qquad (4.3\text{-}19)$$

Note that because the second Frechet differential is proportional to the cost functional evaluated at $\eta(t)$, the cost functional itself is a continuous mapping.

4.3.3 The Generalized Taylor Expansion

It is well known from elementary calculus that the function of a real variable, $f(x)$, can be written as a Taylor series, i.e.,

$$f(x+\Delta x) = f(x) + f'(x)\,\Delta x + \frac{1}{2} f''(x)\,(\Delta x)^2 + \ldots + \frac{1}{m!} f^{(m)}(x)\,(\Delta x)^m + \ldots \qquad (4.3\text{-}20)$$

It can be shown that the Taylor series can be generalized for functionals that map one linear space to another[19,20]. In this case the Taylor expansion for the cost functional is expressed by

$$\delta J(g,\eta,\beta) = \lim_{\varepsilon\to 0} \frac{d}{d\varepsilon} \left[2\ \mathrm{Re}\{\iint_{-\infty}^{\infty} \chi_{x,g+\varepsilon\beta}(\tau,\phi)\ \chi^*_{x,\eta}(\tau,\phi)\ R_S(\tau,\phi)\ d\tau d\phi\} \right]$$

$$= \lim_{\varepsilon\to 0} \frac{d}{d\varepsilon} \left[2\ \mathrm{Re}\{\iint_{-\infty}^{\infty} \chi_{x,g}(\tau,\phi)\ \chi^*_{x,\eta}(\tau,\phi)\ R_S(\tau,\phi)\ d\tau d\phi\} \right.$$

$$\left. + 2\ \varepsilon\ \mathrm{Re}\{\iint_{-\infty}^{\infty} \chi_{x,\beta}(\tau,\phi)\ \chi_{x,\eta}(\tau,\phi)\ R_S(\tau,\phi)\ d\tau d\phi\} \right]$$

$$= 2\ \mathrm{Re}\{\iint_{-\infty}^{\infty} \chi_{x,\beta}(\tau,\phi)\ \chi^*_{x,\eta}(\tau,\phi)\ R_S(\tau,\phi)\ d\tau d\phi\}. \qquad (4.3\text{-}14)$$

By its definition, the second Gateaux derivative is just the first Gateaux derivative of $\delta J(g,\eta)$ with respect to $g(t)$. In effect, $\delta J(g,\eta)$ has been treated no differently than any other functional whose first Gateaux derivative has been sought. Thus, $\delta^2 J(g,\eta,\beta)$ gives the first order change in $\delta J(g,\eta)$ when $g(t)$ changes to $g(t)+\beta(t)$.

As with the first Gateaux derivative, $\delta^2 J(g,\eta,\beta)$ describes a continuous and unique mapping from $L^1(R^1) \cap L^2(R^2)$ if it is also the Frechet derivative of $\delta J(g,\eta)$ with respect to $g(t)$. Equation (4.3-13) describes a second Frechet derivative if $\delta J(g,\eta)$ is a Frechet derivative of $J(g)$ and if for a fixed $g(t)$ in $L^1(R^1) \cap L^2(R^1)$, and $\beta(t)$ an arbitrary element in $L^2(R^1)$, then

$$\lim_{\|\beta\|_2\to 0} \frac{|\delta J(g+\beta,\eta)-\delta J(g,\eta)-\delta^2 J(g,\eta,\beta)|}{\|\beta\|_2} = 0. \qquad (4.3\text{-}15)$$

Without loss of generality, the increment $\beta(t)$ can be replaced by $\varepsilon z(t)$ where ε is a real constant and $\|z\|_2 = 1$. The differential of the two first Frechet derivatives of $J(g)$ in the numerator of (4.3-15) can be found from (4.3-14) and (4.3-6) to be

$$\delta J(g+\beta,\eta) - \delta J(g,\eta)$$

$$= 2\ \mathrm{Re}\{\iint_{-\infty}^{\infty} \chi_{x,\beta}(\tau,\phi)\ \chi^*{}_{x,\eta}(\tau,\phi)\ R_S(\tau,\phi)\ d\tau d\phi\}$$

$$= \delta^2 J(g,\eta,\beta). \qquad (4.3\text{-}16)$$

$$\lim_{\varepsilon \to 0} \frac{|J(x+\varepsilon z)-J(x)-\delta J(g,\varepsilon z)|}{\|\varepsilon z\|_2}$$

$$= \lim_{\varepsilon \to 0} |\varepsilon| \int\int_{-\infty}^{\infty} |\chi_{x,z}(\tau,\phi)|^2 R_s(\tau,\phi)\, d\tau d\phi = 0. \qquad (4.3\text{-}12)$$

This shows that $\delta J(g,\eta)$ is a Frechet derivative and that it is a unique and continuous mapping from the set of all functions in $L^1(R^1) \cap L^2(R^1)$ to R^1.

4.3.2 The Second Gateaux Derivative

Although the second Gateaux derivative will not be used in the development of the optimization procedure presented later, it will be useful in the analysis of its performance and convergence. Furthermore, the definition ultimately used does not express the second Gateaux derivative in its most general form; however, it will be suitable for analyzing the behavior of the cost functional.

The second Gateaux derivative of the cost functional $J(g)$ with increments $\eta(t)$ and $\beta(t)$, where $g(t)$ is in $L^1(R^1)$ and $L^2(R^1)$, and $\eta(t)$ and $\beta(t)$ are arbitrary elements of $L^2(R^1)$ is given by[19,20]

$$\delta^2 J(g,\eta,\beta) = \lim_{\varepsilon \to 0} \frac{d}{d\varepsilon} \delta J(g+\varepsilon\beta,\eta). \qquad (4.3\text{-}13)$$

In section 4.3.1 the first Gateaux derivative was expressed by (4.3-6), thus, by applying the definition in (4.3-13), and using the property of the cross-ambiguity function given by (4.3-3), the second Gateaux derivative is

$$\delta J(g,\eta) = 2\ \mathrm{Re}\ \{\int_{-\infty}^{\infty} \eta(t)\Phi^*(t)\ dt\} = 2\ \mathrm{Re}\{\langle \eta, \Phi \rangle\} \qquad (4.3\text{-}8)$$

where $\Phi(t)$ is called the 'gradient function' defined as

$$\Phi(t) = \iint_{-\infty}^{\infty} \chi^*_{x,g}(\tau,\phi)\ R_S(\tau,\phi)\ x(t-\tau)\ e^{j2\pi\phi(t-\tau/2)}\ d\tau d\phi. \qquad (4.3\text{-}9)$$

The properties of the gradient function will be discussed in section 4.3.4.

The Gateaux derivative of $J(g)$ as given in (4.3-6) and (4.3-8) defines a linear transformation (mapping) from the set of all functions in $L^1(R^1) \cap L^2(R^1)$ to R^1. However, from its definition, the existence of a Gateaux derivative does not imply that it is a continuous or a unique mapping of one linear space to another. This occurs because the norm of the space $L^2(R^1)$ is not involved in the definition given by (4.3-1). Continuity and uniqueness can only be guaranteed by a Frechet derivative.

By definition, the Gateaux derivative $\delta J(g,\eta)$ is also a Frechet derivative[2,19,20] if for a fixed $g(t)$ in $L^1(R^1)$ and $L^2(R^1)$ and an arbitary $\eta(t)$ in $L^2(R^1)$, then

$$\lim_{\|\eta\|_2 \to 0} \frac{|J(x+\eta)-J(x)-\delta J(g,\eta)|}{\|\eta\|_2} = 0\ . \qquad (4.3\text{-}10)$$

Without loss of generality, the increment $\eta(t)$ can be replaced by $\varepsilon z(t)$ where ε is a real constant and $\|z\|_2 = 1$. The numerator of (4.3-10) can be found from (4.1-1), (4,3-5), and (4.3-6), i.e.

$$J(g+\varepsilon z) - J(g) - \delta J(g,\varepsilon\eta) = \varepsilon^2 \iint_{-\infty}^{\infty} |\chi_{x,z}(\tau,\phi)|^2\ R_S(\tau,\phi)\ d\tau d\phi. \qquad (4.3\text{-}11)$$

Applying (4.3-11) to (4.3-10) gives

$$\iint_{-\infty}^{\infty} |\chi_{x,g+\varepsilon\eta}(\tau,\phi)|^2 R_S(\tau,\phi)\, d\tau d\phi$$

$$= \iint_{-\infty}^{\infty} |\chi_{x,g}(\tau,\phi)|^2 R_S(\tau,\phi)\, d\tau d\phi$$

$$+ 2\varepsilon \iint_{-\infty}^{\infty} \mathrm{Re}\{\chi_{x,g}(\tau,\phi)\, \chi^*_{x,\eta}(\tau,\phi)\} R_S(\tau,\phi)\, d\tau d\phi$$

$$+ \varepsilon^2 \iint_{-\infty}^{\infty} |\chi_{x,\eta}(\tau,\phi)|^2 R_S(\tau,\phi)\, d\tau d\phi$$

$$= J(g+\varepsilon\eta) \qquad (4.3\text{-}5)$$

which is a second degree polynomial in ε. Evaluating the derivative of (4.3-5) with respect to ε and taking the limit as $\varepsilon \to 0$ gives the first Gateaux differential of the cost functional $J(g)$ as

$$\delta J(g,\eta) = 2 \iint_{-\infty}^{\infty} \mathrm{Re}\{\chi_{x,g}(\tau,\phi)\, \chi^*_{x,\eta}(\tau,\phi)\} R_S(\tau,\phi)\, d\tau d\phi$$

$$= 2\,\mathrm{Re}\left\{\iint_{-\infty}^{\infty} \chi_{x,g}(\tau,\phi)\, \chi^*_{x,\eta}(\tau,\phi)\, R_S(\tau,\phi)\, d\tau d\phi\right\}. \qquad (4.3\text{-}6)$$

Equation (4.3-6) can be rewritten into a form that will be convenient later. This is done by replacing the conjugated uncertainty function in the integrand by its definition in (3.2-37), changing variable of integration, and rearranging terms as follows:

$$\delta J(g,\eta)$$

$$= 2\,\mathrm{Re}\left\{\iint_{-\infty}^{\infty} \chi_{x,g}(\tau,\phi) \left[\int_{-\infty}^{\infty} x(t-\tau/2)\, \eta^*(t+\tau/2)\, e^{j2\pi\phi t}\, dt\right]^* R_S(\tau,\phi)\, d\tau d\phi\right\}$$

$$= 2\,\mathrm{Re}\left\{\iint_{-\infty}^{\infty} \chi_{x,g}(\tau,\phi) \left[\int_{-\infty}^{\infty} x^*(t-\tau)\, \eta(t) e^{-j2\pi\phi(t-\tau/2)}\, dt\right] R_S(\tau,\phi)\, d\tau d\phi\right\}$$

$$= 2\,\mathrm{Re}\left\{\int_{-\infty}^{\infty} \eta(t) \left[\iint_{-\infty}^{\infty} \chi_{x,g}(\tau,\phi)\, R_S(\tau,\phi)\, x^*(t-\tau)\, e^{-j2\pi\phi(t-\tau/2)}\, d\tau d\phi\right] dt\right\}. \qquad (4.3\text{-}7)$$

Equation (4.3-7) can be more compactly written as

second Gateaux derivatives of the cost functional. They are often given the interpretation of being generalized directional derivatives over a linear space, and in the engineering literature these derivatives are referred to as the first and second variation.

Let $g(t)$ be an element of $L^1(R^1)$ and $L^2(R^1)$ and $\eta(t)$ be an arbitrary element of $L^2(R^1)$, then

$$\delta J(g,\eta) = \lim_{\varepsilon \to o} \frac{d}{d\varepsilon} J(g+\varepsilon\eta) \tag{4.3-1}$$

is the first Gateaux differential of $J(g)$ with increment $\eta(t)$[2,19,20]. To start, it is necessary to find the derivative on the right side of (4.3-1), therefore,

$$\frac{d}{d\varepsilon} J(g+\varepsilon\eta) = \frac{d}{d\varepsilon} \int\int_{-\infty}^{\infty} |\chi_{x,g+\varepsilon\eta}(\tau,\phi)|^2 \, R_S(\tau,\phi) \, d\tau d\phi \, . \tag{4.3-2}$$

The integral in (4.3-2) can be expanded as a polynomial in ε. From the definition of the uncertainty function by (3.2-37),

$$\begin{aligned} \chi_{x,g+\varepsilon\eta}(\tau,\phi) &= \int_{-\infty}^{\infty} x(t-\tau/2) \, [g(t+\tau/2) + \varepsilon\eta(t+\tau/2]^* \, e^{j2\pi\phi t} \, dt \\ &= \int_{-\infty}^{\infty} x(t-\tau/2) \, g^*(t+\tau/2) \, e^{j2\pi\phi t} \, dt \\ &\quad + \varepsilon \int_{-\infty}^{\infty} x(t-\tau/2) \, \eta^*(t+\tau/2) \, e^{j2\pi\phi t} \, dt \\ &= \chi_{x,g}(\tau,\phi) + \varepsilon \, \chi_{x,\eta}(\tau,\phi). \end{aligned} \tag{4.3-3}$$

It follows that the cross-ambiguity function derived from (4.3-3) is

$$\begin{aligned} |\chi_{x,g+\varepsilon\eta}(\tau,\phi)|^2 &= |\chi_{x,g}(\tau,\phi)|^2 + 2 \, \mathrm{Re}\{\chi_{x,g}(\tau,\phi) \, \chi^*_{x,\eta}(\tau,\phi)\} \, \varepsilon \\ &\quad + |\chi_{x,\eta}(\tau,\phi)|^2 \, \varepsilon^2 \, . \end{aligned} \tag{4.3-4}$$

Substituting (4.3-4) into the integral of (4.3-2) gives

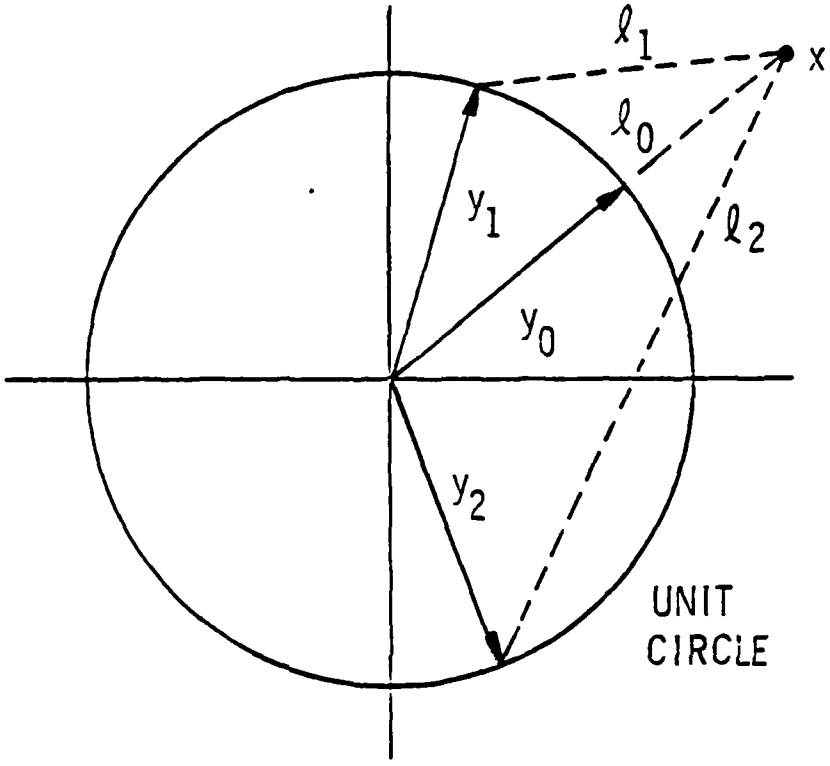

$$\ell_0 < \ell_1 < \ell_2$$

$$\ell_0 = \min_{y \in S} \| x-y \|_2^2 = \| x-y_0 \|_2^2$$

Figure 10. The set S in R^2 consisting of all vectors lying on the unit circle.

By Theorem 4.1, the supremum on the right side is uniquely known, giving

$$\inf_{y(t) \in S} \|x-y\|_2^2 = \|x\|_2^2 + 1 - 2\|x\|_2. \tag{4.2.8}$$

where $y(t) = x(t)/\|x\|_2$. The right side of (4.2-8) is a quadratic equation of the norm, and it can be easily verified that its value is always greater than or equal to zero. Thus, the unique best approximation to any x(t) with a non-zero norm by an element of the set S defined by (4.2-5) is $y_o(t) = x(t)/\|x\|_2$. This completes the proof of the theorem.

Although Theorem 4.2 is stated in terms of $L^2(R^1)$, it can extend to other Hilbert spaces. This can be illustrated by considering a Hilbert space familiar to nearly everyone; the set of all two-dimensional vectors R^2 (the real plane). Figure 10 shows a portion of R^2 near the origin and the set S, which in this case is the unit circle. Also shown is the vector x and its best approximation in the set S, the vector y_o. It is intuitively clear that the best approximation is mearly a scaled version of x that has unity length. Other vectors in S are shown, and it can be seen that the norm of the difference vectors between them and the vector x are not minimal.

4.3 Gateaux Derivatives of the Expected Matched Filter Output

4.3.1 The First Gateaux Derivative

As mentioned in the introduction to this chapter, the cost functional used in the optimization of the matched filter receiver is its expected output subject to the constraint that the value of the norm of both the processing signal and transmit signal is unity. To develop and analyze the optimization procedure, it is necessary to find the first and

Proof By the properties of the complex numbers and the Schwartz inequality

$$\mathrm{Re}\langle x,y\rangle \leq |\langle x,y\rangle| \leq \|x\|_2 \, \|y\|_2. \tag{4.2-3}$$

The right inequality of (4.2-3) is an equality if and only if $y(t) = \lambda\, x(t)$ where $\lambda \in R^1$. Because $y(t)$ is an element of S, either $\lambda = 1/\|x\|_2$ or $\lambda = -1/\|x\|_2$, causing $\langle x,y\rangle$ to be a real quantity, thus

$$\mathrm{Re}\{\langle x,y\rangle\} = \pm \langle x,y\rangle = \pm \|x\|_2. \tag{4.2-4}$$

Therefore, the left inequality of (4.2-3) is an equality and $\mathrm{Re}\{\langle x,y\rangle\}$ is maximized only when $\lambda = 1/\|x\|_2$. Equation (4.2-2) follows immediately.

Theorem 4.1 is used to prove the following theorem.

Theorem 4.2 Let S be the set of all functions in $L^2(R^1)$ whose norm is unity. For any non-zero element $x(t)$ in $L^2(R^1)$, the unique best approximation by an element $y_o(t)$ in S is given by $y_o(t) = x(t)/\|x\|_2$.

Proof Finding the best approximation is defined as a minimum norm problem; in other words, an element $y_o(t)$ is sought such that

$$\|x-y_o\|_2^2 = \inf_{y(t) \in S} \|x-y\|_2^2 > 0. \tag{4.2-5}$$

In the Hilbert space $L^2(R^1)$ the norm can be defined in terms of the inner product, thus (4.2-5) can be restated as

$$\begin{aligned} \inf_{y(t) \in S} \|x-y\|_2^2 &= \inf_{y(t) \in S} \langle x-y, x-y\rangle \\ &= \inf_{y(t) \in S} \{\|x\|_2^2 + \|y\|_2^2 - 2\,\mathrm{Re}\{\langle x,y\rangle\}\}. \end{aligned} \tag{4.2-6}$$

Since $y \in S$ then $\|y\|_2^2 = 1$, therefore,

$$\inf_{y(t) \in S} \|x-y\|_2^2 = \|x\|_2^2 + 1 - 2 \sup_{y(t) \in S} \mathrm{Re}\{\langle x,y\rangle\}. \tag{4.2-7}$$

In section 4.2 the set of unit energy signals is discussed, and a theorem is stated and proved giving the best approximation of any element in the space $L^2(R^1)$ by a unit energy signal. In section 4.3, the first and second Gateaux derivatives (also known as first and second variations) of J(g) are derived as well as its generalized Taylor expansion, and in section 4.4 the procedure for optimizing J(g) subject to the constraints (4.1-2) and (4.1-3) is presented. Finally, in section 4.5 several numerical examples of optimizing a matched filter receiver using this procedure are given.

4.2 The Set of Unit Energy Signals

As indicated in Chapter 1, all functions used to represent signals will be elements of $L^2(R^1)$ and $L^1(R^1)$. Furthermore, it was established in section 3.3 that the energies of both the transmit and processing signals are unity. Thus, it follows that the set of all functions in $L^2(R^1)$ whose norm is equal to unity is of considerable importance to the development of the theory presented in this chapter. Two theorems are stated and proved below. The second theorem will be applied in the development of the optimization procedure developed in Chapter 4.4.

Theorem 4.1 Let x(t) and y(t) be non-zero elements of the complex Hilbert space $L^2(R^1)$. Let y(t) be an element of the set of all functions in $L^2(R^1)$ with unit norm (unit energy), i.e.,

$$S = \{y(t) \in L^2(R^1) \mid \|y\|_2 = 1\}. \tag{4.2-1}$$

If x(t) is fixed then the value of $\mathrm{Re}\{\langle x,y\rangle\}$ is maximized if and only if $y(t) = x(t)/\|x\|_2$ giving

$$\sup_{y(t) \in S} \mathrm{Re}\{\langle x,y\rangle\} = \|x\|_2. \tag{4.2-2}$$

CHAPTER 4

OPTIMAL SIGNAL DETECTION

4.1 Introduction

In this chapter an iterative optimization procedure is developed to increase the expected matched filter receiver response to a signal that has been transmitted through a communication channel whose average scattering properties are known. As might be expected, the cost functional used in this procedure is

$$J(g) = E\{|\ell|^2\} = \int_{-\infty}^{\infty}\int R_S(\tau,\phi)\ |\chi_{x,g}(\tau,\phi)|^2\ d\tau d\phi, \tag{4.1-1}$$

where an increase in the value of $J(g)$ is sought subject to the constraints

$$\|x\|_2^2 = \int_{-\infty}^{\infty} |x(t)|^2\ dt = 1, \tag{4.1-2}$$

$$\|g\|_2^2 = \int_{-\infty}^{\infty} |g(t)|^2\ dt = 1. \tag{4.1-3}$$

In other words, both the transmit and processing signals have unit energy. The cost functional is defined for all $x(t)$ and $g(t)$ in $L^2(R^1)$, and this can be shown by examining the integrand of (4.1-1). Because $x(t)$ and $g(t)$ have finite energy, the value of the cross-ambiguity function is bounded for all τ and ϕ by (3.2-56). Furthermore, it was shown in section 3.2.3 that the scattering function has finite volume, thus

$$J(g) \leq \|x\|_2\ \|g\|_2 \int_{-\infty}^{\infty}\int R_S(\tau,\phi)\ d\tau d\phi < \infty, \tag{4.1-4}$$

showing $J(g)$ exists for all $x(t)$ and $g(t)$ in $L^2(R^1)$. In fact, it means that $J(g)$ is a bounded functional over the space $L^2(R^1)$.

function is bounded by unity the constant K is constrained by

$$K \leq \frac{1}{\max\limits_{R_1 \cap R_2} R_{S_{CHN}}(\tau,\phi)} , \tag{3.3-9}$$

thereby causing the right side of (3.3-8) to be less than or equal to one for all $(\tau,\phi) \in R_1 \cap R_2$.

Equations (3.3-8) and (3.3-9) imply that if the cross-ambiguity and scattering functions are constrained to be non zero in the regions R_1 and R_2, respectively, then the expected value of the matched filter receiver response to the channel output is maximized if the cross-ambiguity function has the same shape as the channel scattering function in their region of intersection in the (τ,ϕ) plane. If the regions R_1 and R_2 have finite areas of nonintersection, then some of the volume of the cross-ambiguity and channel scattering functions are lost when their product, the integrand of (3.2-38) is formed. This implies that an improvement in the matched filter response can occur if the cross ambiguity function and the scattering function subtend the same region in the (τ,ϕ) plane. Since the channel scattering function is not a free parameter, improvement in receiver performance can only be attained by altering the shape of the cross-ambiguity function which can be done by changing either the transmit signal, the processing signal, or both. A method for optimizing the matched filter output by altering the processing signal is presented in Chapter 4.

Consider the expected value of the matched filter receiver output to a received signal which was shown in section 3.2.2 to be given by

$$E\{|\ell_{CHN}|^2\} = \int_{-\infty}^{\infty}\int |\chi_{x,g}(\tau,\phi)|^2 R_{S_{CHN}}(\tau,\phi)\, d\tau d\phi. \qquad (3.2\text{-}38)$$

If R_1 is defined to be the region of the (τ,ϕ) plane where the cross-ambiguity function is non-zero, and R_2 is defined to be the region where the scattering function is non-zero, then (3.2-38) can be restated as

$$E\{|\ell_{CHN}|^2\} = \iint_{R_1 \cap R_2} |\chi_{x,g}(\tau,\phi)|^2 R_{S_{CHN}}(\tau,\phi)\, d\tau d\phi. \qquad (3.3\text{-}5)$$

By the Schwartz inequality an upper bound for (3.3-5) can be found,

$$\begin{aligned} E\{|\ell_{CHN}|^2\} &= \iint_{R_1 \cap R_2} |\chi_{x,g}(\tau,\phi)|^2 R_{S_{CHN}}(\tau,\phi)\, d\tau d\phi \\ &\leq \int_{-\infty}^{\infty}\int |\chi_{x,g}(\tau,\phi)|^2 d\tau d\phi \int_{-\infty}^{\infty}\int R_{S_{CHN}}(\tau,\phi)\, d\tau d\phi \\ &= \frac{E_r}{E_x} = E_r \leq 1. \end{aligned} \qquad (3.3\text{-}6)$$

Regardless of its statistical nature, the matched filter output is, in fact, always less than unity because from (3.2-27), (3.3-1) and (3.3-2),

$$\begin{aligned} |\ell_{CHN}|^2 &= \left| \int_{-\infty}^{\infty} y_{CHN}(t)\, g^*(t)\, dt \right|^2 \\ &\leq \int_{-\infty}^{\infty} |y_{CHN}(t)|^2 dt \int_{-\infty}^{\infty} |g(t)|^2 dt \\ &\leq \int_{-\infty}^{\infty} |x(t)|^2 dt \int_{-\infty}^{\infty} |g(t)|^2 dt = 1. \end{aligned} \qquad (3.3\text{-}7)$$

From the Schwartz inequality the matched filter receiver output can attain its bound if and only if

$$|\chi_{x,g}(\tau,\phi)|^2 = K\, R_{S_{CHN}}(\tau,\phi) \quad \text{for } (\tau,\phi) \quad R_1 \cap R_2, \qquad (3.3\text{-}8)$$

where K is a positive real constant. Because the cross-ambiguity

Property 1: The gradient function $\Phi(t)$ is a bounded function if the transmit signal $x(t)$ is also bounded, i.e., $|x(t)| \leq K$ for all $t \in R^1$.

This can be shown by first finding the magnitude of $\Phi(t)$ and applying the Schwartz inequality to (4.3-9) as follows:

$$|\Phi(t)| \leq \int_{-\infty}^{\infty}\int |\chi_{x,g}(\tau,\phi)|\, R_S(\tau,\phi)\, |x(t-\tau)|\, d\tau d\phi$$

$$\leq K \int_{-\infty}^{\infty}\int |\chi_{x,g}(\tau,\phi)|\, R_S(\tau,\phi)\, d\tau d\phi. \qquad (4.3\text{-}24)$$

Furthermore, because the scattering function has finite volume, and $|\chi_{x,g}(\tau,\phi)| \leq 1$ by (3.3-4),

$$|\Phi(t)| \leq K \int_{-\infty}^{\infty}\int R_S(\tau,\phi)\, d\tau d\phi < \infty, \qquad (4.3\text{-}25)$$

so $\Phi(t)$ is a bounded function.

Property 2: The gradient function $\Phi(t)$ is an element of $L^1(R^1)$ and $L^2(R^1)$.

Showing that $\Phi(t) \in L^1(R^1)$ can be done by using (4.3-24),

$$\int_{-\infty}^{\infty} |\Phi(t)|\, dt \leq \int_{-\infty}^{\infty} \left[\int_{-\infty}^{\infty}\int |\chi_{x,g}(\tau,\phi)|\, R_S(\tau,\phi)\, |x(t-\tau)|\, d\tau d\phi\right] dt$$

$$= \int_{-\infty}^{\infty}\int |\chi_{x,g}(\tau,\phi)|\, R_S(\tau,\phi) \left[\int_{-\infty}^{\infty} |x(t-\tau)|\, dt\right] d\tau d\phi. \qquad (4.3\text{-}26)$$

Since $x(t)$ is in $L^1(R^1)$ and $L^2(R^1)$ and $|\chi_{x,g}(\tau,\phi)| \leq 1$,

$$\int_{-\infty}^{\infty} |\Phi(t)|\, dt \leq \|x\|_1 \int_{-\infty}^{\infty}\int R_S(\tau,\phi)\, d\tau d\phi < \infty. \qquad (4.3\text{-}27)$$

Hence, $\Phi(t)$ is magnitude integrable, and it is an element of $L^1(R^1)$. Also, because it is bounded, by Theorem 2.7 it is also an element of $L^2(R^1)$.

Property 3: The inner product of the processing signal g(t) and the gradient function $\Phi(t)$ is equal to the value of the cost functional, i.e.,

$$\langle g,\Phi\rangle = \int_{-\infty}^{\infty} g(t)\ \Phi^*(t)\ dt = J(g)\ . \tag{4.3-28}$$

This is shown by expanding the left side of (4.3-28) using the definition of the gradient function in (4.3-9) and rearranging the integrand as follows:

$$\begin{aligned}\langle g,\Phi\rangle &= \int_{-\infty}^{\infty} g(t)\left[\iint_{-\infty}^{\infty} \chi_{x,g}(\tau,\phi)\ R_S(\tau,\phi)\ x^*(t-\tau)\ e^{-j2\pi\phi(t-\tau/2)}\ d\tau d\phi\right] dt \\ &= \iint_{-\infty}^{\infty} \chi_{x,g}(\tau,\phi)\ R_S(\tau,\phi)\left[\int_{-\infty}^{\infty} x^*(t-\tau)\ g(t)\ e^{-j2\pi\phi(t-\tau/2)}\ dt\right] d\tau d\phi \\ &= \iint_{-\infty}^{\infty} \chi_{x,g}(\tau,\phi)\ R_S(\tau,\phi)\left[\int_{-\infty}^{\infty} x(t-\tau/2)\ g^*(t+\tau/2)\ e^{j2\pi\phi t}\ dt\right]^* d\tau d\phi.\end{aligned} \tag{4.3-29}$$

The bracketed term in the integrand of (4.3-29) is equal to the uncertainty function $\chi_{x,g}(\tau,\phi)$, so the equation can be rewritten as

$$\langle g,\Phi\rangle = \iint_{-\infty}^{\infty} |\chi_{g,x}(\tau,\phi)|^2\ R_S(\tau,\phi)\ d\tau d\phi. \tag{4.3-30}$$

But the right side of (4.3-30) is the cost functional, thus $\langle g,\Phi\rangle = J(g)$.

By itself, this property is of little consequence. It is, however, useful in establishing the next, and final, property of the gradient function.

Property 4: The norm of the gradient function $\Phi(t)$ is greater than or equal to the value of the cost functional.

Because both $g(t)$ and $\Phi(t)$ are elements of $L^1(R^1)$ and $L^2(R^1)$ they both have finite energies, in fact, $\|g\|_2 = 1$ by convention. Therefore, by applying the Schwartz inequality to (4.3-28) gives

$$J(g) = |J(g)| = |\langle g, \Phi \rangle| \leq \|g\|_2 \, \|\Phi\|_2 = \|\Phi\|_2. \tag{4.3-31}$$

4.4 Optimization of the Expected Matched Filter Output

4.4.1 The Increment of the Cost Functional

In section 4.3.3 it was shown that the cost functional could be expanded into the generalized Taylor series

$$J(g+\eta) = J(g) + 2\,\mathrm{Re}\{\int_{-\infty}^{\infty} \eta(t)\, \Phi^*(t)\, dt\} + J(\eta), \tag{4.3-23}$$

where $g(t)$ is the processing signal and an element of $L^1(R^1)$ and $L^2(R^1)$, $\eta(t)$ is an arbitrary element of $L^2(R^1)$, and $\Phi(t)$ is the gradient function given by

$$\Phi(t) = \iint_{-\infty}^{\infty} \chi^*_{x,g}(\tau,\phi)\, R_S(\tau,\phi)\, x(t-\tau)\, e^{j2\pi\phi(t-\tau/2)}\, d\tau d\phi. \tag{4.3-9}$$

Consider the increment of the cost functional $J(g)$ with increment $\eta(t)$, defined as

$$\begin{aligned} \Delta J(g,\eta) &= J(g+\eta) - J(g) \\ &= 2\,\mathrm{Re}\{\int_{-\infty}^{\infty} \eta(t)\, \Phi^*(t)\, dt\} + J(\eta). \end{aligned} \tag{4.4-1}$$

Since $J(\eta)$ is always a non-negative number, if the increment $\Delta J(g,\eta)$ is to be positive, then it is necessary to choose $\eta(t)$ in such a fashion to guarantee that the first Gateaux derivative, the integral term in (4.4-1), is positive. This can be done by choosing the increment $\eta(t)$ to be

$$\eta(t) = \gamma\, \Phi(t) \tag{4.4-2}$$

where ρ is a positive real number. Using this rule causes the increment of the cost functional to become

$$\Delta J(g,\eta) = 2\,\gamma \int_{-\infty}^{\infty} |\Phi(t)|^2\,dt + J(\gamma\Phi) = 2\,\gamma\,\|\Phi\|_2^2 + J(\gamma\Phi) > 0\ . \qquad (4.4\text{-}3)$$

Notice that by the Schwartz inequality, choosing the increment using (4.4-2) maximizes the value of the first Gateaux derivative.

The choice of the name 'gradient function' for the function $\Phi(t)$ can now be easily explained. Consider the analogy of being at some point on a surface which can be modeled as a function of two real variables $f(x,y)$. If one wants to move in the direction that will cause the greatest positive change in elevation, then one moves in the direction of the gradient vector given by

$$\nabla f(x,y) = \frac{\partial f}{\partial x}(x,y)\,\vec{i} + \frac{\partial f}{\partial y}(x,y)\,\vec{j}. \qquad (4.4\text{-}4)$$

By choosing the direction vector of travel to be $\vec{v} = \gamma\,\nabla f(x,y)$ where γ is a positive real scalar will, to first order, guarantee a positive increase in elevation, denoted by h, which is approximately

$$\Delta h = \gamma\,\|\nabla f(x,y)\|^2 \qquad (4.4\text{-}5)$$

where $\|\cdot\|$ is the vector norm given by the Pythagorean theorem. Notice the similarity between (4.4-4) and the first term on the right side of (4.4-3).

Equation (4.4-4) essentially extends from the concept of a directional derivative. In the general case the value of the change in elevation approximated by

$$\Delta h = \langle \gamma\vec{n},\ \nabla f(x,y)\rangle = \gamma\,\langle \vec{n}, \nabla f(x,y)\rangle, \qquad (4.4\text{-}6)$$

where $\vec{n}$ is a direction vector with unity length and γ is the horizontal length of travel. This relates well to the first Gateaux derivative

(first variation) $\delta J(g,\eta)$, which is to first order an estimate of the change of the value of the cost functional when the function $g(t)$ changes to $g(t) + \eta(t)$. In this case, if $\eta(t) = \gamma\, z(t)$ then

$$\delta J(g,\gamma z(t)) = 2\ \mathrm{Re}\{\int_{-\infty}^{\infty} \gamma\, z(t)\ \Phi^*(t)\ dt\} = 2\ \gamma\ \mathrm{Re}\{\langle z,\Phi\rangle\}. \qquad (4.4\text{-}7)$$

Since both (4.4-6) and (4.4-7) are of a similar form it is natural to refer to $g(t)$ as the 'gradient function.'

4.4.2 The Gradient Projection Algorithm

In the last section, it was shown that if the increment $\eta(t)$ was a scaled replica of the gradient function $\Phi(t)$, then the increment of the cost functional is positive. If this approach is used to choose a new processing signal $\hat{g}(t)$ by letting $\hat{g}(t) = g(t) + \eta(t)$, then it can be seen immediately that there is no guarantee that this processing signal has unit energy. Therefore, the increment $\eta(t)$ must be chosen not only to insure a positive change in the cost functional but also guarantee that the new processing signal has a unity norm. In other words, $\hat{g}(t) = g(t) + \eta(t)$ is an element of the set S where

$$S = \{y \in L^2(R^1) \mid \|y\|_2 = 1\}. \qquad (4.2\text{-}1)$$

One way to do this is to set $\eta(t) = \gamma\ \Phi(t)$, giving a new processing signal equal to $g(t) + \gamma\ \Phi(t)$ and then projecting this function onto the set S by using its best approximation in S which by Theorem 4.2 is

$$\hat{g}(t) = \frac{g(t) + \gamma\ \Phi(t)}{\|g+\gamma\Phi\|_2}. \qquad (4.4\text{-}8)$$

The actual increment, denoted as $\delta g(t)$, in this case is

$$\delta g(t) = \hat{g}(t) - g(t) = \frac{g(t) + \gamma\ \Phi(t)}{\|g+\gamma\Phi\|_2} - g(t). \qquad (4.4\text{-}9)$$

Figure 11 illustrates the process of choosing a new processing signal if the analogy of signals represented by vectors is used.

The method of choosing a new processing signal presented above will be applied recursively to increase the value of the cost function, which in turn implies that the expected value of the matched filter receiver will increase. In terms of the processing signal, this means it will more closely match the form of the signal at the output of the channel whose scattering function is $R_{S_{CHN}}(\tau,\phi)$.

The cost functional, defined as the expected value of the matched filter receiver output to the channel output, given by

$$J(g) = \int\int_{-\infty}^{\infty} |\chi_{x,g}(\tau,\phi)|^2 \, R_{S_{CHN}}(\tau,\phi) \, d\tau d\phi \, , \qquad (4.4\text{-}10)$$

will be increased recursively using the following procedure:

1. Choose a transmit signal x(t) and an initial processing signal $g_1(t)$.
2. Calculate the initial uncertainty function $\chi_{x,g_1}(\tau,\phi)$.
3. Calculate the gradient function given by

$$\Phi_i(t) = \int\int_{-\infty}^{\infty} \chi^*_{x,g_i}(\tau,\phi) \, R_{S_{CHN}}(\tau,\phi) \, x(t-\tau) \, e^{j2\pi\phi(t-\tau/2)} \, d\tau d\phi. \qquad (4.4\text{-}11)$$

4. Form the new processing signal

$$g_{i+1}(t) = \frac{g_i(t) + \gamma \, \Phi_i(t)}{\|g_i + \gamma \Phi_i\|_2} \, . \qquad (4.4\text{-}12)$$

5. Calculate the uncertainty function $\chi_{x,g_{i+1}}(\tau,\phi)$.
6. Calculate the cost functional $J(g_{i+1})$.
7. Return to step 3 or stop if a maximum amount of interations have been reached or the value of $J(g_{i+1})$ equals or exceeds a predetermined threshold.

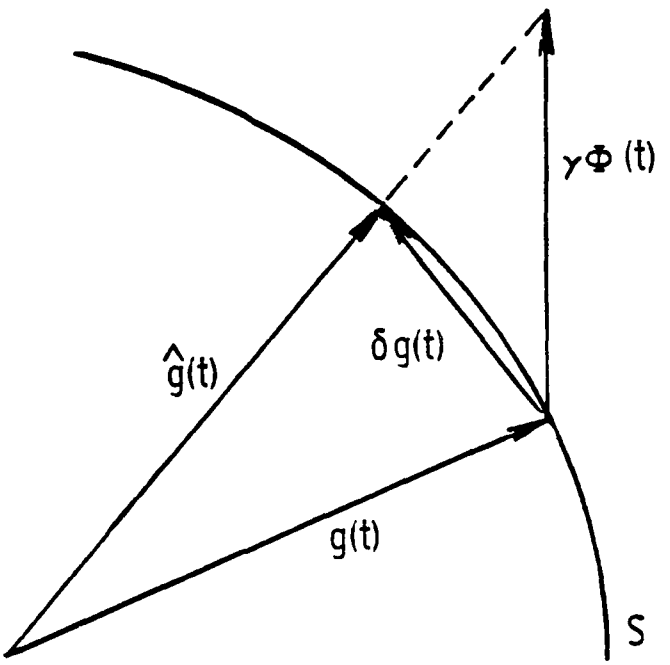

Figure 11. Visualizaton of the projection algorithm The signal $g(t) + \gamma\ \phi(t)$ is best approximated by $\hat{g}(t)$ in the set S.

In general, there is no way to perform each step in closed form. In particular, closed form calculation of the cross-ambiguity or gradient functions presents an unwieldy task. Therefore, all the equations must be discretized and the optimization procedure done numerically.

4.4.3 Convergence of the Gradient Projection Algorithm

Determining the convergence of the gradient projection algorithm presented in section 4.4.2 is done by examining the behavior of the increment of the cost functional. By showing that the increment is always a non-zero positive value for any non-zero positive step size γ will imply that the sequence $\{J(g_i)\}_{n=1}^{\infty}$ monotonically increases and will converge because it is bounded.

To begin, it is necessary to determine the processing signal increment for the i-th step of the recursive algorithm which by (4.4-9) is

$$\delta g_i(t) = \frac{g_i(t) + \gamma\, \Phi_i(t)}{\|g_i+\gamma\Phi_i\|_2} - g_i(t). \tag{4.4-13}$$

Substituting (4.4-13) into (4.4-1) gives the increment of the cost functional at the i-th iteration as

$$\begin{aligned}\Delta J(g_i,\delta g_i) &= 2\ \mathrm{Re}\{\langle \delta g_i, \gamma\Phi_i\rangle\} + J(\delta g_i)\\ &= \frac{2\ \mathrm{Re}\{\langle g_i,\Phi_i\rangle+\langle\Phi_i,\Phi_i\rangle\gamma\}}{\|g_i+\gamma\Phi_i\|_2} - 2\ \mathrm{Re}\{\langle g_i,\Phi_i\rangle\} + J(\delta g_i).\end{aligned} \tag{4.4-14}$$

By property 3 of the gradient function, the numerator in (4.4-14) can be restated as

$$\begin{aligned}2\ \mathrm{Re}\{\langle g_i\Phi_i\rangle+\langle\Phi_i,\Phi_i\rangle\gamma\} &= 2\ \mathrm{Re}\{J(g_i)+\|\Phi_i\|_2^2\gamma\}\\ &= 2\ [J(g_i) + \|\Phi_i\|_2^2\ \gamma].\end{aligned} \tag{4.4-15}$$

Because $J(g_i)$, $\|\Phi_i\|_2^2$, and γ are all real numbers the operation of finding the real part of the complex number is not required in (4.4-15). The denominator of the first term on the right side of (4.4-14) can also be simplified using (2.2-8), property 3 of the gradient function, and the fact that $g_i(t)$ is a unit energy signal as follows:

$$\begin{aligned}\|g_i+\gamma\Phi_i\|_2^2 &= \langle g_i+\gamma\Phi_i, g_i+\gamma\Phi_i\rangle \\ &= \langle g_i,g_i\rangle + 2\,\mathrm{Re}\{\langle g_i,\Phi_i\rangle\}\,\gamma + \langle\Phi_i,\Phi_i\rangle\,\gamma^2 \\ &= 1 + 2\,J(g_i)\,\gamma + \|\Phi_i\|_2^2\,\gamma^2. \end{aligned} \tag{4.4-16}$$

Therefore, by (4.4-15) and (4.4-16), the increment of the cost functional is

$$\Delta J(g_i,\delta g_i) = \frac{2\,[J(g_i) + \|\Phi_i\|_2^2\,\gamma]}{\sqrt{1 + 2\,J(g_i)\,\gamma + \|\Phi_i\|_2^2\,\gamma^2}} - 2\,J(g_i) + J(\delta g_i). \tag{4.4-17}$$

Since $J(\delta g_i)$ is always a positive value, it is only necessary to determine if the sum of the first two terms of the right side of (4.4-17), the first Gateaux derivative of $J(g_i)$, is always positive. By examination of (4.4-17), it is seen that the first Gateaux derivative is a function of the step size γ, therefore,

$$F(\gamma) \triangleq \delta J(g_i,\delta g_i) = \frac{2\,[J(g_i) + \|\Phi_i\|_2^2\,\gamma]}{\sqrt{1 + 2\,J(g_i)\,\gamma + \|\Phi_i\|_2^2\,\gamma^2}} - 2\,J(g_i). \tag{4.4-18}$$

The function $F(\gamma)$ is continuous for all $\gamma > 0$ and can be shown to be monotonic by examining its first derivative. Since differentiating (4.4-18) involves considerable algebraic manipulation, the details are omitted here, and only the result stated, which is

$$\frac{dF(\gamma)}{d\gamma} =$$

$$\frac{2\,[\|\phi_i\|_2^2 - J(g_i)^2]\,\|g_i+\gamma\phi_i\|_2}{\|\Phi_i\|_2^4\,\gamma^4 + 4\,J(g_i)\,\|\Phi_i\|_2^2\,\gamma^3 + 2\,[\|\Phi_i\|_2^2 + 2\,J(g_i)^2]\,\gamma^2 + 4\,J(g_i)\,\gamma + 1}\,. \tag{4.4-19}$$

The denominator of (4.4-19) is a polynomial in γ with positive coefficients because both $J(g_i)$ and $\|\Phi_i\|_2$ are positive; therefore, for all $\gamma \geq 0$ its value is always greater than or equal to 1. As for the numerator, it is always non-negative since the norm term is always positive, and because by property 4 of the gradient function,

$$\|\Phi_i\|_2^2 \geq J(g_i)^2. \tag{4.4-20}$$

Therefore, for all $\gamma \geq 0$, the first derivative of $F(\gamma)$ is non-negative. From elementary calculus it is known that if the first derivative of a function is non-negative on an interval, then the function monotonically increases on that interval; consequently, $F(\gamma)$, or the first Gateaux derivative $\delta J(g_i,\delta g_i)$, increases monotonically for γ in $[0,\infty)$. If the step γ is zero, then from (4.4-13) and (4.4-18)

$$\delta J(g_i,\delta g_i) = \delta J(g_i,0) = F(0) = 0\,. \tag{4.4-21}$$

Thus $F(\gamma) = \delta J(g_i,\delta g_i)$ is non-zero for all $\gamma > 0$. It now follows that because the second Gateaux derivative is always non-negative, then

$$\Delta J(g_i,\delta g_i) > 0 \quad \text{for all } \gamma > 0\,. \tag{4.4-22}$$

This in turn implies

$$J(g_{i+1}) > J(g_i) \quad \text{for all } \gamma > 0. \tag{4.4-23}$$

From (4.4-23) it is guaranteed that the sequence $\{J(g_i)\}_{n=1}^{\infty}$ monotonically increases if $\gamma > 0$. Furthermore, the sequence is bounded from above by (3.3-6) giving $J(g_i) < 1$. From elementary calculus, it is

known that a bounded monotonic sequence of real numbers is convergent. Thus,

$$\lim_{i\to\infty} J(g_i) = J_{op} \leq 1 \ . \tag{4.4-24}$$

The analysis presented above proves that the gradient projection algorithm will increase the expected matched filter output. It should be noted that it does not guarantee that the sequence of processing signals, $\{g_i\}_{n=1}^{\infty}$, converges. However, what is guaranteed is that each successive $g_i(t)$ produces a better average receiver output. This extends from the fact that the cross-ambiguity function is not unique for a given pair of transmit and processing signals. Since the value of the expected matched filter output, the cost functional

$$J(g_i) = \int\int_{-\infty}^{\infty} |\chi_{x,g_i}(\tau,\phi)|^2 R_{S_{CHN}}(\tau,\phi)\, d\tau d\phi \tag{4.4-25}$$

is related to $g_i(t)$ via the cross-ambiguity function, the value of $J(g_i)$ is not unique for a given $g_i(t)$. It should be realized that this does not invalidate the optimization procedure presented in this chapter since it does insure an increase in $J(g_i)$. Therefore, the nonuniqueness of each $g_i(t)$ in the optimization sequence is of little consequence.

4.5 Examples of Matched Filter Optimization

Since the optimization procedure presented in section 4.4.2 must be implemented on a digital computer, it is necessary to discretize the equations used in the procedure.

Consider the uncertainty function derived in Chapter 3 and given by

$$\chi_{x,g}(\tau,\phi) = \int_{-\infty}^{\infty} x(t-\tau/2)\, g^*(t+\tau/2)\, e^{j2\pi\phi t}\, dt \ . \tag{3.2-37}$$

By invoking a change of variable and defining the function

$$v(t,\phi) = g^*(t)\, e^{j2\pi\phi t} , \tag{4.5-1}$$

equation (3.2-37) can be restated as

$$\chi_{x,g}(\tau,\phi) = e^{j\pi\phi\tau} \int_{-\infty}^{\infty} x(t-\tau)\, v(t,\phi)\, dt . \tag{4.5-2}$$

The integral in (4.5-2) can be approximated by a sum by setting $\phi = \ell(\Delta\phi)$, $t = m(\Delta t)$, and $\tau = n(\Delta\tau)$, and by replacing the integral sign by a summation symbol giving

$$\chi_{x,g}(n(\Delta\tau),\ell(\Delta\phi)) \simeq e^{-j\pi n\ell(\Delta\phi)(\Delta\tau)} \sum_{m=1}^{M} x(m(\Delta t)-n(\Delta\tau))\, v(m(\Delta t),\ell(\Delta\phi))\, \Delta t. \tag{4.5-3}$$

A simplification can be made by setting $\Delta\tau = \Delta t$, thus allowing the definition of the discrete sequences

$$\begin{aligned} x(m(\Delta t)-n(\Delta\tau)) &= x((m-n)(\Delta\tau)) \\ &\triangleq \hat{x}(m-n) \end{aligned} \tag{4.5-4}$$

$$\begin{aligned} v(m(\Delta t),\ell(\Delta\phi)) &= v(m(\Delta\tau),\ell(\Delta\phi)) \\ &\triangleq \hat{v}(m,\ell) . \end{aligned} \tag{4.5-5}$$

Substituting (4.5-4) and (4.5-5) back into (4.5-3) gives for the discretized uncertainty function

$$\chi_{x,g}(n(\Delta\tau),\ell(\Delta\phi)) = \Delta\tau\, e^{-j\pi n\ell(\Delta\tau)(\Delta\phi)} \sum_{m=1}^{M} \hat{x}(m-n)\hat{v}(m,\ell). \tag{4.5-6}$$

The summation in (4.5-6) is actually a correlation between the sequence $\hat{x}(n)$ and $\hat{v}(n,\ell)$, so it can be calculated using discrete Fourier transforms.[18] Therefore, it can be shown that (4.5-6) can be written as

$$\chi_{x,g}(n(\Delta\tau),\ell(\Delta\phi)) = \Delta\tau\, e^{-j\pi n\ell(\Delta\phi)(\Delta\tau)}\ \mathrm{IDFT}\{\mathrm{DFT}(x(-n))\ \mathrm{DFT}(\hat{v}(n,\ell))\} \tag{4.5-7}$$

where

$$\mathrm{DFT}(x(n)) = \sum_{n=0}^{N-1} x(n)\, e^{-j2\pi kn/N} = X(k) \tag{4.5-8}$$

is the forward discrete Fourier transform of the sequence x(n) and

$$\mathrm{IDFT}(X(k)) = \frac{1}{N}\sum_{k=0}^{N-1} X(k)\, e^{j2\pi kn/N} \tag{4.5-9}$$

is the inverse discrete Fourier transform of the sequence of Fourier coefficients X(k).

Another equation that requires discretization is the formula for the gradient function given by

$$\phi(t) = \int\int_{-\infty}^{\infty} \chi^*_{x,g}(t,\phi)\, R_{S_{CHN}}(\tau,\phi)\, x(t-\tau)\, e^{j2\pi\phi(t-\tau/2)}\, d\tau d\phi. \tag{4.5-10}$$

By defining the functions

$$\theta(\tau,\phi) \triangleq \chi^*_{x,g}(\tau,\phi)\, R_{S_{CHN}}(\tau,\phi)\, e^{-j\pi\phi\tau} \tag{4.5-11}$$

$$w(t,\phi) \triangleq x^*(t)\, e^{j2\pi\phi t} \tag{4.5-12}$$

equation (4.5-10) can be restated as

$$\begin{aligned}\phi(t) &= \int\int_{-\infty}^{\infty} \theta(\tau,\phi)\, w(t-\tau,\phi)\, d\tau d\phi \\ &= \int_{-\infty}^{\infty}\left[\int_{-\infty}^{\infty} \theta(\tau,\phi)\, w(t-\tau,\phi)\, d\tau\right] d\phi \\ &= \int_{-\infty}^{\infty} \theta(t,\phi)*w(t,\phi)\, d\phi\ .\end{aligned} \tag{4.5-13}$$

As before, the integral in (4.5-13) can be approximated by a sum by

setting $\phi = \ell\ (\Delta\phi)$ and $t = n\ (\Delta\tau)$ and by replacing the integral sign by a summation symbol giving

$$\Phi(n(\Delta\tau)) = \sum_{\ell} [\theta(n(\Delta\tau),\ell(\Delta\phi))*x(n(\Delta\tau),\ell(\Delta\phi))\ \Delta\tau]\ \Delta\phi\ . \quad (4.5\text{-}14)$$

By defining the two-dimensional sequences

$$\theta(n(\Delta\tau),\ell(\Delta\phi)) \triangleq \hat{\theta}(n,\ell), \quad (4.5\text{-}15)$$

$$w(n(\Delta\tau),\ell(\Delta\phi)) \triangleq \hat{w}(n,\ell), \quad (4.5\text{-}16)$$

$$\Phi(n(\Delta\tau)) \triangleq \hat{\Phi}(n), \quad (4.5\text{-}17)$$

and substituting them into (4.5-14) gives

$$\hat{\Phi}(n) = (\Delta\tau)\ (\Delta\phi) \sum_{\ell} \hat{\theta}(n,\ell)*w(n,\ell), \quad (4.5\text{-}18)$$

where the discrete convolution inside the sum of (4.5-18) is with respect to the variable n. Again the convolution can be calculated using discrete Fourier transform, therefore

$$\hat{\Phi}(n) = (\Delta\tau)\ (\Delta\phi) \sum_{\ell} \text{IDFT}\{\text{DFT}(\theta(n,\ell))\ \text{DFT}(w(n,\ell))\}\ . \quad (4.5\text{-}19)$$

Now that the equations giving the uncertainty function and gradient function are in a useable form, the gradient projection algorithm can now be stated in a form suitable for implementation on a digital computer:

1. Choose a discretized transmit signal $\hat{x}(n)$ and an initial discretized processing signal $\hat{g}_1(n)$.
2. Calculate the initial discretized uncertainty function $\chi_{\hat{x},\hat{g}_1}(n,\ell)$.
3. Calculate $\theta_i(n,\ell)$ and $w_i(n,\ell)$.
4. Calculate the gradient function $\hat{\Phi}_i(n)$ using (4.5-19).
5. Form the new discretized processing signal

AD-A151 226 RECEIVER OTTIMIZATION FOR DETECTION IN DOUBLY SPREAD COMMUNICATION CHANNE..(U) PENNSYLVANIA STATE UNIV UNIVERSITY PARK APPLIED RESEARCH LAB.. D M DRUMHELLER 2/2

UNCLASSIFIED 10 DEC 84 ARL/PSU/TM-84-185 F/G 17/2.1 NL

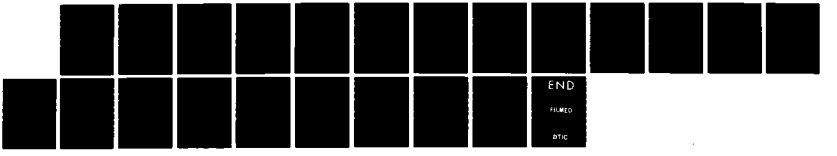

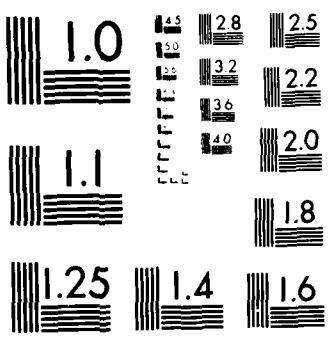

$$\hat{g}_{i+1}(n) = \frac{\hat{g}_i(n) + \gamma\, \hat{\phi}_i(n)}{\Delta\tau \sqrt{\sum_n |\hat{g}_i(n)+\gamma\hat{\phi}_i(n)|^2}} . \qquad (4.4\text{-}20)$$

6. Calculate the discretized uncertainty function $\chi_{\hat{x},\hat{g}_{i+1}}(n,\ell)$.

7. Calculate the value of the cost functional using

$$J_{i+1} = (\Delta\tau)\,(\Delta\phi) \sum_n \sum_\ell |\chi_{\hat{x},\hat{g}_{i+1}}(n,\ell)|^2 R_{S_{TGT}}(n,\ell) \qquad (4.4\text{-}21)$$

where

$$R_{S_{CHN}}(n,\ell) \triangleq R_{S_{CHN}}(n(\Delta\tau),\ell(\Delta\phi)). \qquad (4.5\text{-}22)$$

8. Return to step 3 or stop if a maximum amount of iterations have been reached or the value of J_{i+1} equals or exceeds a predetermined threshold.

The version of the gradient projection algorithm given above was implemented on the VAX11/782 at the Applied Research Laboratory. The algorithm was written as a FORTRAN 77 program, was run in a low priority batch queue, and for these examples required about one hour of CPU time.

The transmit signal and initial processing signal are both analytic signals with ten percent raised cosine windows. Both were linear frequency modulated with the transmit signal being a 200 Hz upchirp and the processing signal a 200 Hz downchirp. Figures 12 and 13 show the magnitude and the real and imaginary parts of the envelopes of both signals. Figure 14 shows the initial cross-ambiguity function derived from these two signals. Figure 15 shows the scattering function which consists of three two-dimensional Guassian pulses each with $\sigma_\tau = 0.015$ sec. and $\sigma_\phi = 25.0$ Hz. One pulse is centered on the τ axis at $\tau = 0.065$ sec. and the remaining two pulses are centered at $\tau = 0.155$ sec. and $\phi =$

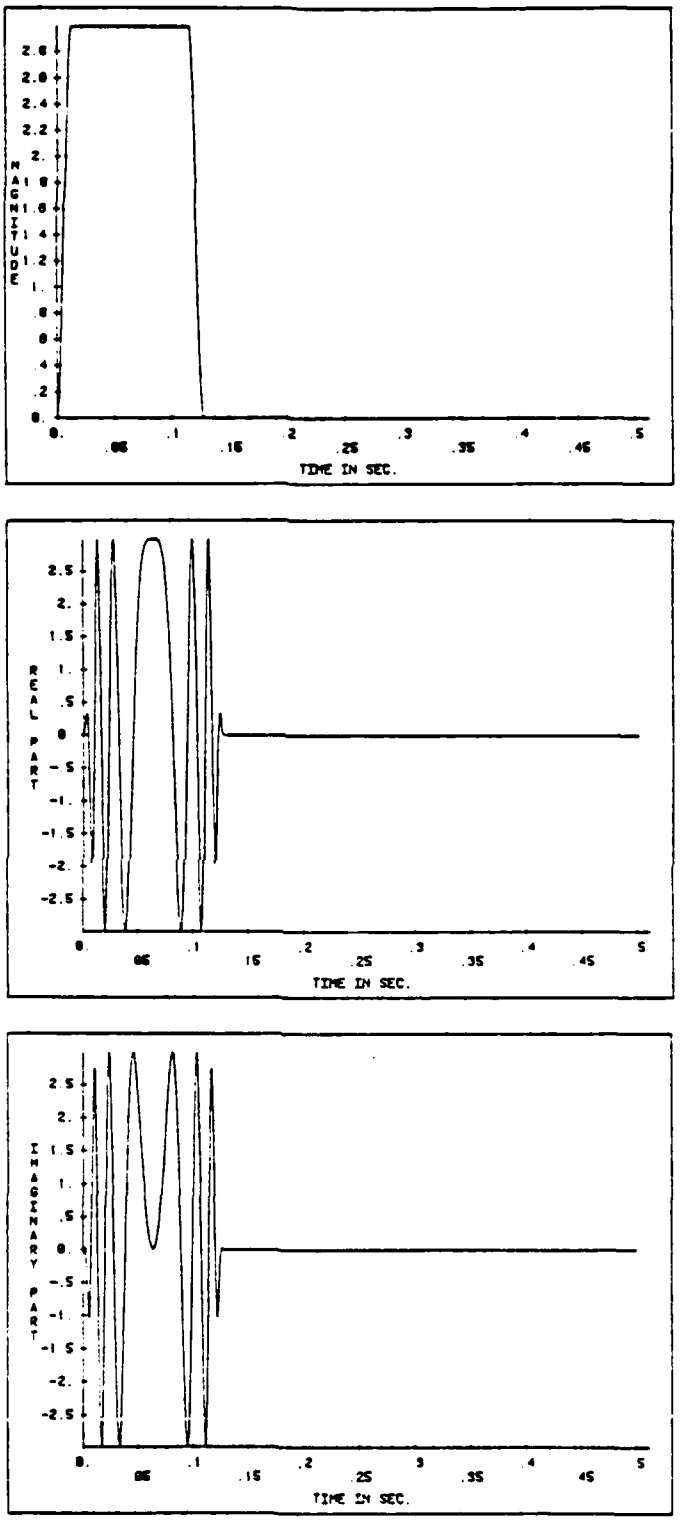

Figure 12. The magnitude and the real and imaginary parts of the transmit signal envelope for the first example.

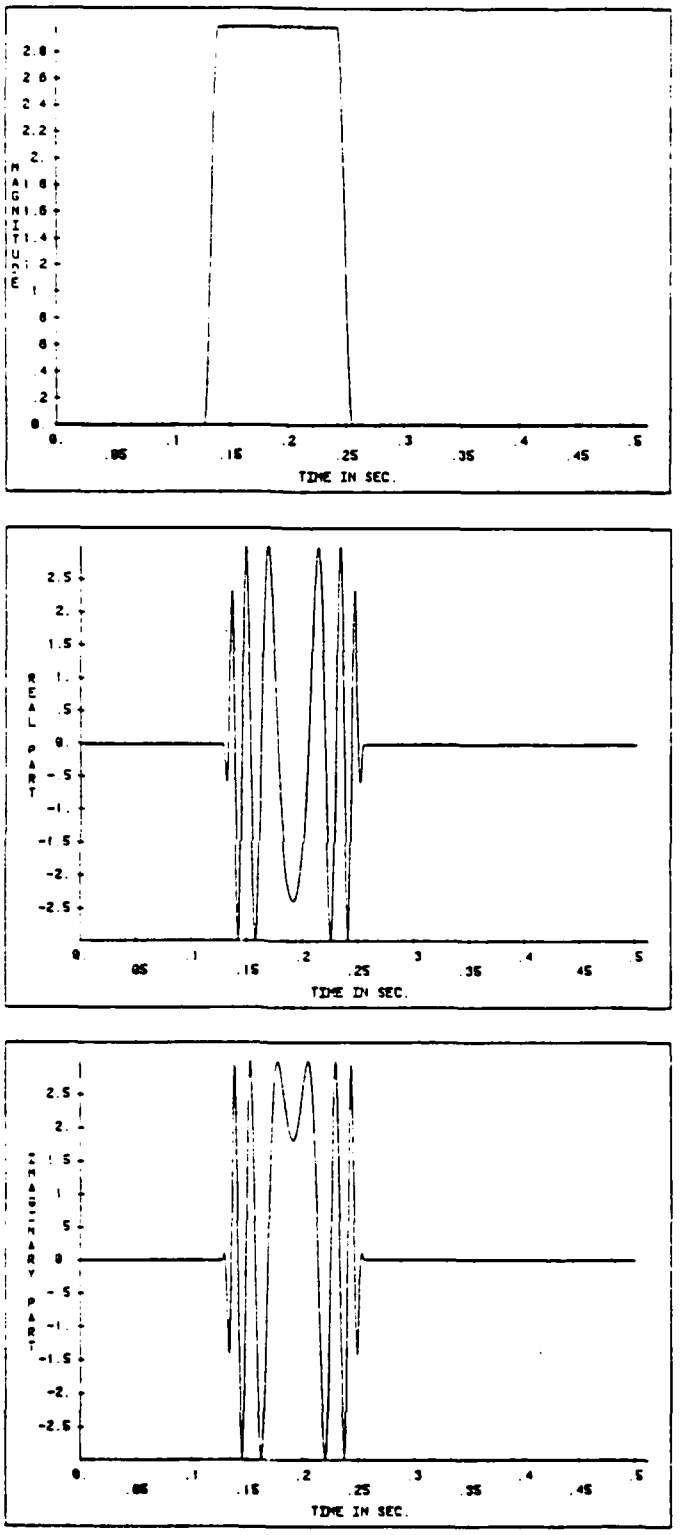

Figure 13. The magnitude and the real and imaginary parts of the original processing signal envelope for the first example.

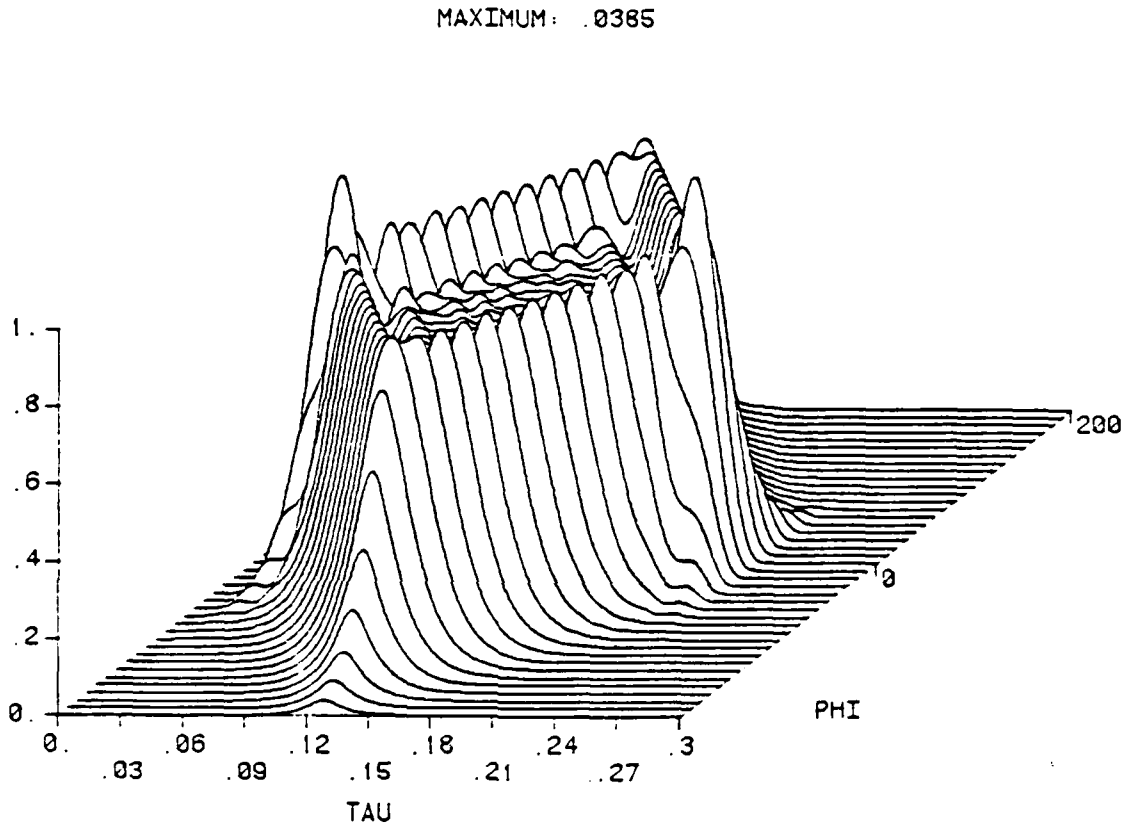

Figure 14. The original cross-ambiguity function for the first and third example.

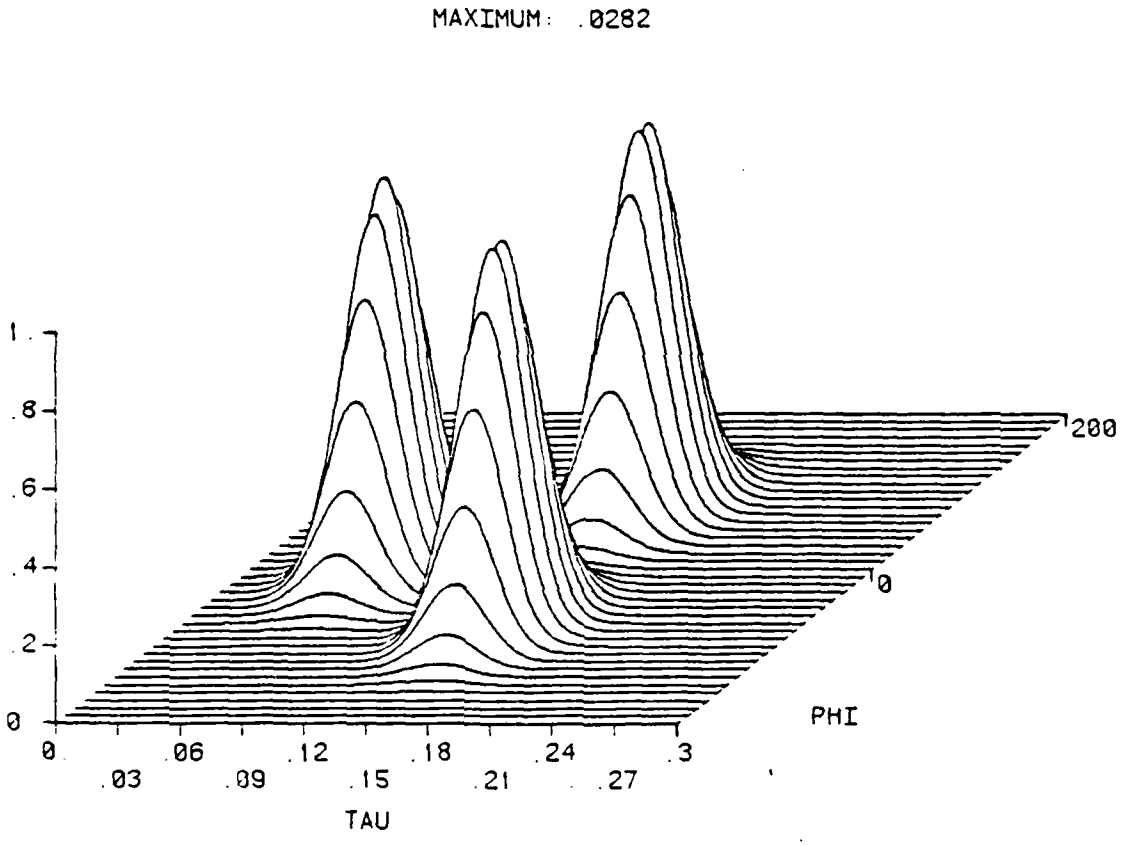

Figure 15. A scattering function consisting of three two-dimensional Gaussian pulses.

± 75 Hz. Furthermore, the pulses have been scaled so that the volume of the scattering function (the ratio of the average return energy to the transmit energy) is 0.2. For the discretization of all functions, the values $\Delta t = \Delta\tau = 0.00025$ sec and $\Delta\phi = 10$ Hz were used and the step size was set at $y = 5.0$.

The program iterated 15 times, and an increase in the cost functional occurred at each iteration. This is shown in Figure 16. Figure 17 shows the magnitude and real and imaginary parts of the final processing signal and Figure 18 shows the cross-ambiguity function derived from the transmit signal and final processing signal.

By comparing Figures 14 and 18, it can be seen that the volume of the cross-ambiguity function has been redistributed from one large plateau into two ridges. Each of these ridges subtends nearly the same region in the $(\tau-\phi)$ plane as do the three Gaussian pulses of the scattering function; in fact, by close inspection of large ridge it can be seen that the ends of the ridge have assumed a shape similar to two of the pulses in the scattering function. What occurred during the optimization procedure is that the processing signal was altered to cause the volume of the resulting cross-ambiguity function to collect in the same locations as the pulses in the scattering function and if possible cause the cross-ambiguity function to assume the same shape. This follows the principle developed in section 3.3, which said that the expected matched filter receiver output is maximized if the cross-ambiguity function is proportional to the scattering function of the channel. In this case, however, the shape of the cross-ambiguity function never actually matched that of the scattering function. This occurred because the processing signal was only parameter altered during the optimization process.

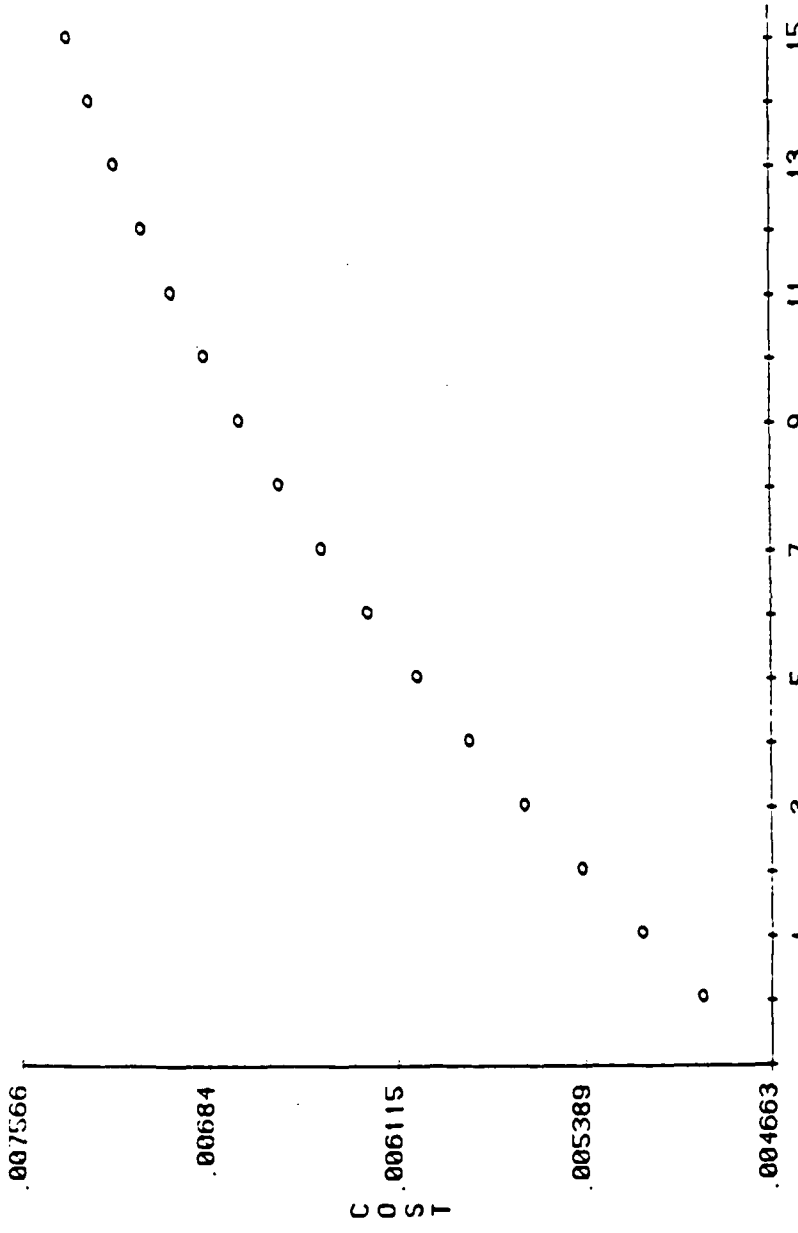

Figure 16. The value of the cost functional at each iteration of the projection algorithm for the first example.

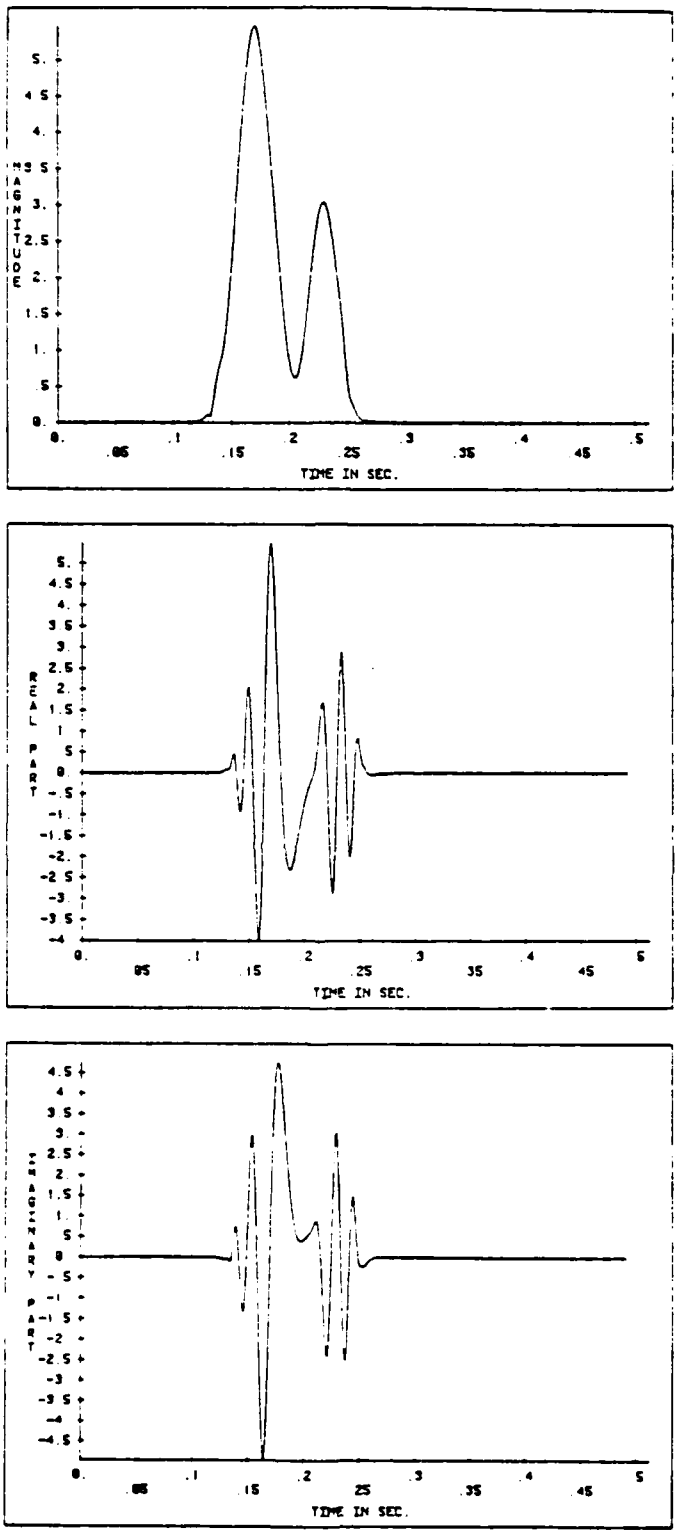

Figure 17. The magnitude and the real and imaginary parts of the final processing signal for the first example.

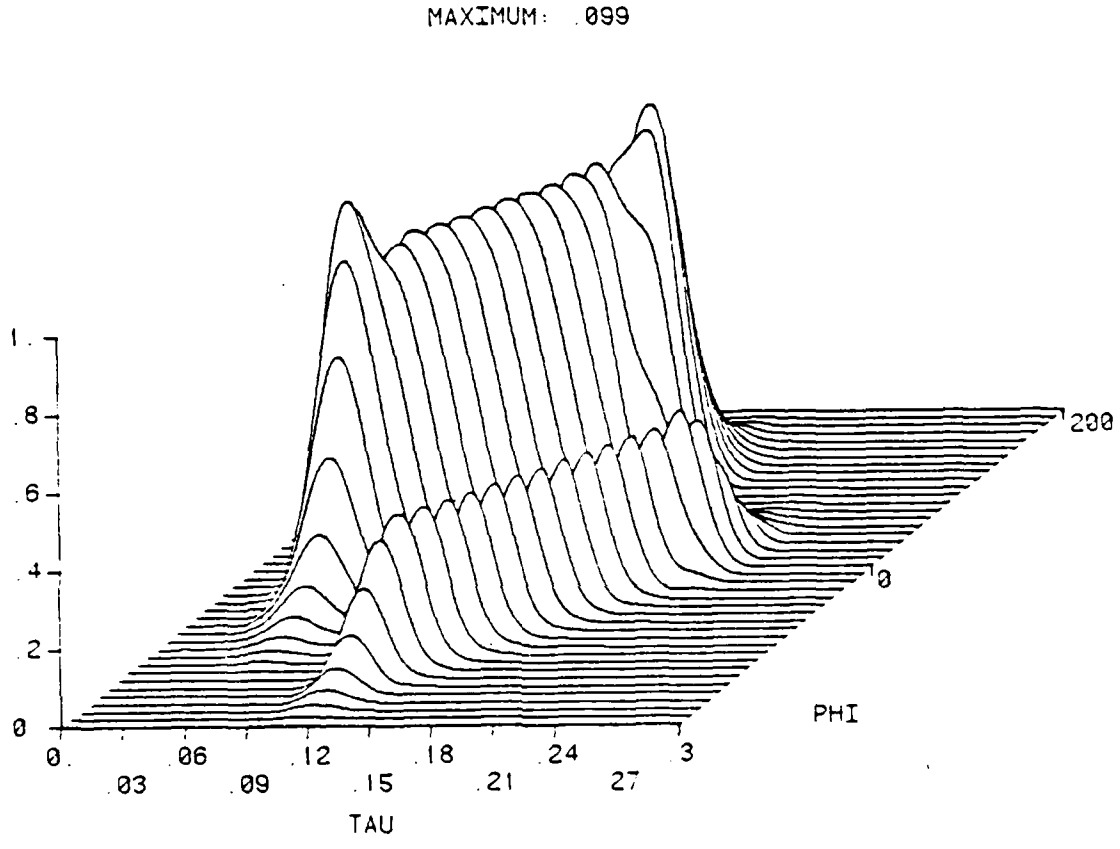

Figure 18. The final cross-ambiguity function for the first example.

It can also be demonstrated that the processing signal generated by the gradiant projection algorithm is highly dependent upon the placement of the initial cross-ambiguity function in the (τ, ϕ) plane and upon the distribution of its volume. Figure 19 shows a cross-ambiguity function derived from an 0.012 sec. transmit signal and an 0.210 sec. processing signal. Both signals were contimuous wave tones with a ten percent raised cosine window. The scattering function used was the same one used in the first example and is shown in Figure 15. By examining Figures 15 and 19, it can be seen that the two high doppler pulses of the scattering function, located at τ = 0.155 sec. and $\phi = \pm$ 75 Hz., are not fully subtended by the cross-ambiguity function. Furthermore, the cross-ambiguity function does not have a large portion of its volume in the region of the (τ, ϕ) plane where the high doppler pulses and the cross-ambiguity function intersect.

As in the first example, the computer program iterated 15 times, and an increase in the cost functional occured at each iteration. This is shown in Figure 20. Figure 21 shows the final cross-ambiguity function. It can be seen that the optimization procedure placed most of the volume of the cross-ambiguity function at the pulse of the scattering funcion located at τ = 0.065 sec. and ϕ = 0 Hz. This is also the same pulse of the scattering function that was completely overlayed by the initial cross-ambiguity function and where it had a significant portion of its volume. Thus, the gradient projection algorithm tends to place the volume of the cross-ambigutiy function over the prominent portions of the scattering function that are best overlayed by the initial cross-ambiguity function.

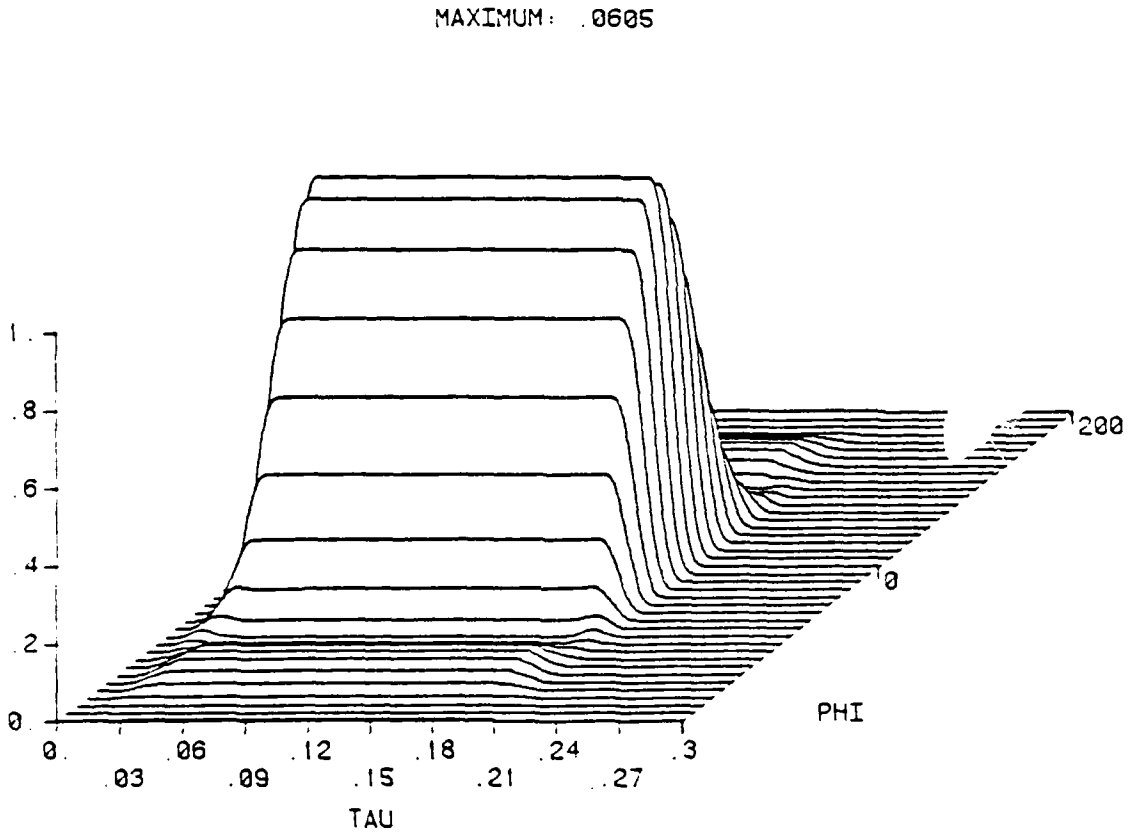

Figure 19. The initial cross-ambiguity function for the second example.

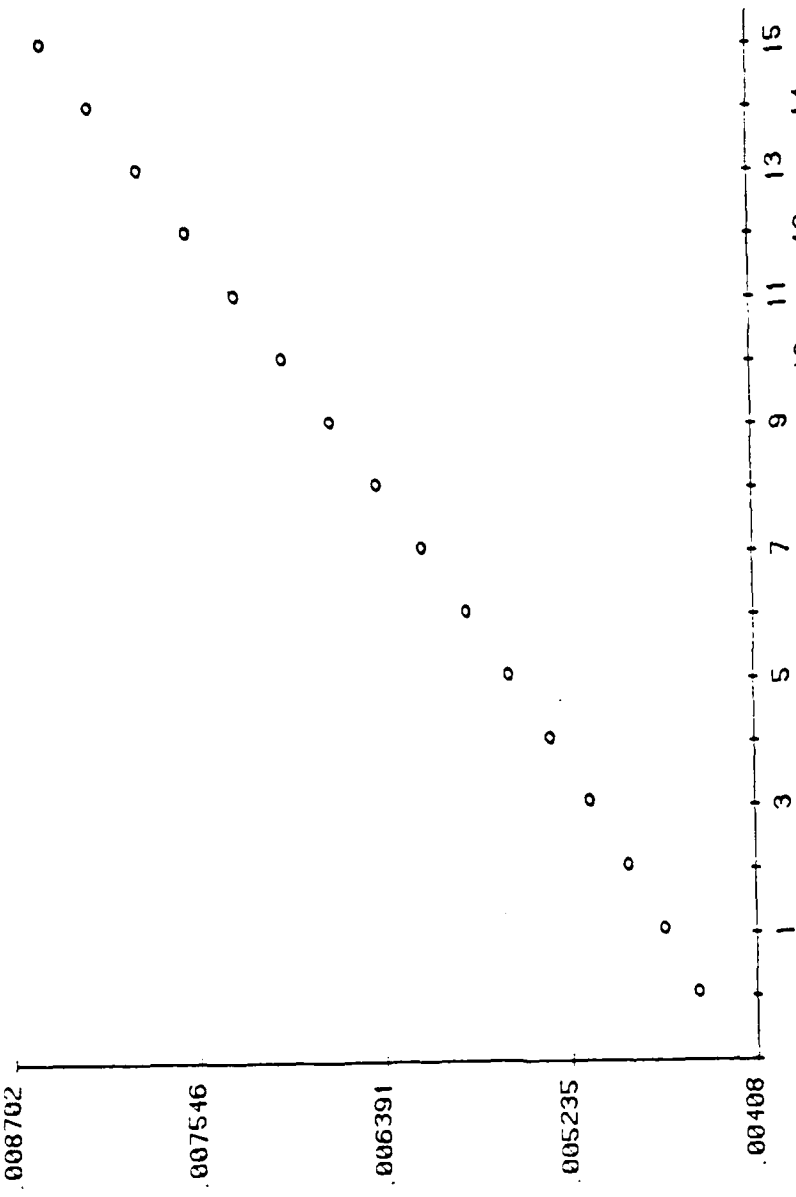

Figure 20. The value of the cost functional at each iteration of the projection algorithm for the second example.

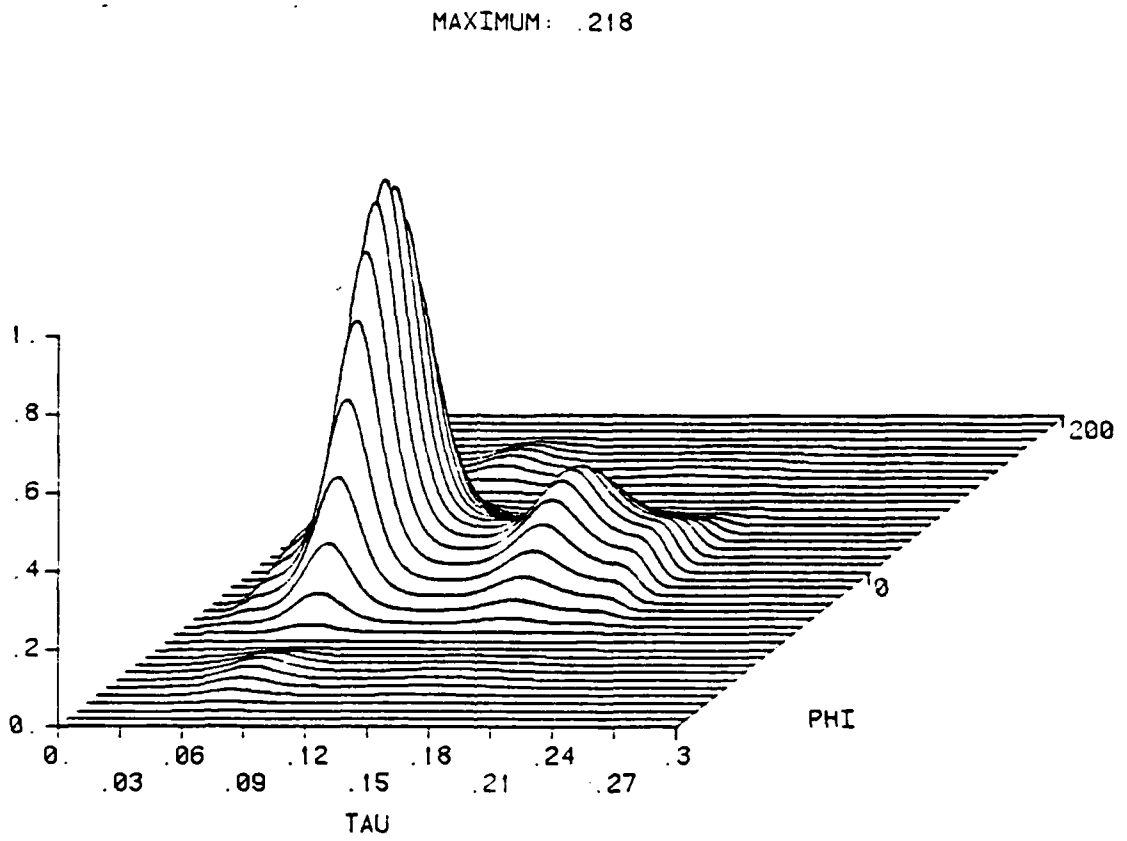

Figure 21. The final cross-ambiguity function for the second example.

Another way to test the validity of the gradient projection algorithm is to have it produce a known result. Figure 22 shows a scattering function that clos 'v models a point scatterer. It is a single gaussian pulse located at $\tau = 0.15$ sec. and $\phi = 0$ Hz. with standard deviations of $\sigma_\tau = 0.002$ sec. and $\sigma_\phi = 2.0$ Hz. The transmit signal and initial processing signal are the same used in the first example where the magnitude and real and imaginary parts of their envelopes are shown in Figures 12 and 13. The initial cross-ambiguity function is shown in Figure 14. The opimization procedure iterated 7 times, and the final cross-ambiguity function is shown in Figure 23. It is an autoambiguity function, which is a cross-ambiguity function derived from equal transmit and processing signals. In effect, the gradient projection algorithm dechirped the 200 Hz. downchirp FM processing signal to a 200 Hz. upchirp FM. It is shown in Van-Trees[11] and is well known in the literature that to optimally detect a point scatterer in the presence of white gaussian noise both the transmit and processing signals must be equal (this gives rise to the autoambiguity function).

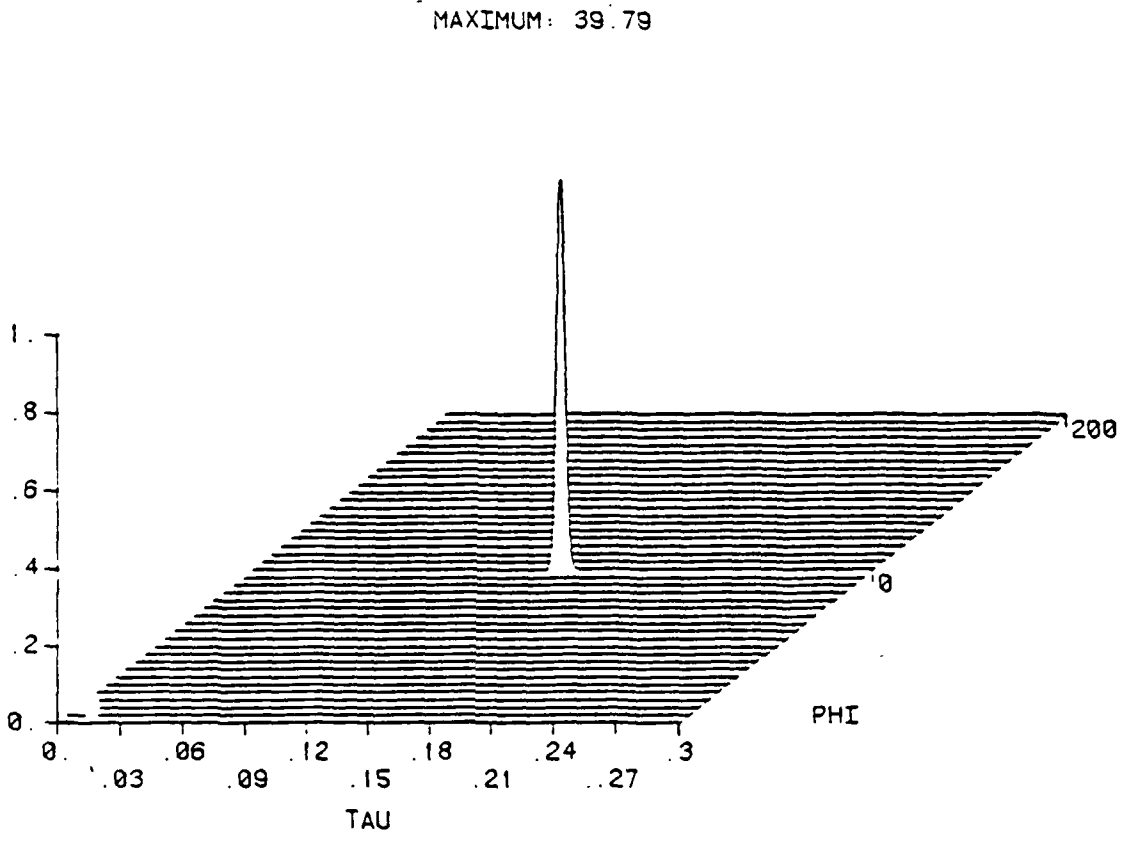

Figure 22. A scattering function modeling a point scatterer.

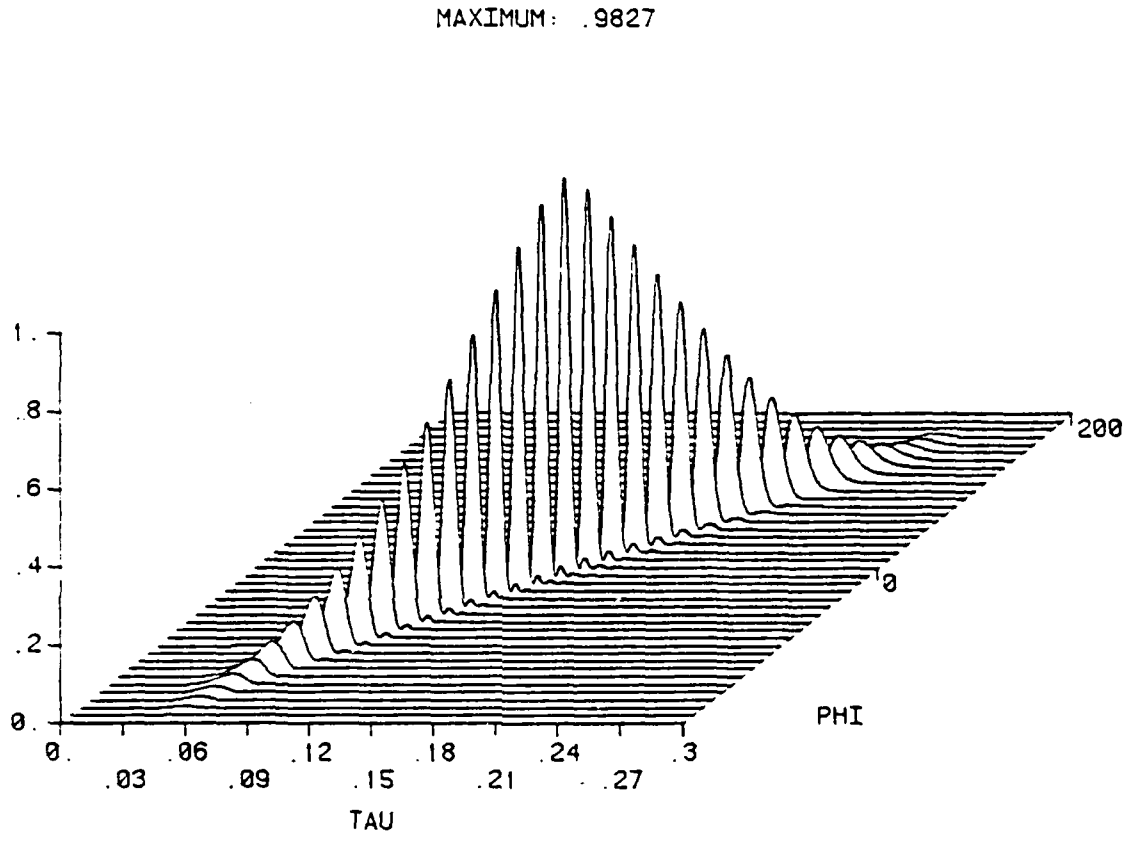

Figure 23. The final cross-ambiguity function for the third example.

CHAPTER 5

SUMMARY AND CONCLUSIONS

The derivation of the scattering function and its three Fourier transforms, under the assumption that it describes a wide sense stationary uncorrelated system (WSSUS), has been presented. Also it was shown that the scattering function can be used to determine the expected output of a matched filter receiver by multiplying it with the cross-ambiguity function and integrating the resulting two-dimensional function. Finally, a method for optimizing the matched filter by altering the processing signal was developed, and a numerical example was given.

It should be pointed out that the cross-ambiguity function is the bridge that links scattering properties via the scattering function to the signals used in detection. It is for this reason that the cross-ambiguity function is of major importance in the design of receivers for signal detection in the communication systems. There are two important results in this thesis related to cross-ambiguity functions. First, it was shown that if a receiver is to maximally detect a signal at the channel output, then the cross-ambiguity function derived from the transmitted signal and the processing signal must be proportional to the channel scattering function. Second, a method was derived to iteratively find an optimum processing signal given a fixed transmit signal and channel scattering function. The validity of the method was demonstrated by producing a known result; specifically, when the channel was modeled by a point scatterer, the cross-ambiguity function converged to an auto-ambiguity function.

There are a number of extensions to this work that could be made. For example, an analysis could be made to determine the rate of convergence of the gradient projection algorithm, and the optimum step size could be determined to accelerate the optimization procedure. To do this, the behavior of the second variation of the cost functional with respect to the step size would have to be examined. Another possible research project would be to develop a method of jointly altering the transmit and processing signals with a global search to produce a better match between the cross-ambiguity and scattering functions. This would be a generalization of the problem addressed in this thesis. It was shown that the optimized processing signal depended upon how well the original cross-ambiguity function overlayed the scattering function and to what extent its volume was placed with respect to the scattering function support. As a result, the optimization procedure converged locally over the whole set of possible transmit and processing signal pairs. The analysis of a procedure where both signals are altered, and the cross-ambiguity function is shifted in the (τ, ϕ) plane, may show that it is possible to globally maximize the expected matched filter output over all admissible transmit and processing signals.

BIBLIOGRAPHY

1. Royden, H. L. Real Analysis. London: The MacMillan Company, 1968.

2. Luenberger, D. G. Optimization by Vector Space Methods. New York: John Wiley and Sons, 1969.

3. Butzer, P. L., Nessel, R. J. Fourier Analysis and Approximation (Vol. I). Birkhäuser Verlag Basel, 1971.

4. Titchmarsh, E. C. Introduction to the Theory of Fourier Integrals. Oxford University Press, 1937.

5. Bachman, G. Elements of Abstract Harmonic Analysis. New York: Academic Press Inc., 1964.

6. Dym, H., McKean, H. P. Fourier Series and Integrals. New York: Academic Press Inc., 1972.

7. Lathi, B. P. Signals, Systems, and Communication. New York: John Wiley and Sons, 1965.

8. Zadeh, L. A., Desoer, C. A. Linear System Theory. McGraw-Hill, 1963.

9. Kailath, T. Channel Characterization: Time Variant Dispersive Channels. In E. J. Baghdady (Ed.), Lectures on Communication System Theory. New York: McGraw-Hill, (1969).

10. Ziomek, L. J. A Scattering Function Approach to Underwater Acoustic Detection and Signal Design. Ph.D. Dissertation. The Pennsylvania State University, 1981.

11. Van Trees, H. L. Detection, Estimation, and Modulation Theory, Part III. New York: John Wiley and Sons, Inc., 1971.

12. Kennedy, R. S. Fading Dispersive Communication Channels. New York, John Wiley and Sons, Inc., 1969.

13. Papoulis, A. Probability, Random Variables, and Stochastic Processes. New York: McGraw-Hill, 1984.

14. Kelly, E. J., Wishner, R. P. Matched Filter Theory for High-Velocity Accelerating Targets. IEEE Transactions on Military Electronics, 56-69, January 1965.

15. Sibul, L. H., Titlebaum, E. L. Volume Properties for the Wideband Ambiguity Function. IEEE Transactions on Aerospance and Electronic Systems, Vol. AES-17(1):83-87, January 1981.

16. Stutt, C. A., Spafford, L. J. A "Best" Mismatched Filter Response for Clutter Discrimination. IEEE Transactions on Information Theory, 280-287, March 1968.

17. Spafford, L. J. Optimum Radar Signal Processing in Clutter. IEEE Transactions on Information Theory, 734-743, September 1968.

18. Oppenheim, A. V., Schafer, R. W. Digital Signal Processing. Englewood Cliffs, NJ: Prentice-Hall Inc., 1975.

19. Lusternik, L. A., Sobolev, V. J. Elements of Functional Analysis. New York: Gordon and Breach, 1968.

20. Milne, R.D. Applied Functional Analysis. Marshfield Mass.: Pitman Publishing Inc., 1980.

DISTRIBUTION LIST FOR UNCLASSIFIED ARL INTERNAL MEMORANDUM 84-185
by D. D. Drumheller, dated 10 December 1984

Commander
Naval Sea Systems Command
Department of the Navy
Washington, DC 20362

Mr. D. Porter, SEA 63R1 Copy #1

Mr. D. C. Houser, SEA 63R-14 Copy #2
Code SEA 9961 (Library) Copy #3

Naval Coastal Systems Center
Panama City, FL 32401

Dr. David Skinner, Code 790 Copy #4

Commanding Officer
Naval Underwater Systems Center
Newport Laboratory
Newport, RI 02840

Dr. J. R. Short, Code 303 Copy #5

University of Texas at Austin
Applied Research Laboratories
P.O. Box 8029
Austin, TX 78712

Dr. J. F. Willman Copy #6

Commander
Naval Ocean Systems Center
San Diego, CA 92152

Mr. J. Campbell, Code 635 Copy #7

Commander
Office of Naval Research
800 North Quincy Street
Arlington, VA 22217

Dr. E. J. Wegman, Code 411SP Copy #8
Dr. A. J. Faulstich, ONT Copy #9

University of Washington
Applied Physics Laboratory
1013 N. E. 40th Street
Seattle, WA 98105

Mr. C. Sienkiewicz Copy #10

Naval Ocean Research Development Activity
NSTL, MS 39529

Mr. R. L. Martin, Code 113 Copy #11

Defense Technical Information Center
Cameron Station
Alexandria, VA 22314
Copy #12,13,14,15, (six)
16, and 17

Director
Applied Research Laboratory
The Pennsylvania State University
P. O. Box 30
State College, PA 16804

C. L. Ackerman Copy #18
R. Stern Copy #19
R. D. Ingram Copy #20
D. W. Ricker Copy #21
L. H. Sibul Copy #22
F. W. Symons Copy #23
J. Tague Copy #24
J. R. Sacha Copy #25
M. A. Matuson Copy #26
J. D. Hatlestad Copy #27
ARL Library Copy #28

END

FILMED

4-85

DTIC